The role of Dot1l in normal hematopoiesis and *MLL* translocation leukemia

by

Stephanie Youngyoon Jo

A dissertation submitted in partial fulfillment
of the requirements for the degree of
Doctor of Philosophy
(Molecular and Cellular Pathology)
in the University of Michigan
2011

Doctoral Committee:

Professor Jay L. Hess, Chair
Professor Ronald J. Koenig
Professor Steven L. Kunkel
Associate Professor Raymond C. Trievel
Assistant Professor Ivan P. Maillard
Assistant Professor Alexey Nesvizhskii

Dedication

To my family

Table of Contents

List of Figures

List of Tables

Abstract

*D*isruptor *o*f *t*elomeric silencing *1-l*ike (Dot1l) is a histone 3 lysine 79 methyltransferase. Studies of constitutive Dot1l knockout mice show that Dot1l is essential for embryonic development and prenatal hematopoiesis. Dot1l also interacts with fusion partners of *M*ixed *L*ineage *L*eukemia (*MLL*) gene, which is commonly translocated in human leukemia. However, the requirement of Dot1l in postnatal hematopoiesis and leukemogenesis of *MLL* translocation proteins have not been conclusively shown. With conditional Dot1l knockout mouse model, we examined the consequences of Dot1l loss in postnatal hematopoiesis and *MLL* translocation leukemia. Deletion of *Dot1l* led to pancytopenia and failure of hematopoietic homeostasis, and Dot1l-deficient cells minimally reconstituted recipient bone marrow in competitive transplantation experiments. In addition, MLL-AF9 cells required Dot1l for oncogenic transformation, while cells with other leukemic oncogenes such as Hoxa9/Meis1 and E2A-HLF did not. Furthermore, both histone methyltransferase activity of Dot1l and interaction with MLL fusion partner are required for transformation by MLL-AF9. In addition, loss of Dot1l affected histone modification at select loci instead of leading to global changes. These findings illustrate a crucial role of Dot1l in normal hematopoiesis, leukemogenesis of specific oncogenes, and histone cross-talk.

CHAPTER I

Introduction

Epigenetic modification is an important mechanism for the regulation of transcription and maintenance of cell identity with cell division. Hence, many histone modifying enzymes have been identified as crucial for maintaining normal hematopoietic stem cells (HSCs) as well as leukemia initiating cells (LICs). *D*isruptor *o*f *t*elomeric silencing *1* (Dot1) is a novel class of histone methyltransferase that was first identified in yeast for its ability to dysregulate gene silencing near telomeres (Feng et al., 2002; Min et al., 2003; Singer et al., 1998). Dot1, and its mammalian homologue, Dot1l (Dot1-like), is currently the only identified histone 3 lysine 79 (H3K79) methyltransferase (Ng et al., 2002a; van Leeuwen et al., 2002). Since its discovery, many studies show an essential role for Dot1l and H3K79 methylation in leukemia, embryonic development, prenatal hematopoiesis, and histone cross-talk (Barry et al., 2010; Chandrasekharan et al., 2010; Slany, 2009). However, the requirement of Dot1l in leukemogenesis and the role of Dot1l in the normal postnatal hematopoiesis have not been definitely shown.

Mixed Lineage Leukemia (*MLL*) gene

The Hess lab became interested in Dot1l while studying leukemias arising from translocations of the *M*ixed *L*ineage *L*eukemia (*MLL*) gene. Work done by the Hess laboratory and others has shown that the *MLL* C-terminal SET domain is a H3K4 methyltransferase (Milne et al., 2001; Nakamura et al., 2002). Further studies have shown that *MLL* interacts with proteins RbBP5, WDR5, and Ash2L, for optimal H3K4 methyltransferase activity (Dou et al., 2006). MLL also requires association with Menin, LEDGF, and MOF for its proper function (Dou et al., 2005; Yokoyama and Cleary, 2008; Yokoyama et al., 2005; Yokoyama et al., 2004). Knockout mouse models have shown that *MLL* is particularly important for the correct *Hox* gene expression and maintenance. *MLL* heterozygous (+/-) mice show slowed growth, hematopoietic abnormalities, and bidirectional shifts in *Hox* expression boundaries. Complete *MLL* deficiency (-/-) is embryonic lethal and is associated with severe defects in *HoxA* and *C* cluster expression (Hanson et al., 1999; Yu et al., 1995). However, the transgenic mice expressing *Mll* lacking the SET domain (MllΔSET) exhibit altered transcription of *Hox* genes and loss of H3K4 methylation but remain viable (Terranova et al., 2006), indicating that regions of Mll other than the SET domain also have important biological activity. This result is notable because the SET domain is lost with the majority of leukemia causing *MLL* translocations (Krivtsov and Armstrong, 2007; Meyer et al., 2009; Rubnitz et al., 1994; Silverman, 2007; Taki et al., 1996).

MLL translocation leukemia

Translocations of *MLL*, located on chromosome band 11q23, are frequently found in acute leukemia and are associated with poor prognosis. *MLL* rearrangements are particularly common in infant leukemia under the age of two, with 70-80% of cases exhibiting *MLL* translocation and pro-B cell lymphoid phenotype (Krivtsov and Armstrong, 2007; Rubnitz et al., 1994; Silverman, 2007; Taki et al., 1996). *MLL* translocations are also found in roughly 10% of adult cases with acute myeloid leukemia (AML), involving over fifty different translocation partners in addition to those presenting with partial tandem duplications (Dou and Hess, 2008; Meyer et al., 2009). While recent studies indicate important function of reverse translocation proteins such as AF4-MLL (Benedikt et al., 2011; Bursen et al., 2010), for the purpose of this thesis, *MLL* translocation refers to the fusion of the N-terminus of MLL and C-terminus of a translocation partner.

Similar to wild type *MLL*, *MLL* fusion proteins upregulate the expression of the *Hox* loci along with the *Hox* cofactor *Meis1*, which are necessary and sufficient for transformation (Ayton and Cleary, 2003; Zeisig et al., 2004). Although rare *MLL* fusion partners are cytoplasmic proteins with self oligomerization domains (Martin et al., 2003; So et al., 2003), greater than 80% of the fusion partners are nuclear proteins, including AF4, AF9, ENL, AF10, and ELL, with t(4;11) (MLL-AF4 fusion), t(11;19) (MLL-ENL fusion), and t(9;11) (MLL-AF9 fusion) being most common (Dou and Hess, 2008; Huret et al., 2001; Krivtsov and Armstrong, 2007; Meyer et al., 2009). Studies performed by the

Hess lab and others have shown that these common translocation partners form a coactivator complex along with the transcriptional elongation machinery pTEFb and chromatin modifier Dot1l (Bitoun et al., 2007; Mohan et al., 2010; Monroe et al., 2010; Mueller et al., 2007; Okada et al., 2006). These studies on MLL and *MLL* translocation proteins led to the following model (Slany, 2009).

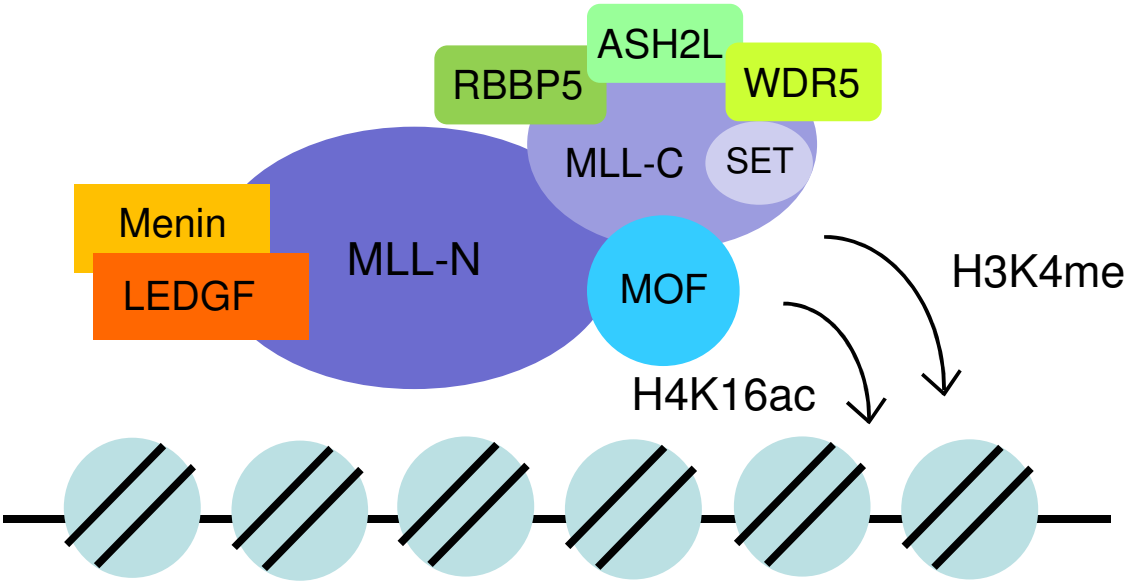

Figure 1.1. Wild type MLL protein complex. C-terminal MLL associates with other proteins for H3K4 methylation and H4K16 acetylation activity. N-terminal MLL associates with LEDGF and Menin for proper gene regulation. C-terminal MLL associates with RBBP5, ASH2L, and WDR5 for H3K4 methylation and also interacts with MOF that acetylates H4K16 residue. Figure modified from Slany, 2009.

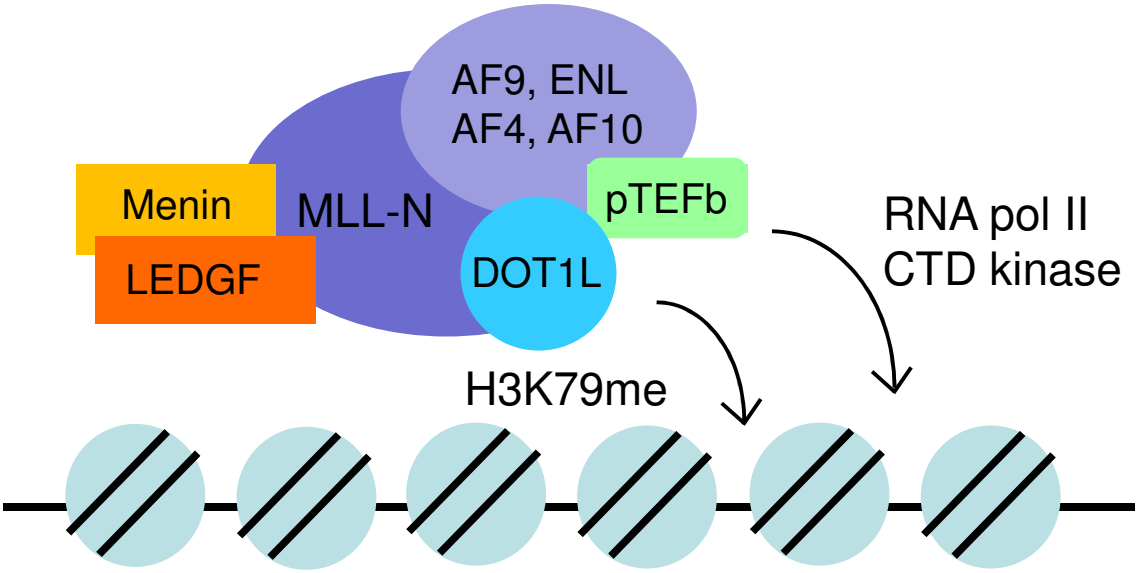

Figure 1.2. The most common *MLL* translocation protein complex. The most common *MLL* translocation partners interact with each and other proteins that promote transcriptional elongation (pTEFb, phosphorylates RNA pol II C-terminal domain, CTD) and modify chromatin (DOT1L, methylates H3K79 residue). Figure modified from Slany, 2009.

Dot1l and *MLL* translocation leukemias

Dot1l is strongly associated with *MLL* translocation leukemias. As mentioned above, multiple studies show that Dot1l interacts with many of the most common *MLL* translocation partners in a complex promoting transcriptional elongation (Bitoun et al., 2007; Mohan et al., 2010; Monroe et al., 2010; Mueller et al., 2007; Okada et al., 2006). Additional evidence from *MLL* translocation containing cell lines and patient samples shows upregulation of H3K79 methylation at *MLL* translocation target genes including *HOXA9* and *MEIS1*, which are critical for leukemogenesis (Krivtsov et al., 2008; Monroe et al., 2010). Furthermore, the loss of H3K79 methylation through knockdown of Dot1l leads to reduced expression of these genes (Krivtsov et al., 2008; Monroe et al., 2010).

However, it is not clear if Dot1l is required for *MLL* translocation-mediated leukemogenesis, and if other leukemia oncogenes also require Dot1l.

Gene regulation by Dot1l and H3K79 methylation

In general, Dot1l and H3K79 methylation are associated with transcriptional activation (Karlić et al., 2010; Steger et al., 2008; Vakoc et al., 2006). Interestingly, the loss of Dot1l seems to regulate a relatively short list of genes instead of globally downregulating the entire transcriptome. This effect has been particularly noted in the context of embryonic stem cells suggesting a specific biological role for Dot1l (Barry et al., 2009). Further studies using constitutive Dot1l knockout mouse models provide additional evidences for a role of Dot1l in stem cell biology. Analyses of Dot1l knock out embryonic stem cells and yolk sac cells show that the loss of Dot1l leads to cell cycle defects, chromosomal aberrations, and prenatal hematopoietic abnormalities (Feng et al., 2010; Jones et al., 2008). However, the two constitutive Dot1l knockout mouse lines are embryonic lethal by E10.5 and E13.5, precluding the examination of Dot1l loss in postnatal mice and in definitive hematopoiesis.

Dot1l and histone cross-talk

Dot1l is currently the only identified H3K79 methyltransferase. Knockout models (Feng et al., 2010; Jones et al., 2008) and knock down studies (Barry et al., 2009; Jacinto et al., 2009) indicate that Dot1l is the major, if not the only, histone methyltransferase responsible for mono-, di-, and tri- H3K79 methylation.

Histone methyltransferase activity of Dot1l is quite unique, requiring the nucleosome for optimal activity unlike many other enzymes that can methylate histone peptides (Feng et al., 2002; Min et al., 2003). Furthermore, studies show that H3K79 methylation requires H2B ubiquitination for enzymatic activity (Kim et al., 2009; Lee et al., 2007; Ng et al., 2002b; Wood et al., 2003). It is also interesting that the same studies show a requirement of H2B ubiquitination for H3K4 methylation. As mentioned above, MLL and DOT1L are closely associated through *MLL* translocation leukemias. Hence, the histone cross-talk between H3K79 methylation, H2B ubiquitination, and H3K4 methylation is of interest. In particular, there has been no study showing if H3K79 methylation is required for H2B ubiquitination or H3K4 methylation in a mammalian system.

Rational of study

Despite its importance in prenatal hematopoiesis and its association with *MLL* translocation leukemia, no conclusive data are available regarding the role of Dot1l in postnatal hematopoiesis and its requirement in leukemogenesis. In addition, while histone cross-talk among H2B ubiquitination, H3K79 methylation, and H3K4 methylation is established in yeast, data in mammalian systems need further studies. Since constitutive Dot1l inactivation leads to early embryonic lethality, we generated conditional Dot1l knockout mice and examined the consequences of Dot1l loss in postnatal hematopoiesis, leukemogenesis by *MLL* translocation, and histone modifications. Dot1l was required for normal hematopoiesis under homeostatic conditions, and the loss of Dot1l led to the cell-

autonomous failure of functional stem cells. In addition, *MLL* translocation leukemia cells were selectively sensitive to the loss of Dot1l compared to cells transformed by other oncogenes such as Hoxa9/Meis1 and E2A-HLF. Furthermore, the loss of H3K79 methylation had minimal effects on global H2B ubiquitination and H3K4 methylation while having dramatic effects on Mll target gene loci. These results indicated that Dot1l is required for maintaining normal HSCs and LICs that depend on *MLL* translocation proteins, and H3K79 methylation plays an important role in the chromatin status of specific gene loci.

CHAPTER II

The role of Dot1l in postnatal hematopoiesis

Because of the close connection between Dot1l and MLL translocation leukemia, we examined the possible connection between Dot1l and normal hematopoiesis. Given that the conventional Dot1l knockout mice are embryonic lethal, we generated conditional knockout mice from sperm obtained from the Knockout Mouse Project.

Materials and Methods

Generation of Dot1l conditional knockout mouse

Sperms containing targeted *Dot1l*$^{-}$ allele (Figure 2.1) were obtained from the Knockout Mouse Project (CSD29070). The targeted allele contained beta-galactosidase (bgal) and neomycin resistance (neo) genes followed by polyA sequences for transcription termination in the intron 1-2 of the *Dot1l* locus. This bgal-neo-polyA cassette is flanked by Flippase Recognition Target (FRT) sequences for sequence-specific recombination with Flippase (FLP). In addition, exon 2 was flanked by loxp sequences for sequence-specific recombination with Cre protein. The bgal-neo-polyA cassette is necessary for selection of mouse

embryonic stem cells that contains the Dot1l- allele for microinjection into recipient embryos. Once the *Dot1l*$^{-}$ allele is correctly passed on, the selection cassette is removed by breeding with FLP positive transgenic mice (Jax 005703, Dot1l^{F}allele, Figure 2.1). The resulting mice were further bred to ubiquitously expressed CreER transgenic mice (Jax 004847) for Cre induction with tamoxifen *in vivo* and 4-hydroxytamoxifen (4-OHT) *in vitro*. Induction of Cre recombinase removes exon 2 (Dot1l$^{\Delta}$ allele, Figure 2.1) resulting in a frameshift mutation and a non-functional truncated protein. Dot1l$^{F/F}$;CreER+ mice were born in mendelian ratios and bred normally. Genotype of animals was confirmed by genomic DNA extraction and PCR (Denville Scientific, DirectAmp kit, CG1100). The strain background of all mice used was C57BL/6. All mice used for experiments were between 6-10 weeks of age. Genotyping primers and control and experimental allele designations are described on tables 2.1 and 2.2.

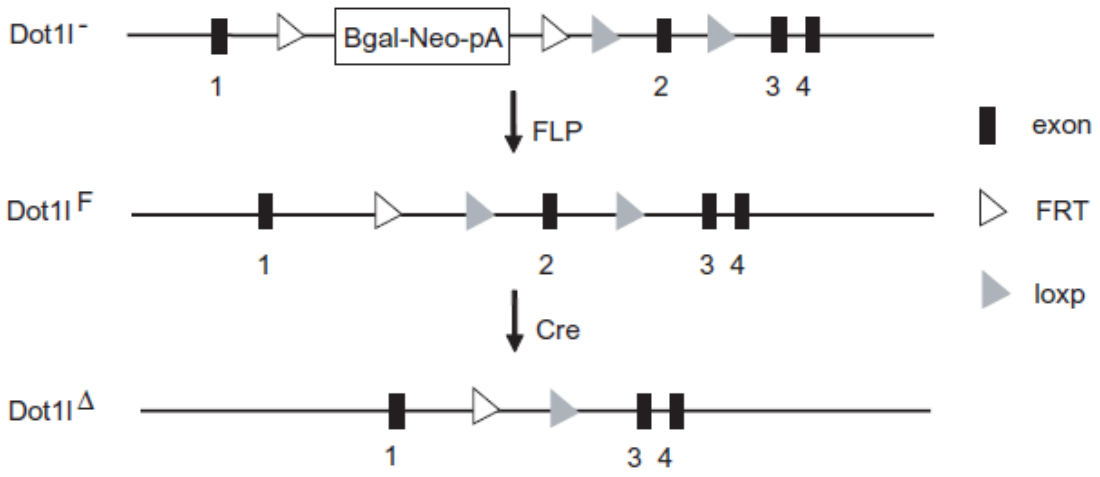

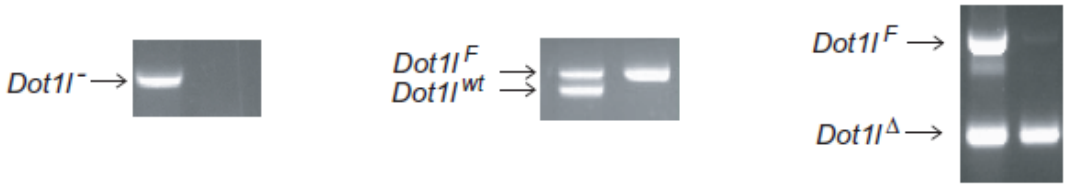

Figure 2.1. Generation of conditional Dot1l knockout mice.
Schematic of conditional *Dot1l* allele. *Dot1l*$^{-}$ allele containing sperm were obtained from the Knockout Mice Project (KOMP, CSD29070). *Dot1l*$^{-}$ mice were bred with FLP transgenic mice for the selection cassette removal (*Dot1l*^{F}). Resulting mice were further bred with CreER transgenic mice for conditional *Dot1l* exon 2 excision (*Dot1l*$^{\Delta}$) with tamoxifen injection or 4-OHT treatment. Loss of exon 2 (*Dot1l*$^{\Delta}$) led to a frame shift mutation and resulted in a non-functional product. Genotyping PCR products were run on 1.5% agarose gels. PCR primers were designed for distinguishing *Dot1l*^{wt}, *Dot1l*$^{-}$, *Dot1l*^{F}, and *Dot1l*$^{\Delta}$ alleles.

Genotyping Primers	*Dot1l*^{wt}	*Dot1l*$^{-}$	*Dot1l*^{F}	*Dot1l*$^{\Delta}$
F: GCCATGGTGTTTGTGTGTCCAGTT R: CCAACTGACCTTGGGCAAGAACAT	No product	312bp	No product	No product
F: GCCTACAGCCTTCATCATTC R: GATAGTCTCAATAATCTCA	527bp	6001bp	634bp	No product
F: GAAGTTCCTATTCCGAAGTT R: GAACCACAGGATGCTTCAG	No product	6294bp /927bp	927bp	244bp
F: CACTGATATTGTAAGTAGTTTGC R: CTAGTGCGAAGTAGTGATCAGG	For FLP allele (~750 bp)			
F: GCATTACCGGTCGATGCAACGAGTGATGAG R: GAGTGAACGAACCTGGTCGAAATCAGTGCG		For Cre allele (~400 bp)		

Table 2.1. Genotyping primers. Four different genotyping primer sets were used for distinguishing *Dot1l*^{wt}, *Dot1l*$^{-}$, *Dot1l*^{F}, and *Dot1l*$^{\Delta}$ alleles.

Control	*Dot1l*$^{+/+}$	*Dot1l*$^{F/F}$*;CreER-* or *Dot1l*$^{wt/wt}$*;CreER+* (*Dot1l*$^{+/+}$)
Experimental	*Dot1l*$^{F/F}$	*Dot1l*$^{F/F}$*;CreER+* (*Dot1l*$^{F/F}$)

Table 2.2. Control and experimental mice genotype designation.

Dot1l excision

Tamoxifen (Sigma T5648) was used *in vivo* for excision of Dot1l. Tamoxifen was dissolved in corn oil (Sigma C8267) at 10mg/ml stock solution and kept at 4^{o}C for a month. The stock was made fresh each month. In order to minimize toxicity from tamoxifen, two doses of 100µg/g body weight were given one day apart (total 200µg/g body weight) via intraperitoneal (IP) injection. 4-hydroxytamoxifen (4-OHT) (Sigma H7904), the active metabolite of tamoxifen, was used for excision of Dot1l *in vitro*. 4-OHT was dissolved in 100% EtOH at 1mM stock solution and kept at -20^{o}C. Again, in order to minimize cell toxicity from prolonged 4-OHT exposure, cells were treated with 5nM of 4-OHT for three days and then moved to fresh growth media.

Peripheral blood collection

Peripheral blood was collected via tail vein. Animals were warmed with heat lamp (100 watt) and placed in mouse tail illuminator (Braintree Scientific, MTI). Once tail veins on the sides were visible, a nick was made with razor blade and blood was collected by capillary action into EDTA coated tube (Ram Scientific 14-915-50). The collected blood was used for genomic DNA extraction and PCR for checking *Dot1l* excision efficiency, complete blood count analysis

for monitoring hematopoiesis, and surface marker staining and flow cytometry for examining specific white blood cell population changes.

Complete blood count (CBC) analysis

For CBC analysis, mice were given 200µg/g of tamoxifen every month for continued Dot1l excision and peripheral blood was collected from mice by tail vein bleed one week after each injection or when mice became moribund. The samples were analyzed on Advia120 (Siemens) or Forcyte (Oxford Science) instruments.

Competitive bone marrow transplantation

Competitive bone marrow transplantation involves transplanting wild type competitor cells with transgenic or knockout cells of interest into recipients that were lethally irradiated. Lethal irradiation should remove recipient hematopoietic system. This method is useful because competitive cells prevent animal death in case the genetically modified cells are unable to reconstitute recipient bone marrow, allowing detailed examination of hematopoietic compartment after transplantation. Hence, it is important to distinguish competitor cells and residual long-lived recipient cells from genetically modified cells. The distinction can be made by utilizing CD45 alleles. CD45 protein is expressed on the cell surface of all nucleated hematopoietic cells (Hermiston et al., 2003). The CD45 alleles are different between mouse strains, and C57BL/6 mice have the CD45.2 allele and

SJL/J mice have the CD45.1 allele (Komura et al., 1975). Since this discovery, B6.SJL mice, which are C57BL/6 mice with CD45.1+ allele, have been generated (Shen et al., 1985). Because the conditional Dot1l knockout mice generated were in C57BL/6 background and therefore CD45.2+, congenic CD45.1+ B6.SJL mice (Taconic Farms, 4007) were used as competitor cells and recipients.

For competitive transplantation, CD45.2+ *Dot1l*$^{+/+}$ or *Dot1l*$^{F/F}$ mice were injected with tamoxifen, and three days later bone marrow cells were harvested. Genomic DNA was extracted from 250,000-500,000 cells (Qiagen, DNeasy kit, 69504) for checking Dot1l excision efficiency. The cells were mixed with wild type CD45.1+ competitors at 1:1 or 3:1 ratio and transplanted into lethally irradiated (900 rad) CD45.1+ recipients. Recipients were lethally irradiated (900 rad) 2-4 hours before transplantation.

For examining cell-autonomous effects of Dot1l, bone marrow cells from CD45.2+ *Dot1l*$^{+/+}$ or *Dot1l*$^{F/F}$ mice were harvested without tamoxifen injection. The cells were mixed with wild type CD45.1+ competitors at 1:1 ratio and transplanted into lethally irradiated recipients. Recipients were injected with tamoxifen once bone marrow was stably reconstituted (8 weeks after transplantation). CBC of recipients was checked before tamoxifen injection to ensure hematopoietic reconstitution.

Flow Cytometry

LSRII (BD Biosciences) was used for analysis of bone marrow and peripheral blood cells. Antibodies were obtained from BD Pharmigen,

eBioscience, or Biolegend (parenthesis indicates clone identification): anti-sca-1 (D7), c-kit (2B8), CD48 (HM48-1), CD150 (mShad150), CD135 (A2F10), IL7Rα (A7R34), CD93 (AA4.1), CD41 (MWReg30), CD105 (MJ7/18), CD16/32 (93), CD45.1 (A20), CD45.2 (104), CD19 (6D5), B220 (30-F11), CD43 (ebioR2/60), IgM (RMM-1), CD11b (M1/70), Gr1 (R86-8C5), CD3 (145-2C11), CD4 (CK1.5), CD8α (53-6.7), TCRβ (H57-597), streptavidin-PE-TexasRed. Lineage positive cells were defined by mouse lineage cocktail (BD Pharmigen 559971). DAPI 1µg/ml (Sigma D9542) was used for dead cell exclusion. Standard buffer (1% FBS, 0.1% sodium azide, 1x PBS) was used for antibody staining. Results were analyzed using FlowJo (TreeStar).

Hematoxylin and Eosin (H & E) stain of bone marrow

Sternums of mice were fixed in 10% phosphate buffered formalin solution for 22-26 hours. H & E stain was performed by the University of Michigan Cancer Center Tissue Core.

Results

Postnatal *Dot1l* deletion leads to pancytopenia

First, we wanted to determine if the loss of Dot1l had adverse effects on the life expectancy of adult mice. *Dot1l* was deleted from 6-10 week old mice utilizing a ubiquitously expressed CreER transgene activated by intraperitoneal (IP) tamoxifen injection (200µg/g body weight). Efficiency of excision was checked by genotyping peripheral blood 1 week after tamoxifen injection.

Although high excision efficiency was initially observed, there was an increase of the non-excised allele when mice were re-genotyped between 4-5 weeks after the first tamoxifen injection. In order to prevent cells with the non-excised allele from repopulating, mice were injected with tamoxifen every month, and peripheral blood was collected for genotyping and CBC analysis 1 week after each injection.

Next, the loss of H3K79 methylation was confirmed by western blot of bone marrow cells 3 weeks after the excision (Figure 2.2) in order to verify that our mouse model indeed led to loss of Dot1l phenotype. The loss of H3K79 dimethylation (H3K79Me2) can be used as proxy for the loss of Dot1l and H3K79 methylation since Dot1l is the only enzyme mediating H3K79 mono-, di-, and tri-methylation (Feng et al., 2010; Jones et al., 2008). While mice were relatively healthy during the first two months, *Dot1l*$^{F/F}$ mice became moribund between 8 to 12 weeks after the first tamoxifen injection (Figure 2.2).

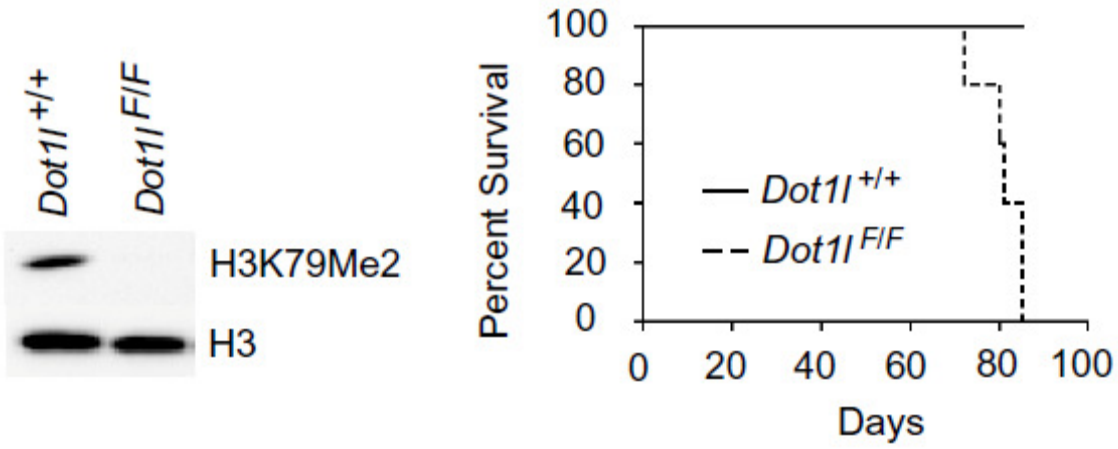

Figure 2.2. Prolonged loss of Dot1l in adult mice leads to death. H3K79me2 western blot of unfractionated bone marrow cells three weeks after *Dot1l* excision. Dot1l$^{F/F}$ cells show loss of H3K79me2. Histone 3 blot was used as loading control.

CBC analysis of moribund mice showed that *Dot1l*$^{F/F}$ mice developed pancytopenia with mean white blood cell count of 2.2x10^3/µl, red blood cell count of 3.2x10^6/µl, and platelet count of 200x10^3/µl, while *Dot1l*$^{+/+}$ mice had normal counts (Figure 2.3). H & E staining of bone marrow from euthanized *Dot1l*$^{F/F}$ mice showed marked hypocellularity compared to control mice (Figure 2.4). These results showed that Dot1l is required for maintaining normal steady-state hematopoiesis.

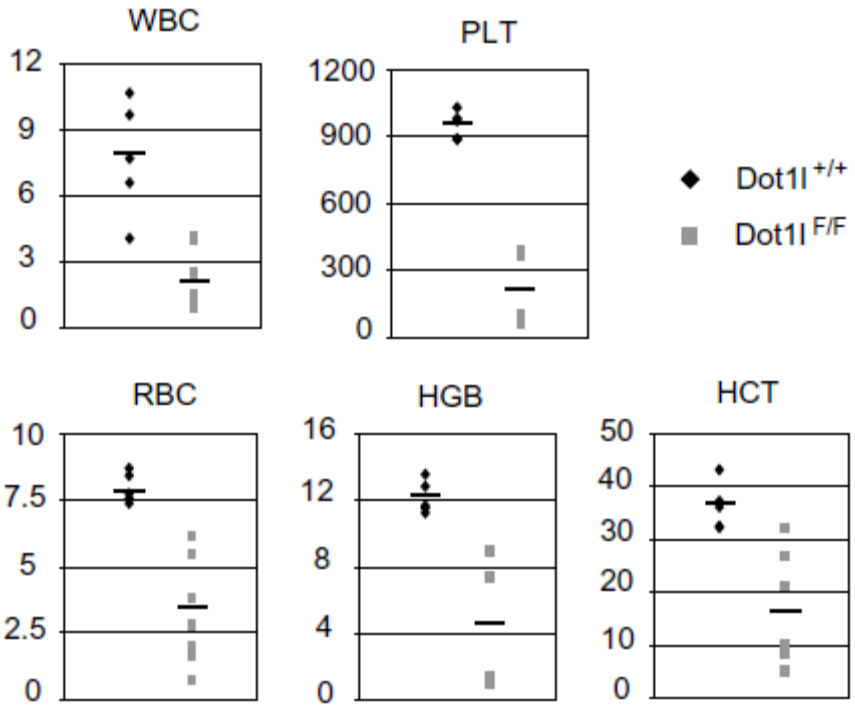

Figure 2.3. CBC analysis. Last CBC analysis before *Dot1l*$^{F/F}$ mice died or had to be euthanized. Data points represent individual animals and bars represent mean.

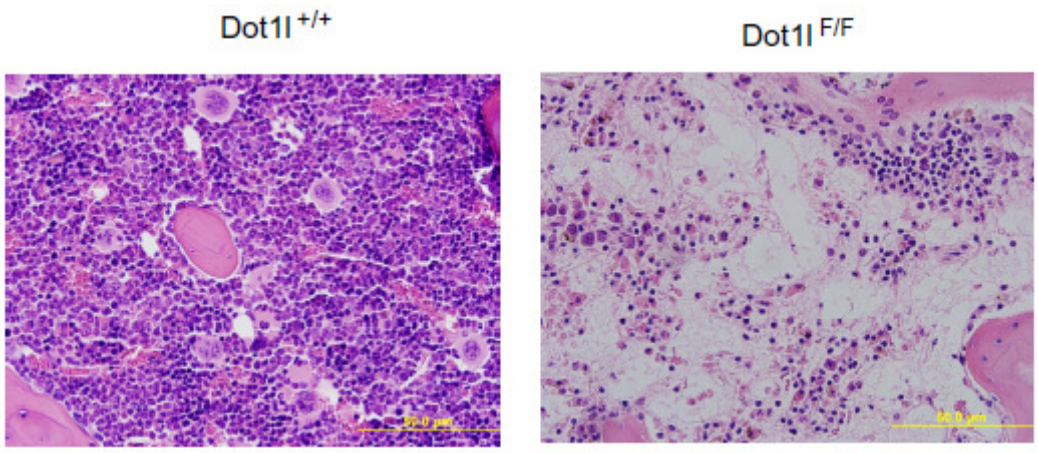

Figure 2.4. H & E stained section of bone marrow. *Dot1l* deletion led to bone marrow hypocellularity in *Dot1l*$^{F/F}$ mice. Tissues were collected when *Dot1l*$^{F/F}$ mice became moribund.

Dot1l deletion leads to depletion of phenotypic HSCs and progenitors

Since pancytopenia after *Dot1l* deletion suggested failure of HSCs or multipotent progenitors, we examined the bone marrow progenitor cell populations by flow cytometry.

First, HSC staining profile of *Dot1l*$^{F/F}$*;CreER-* (*Dot1l*$^{+/+}$), *Dot1l*$^{wt/wt}$*;CreER+* (*Dot1l*$^{+/+}$), and *Dot1l*$^{F/F}$*;CreER+* (*Dot1l*$^{F/F}$) mice were examined in the absence of any treatment to exclude baseline differences between control and experimental animals (refer to Table 2.2). All three genotypes showed similar staining profiles of HSCs (Figure 2.5).

Once it was confirmed that there were no major baseline differences between the control and experimental genotypes, mice were injected with tamoxifen. Three weeks after tamoxifen injection, mice were euthanized and bone marrow cells were harvested for population analysis. A three week point

was chosen based on the observation that by 4-5 weeks post-injection, the few cells that escaped excision competed out the rest of bone marrow.

The harvested bone marrow cells were stained with antibodies for cell surface markers to identify HSCs and progenitors. Frequency of population was calculated based on the total live cell count from each sample obtained from the flow cytometer. Live cells were defined by first gating out red blood cells and DAPI positive dead cells, and then selecting singlet cells and correct size. The definition of each population was immunophenotypically characterized in previous studies (Kiel et al., 2005; Maillard et al., 2009; Pronk et al., 2007). HSC: lineage-, sca1+, ckit+, CD48-, CD150+. Common lymphoid progenitors (CLP): lineage-, IL7Rα+, sca1lo, ckitlo, AA4.1+, CD135+. Megakaryocyte progenitors (MkP): lineage-, sca1lo, ckit+, CD150+, CD41+. Erythroid progenitors (EryP): lineage-, sca1lo, ckit+, CD41-, CD16/32-, CD105+. Granulocyte macrophage progenitors (GMP): lineage-, sca1lo, ckit+, CD41-, CD16/32+, CD105-.

The frequencies of HSCs and progenitors were all significantly decreased in Dot1l-deficient bone marrow compared to control (Figures 2.6 and 2.7). The decrease in frequency was particularly pronounced for HSCs. These results indicated that Dot1l is required for the maintenance of HSCs and lineage specific progenitors in homeostatic conditions.

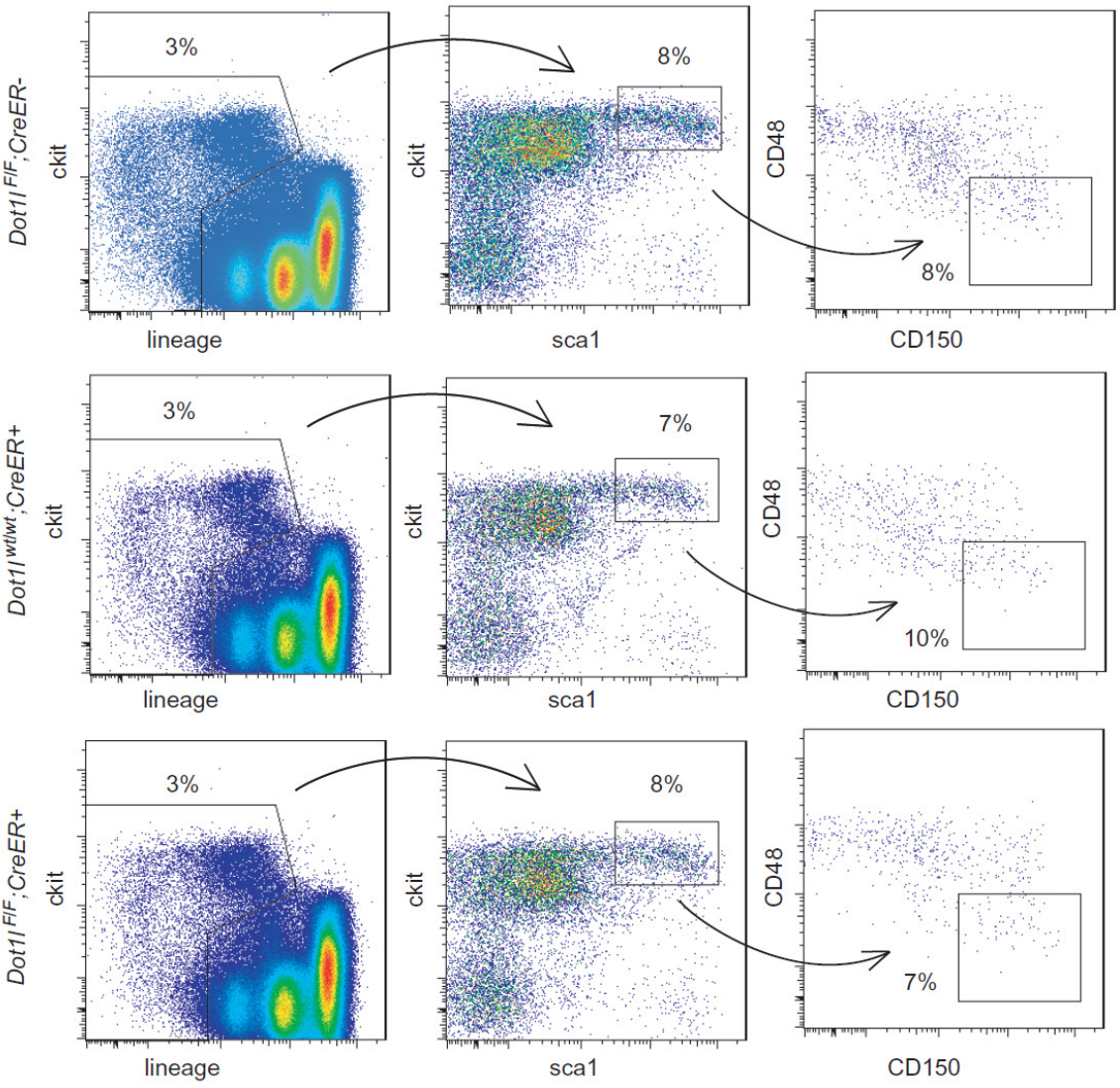

Figure 2.5. Baseline comparison of HSCs in mice lines. Bone marrow cells of *Dot1l*$^{F/F}$*;CreER-*, *Dot1l*$^{wt/wt}$*;CreER+* and *Dot1l*$^{F/F}$*;CreER+* mice were stained for HSCs (lineage-, sca1+, ckit+, CD48-, CD150+). In the absence of tamoxifen injection, all three mice lines showed similar HSC staining profiles. Percentages were based on parent gate.

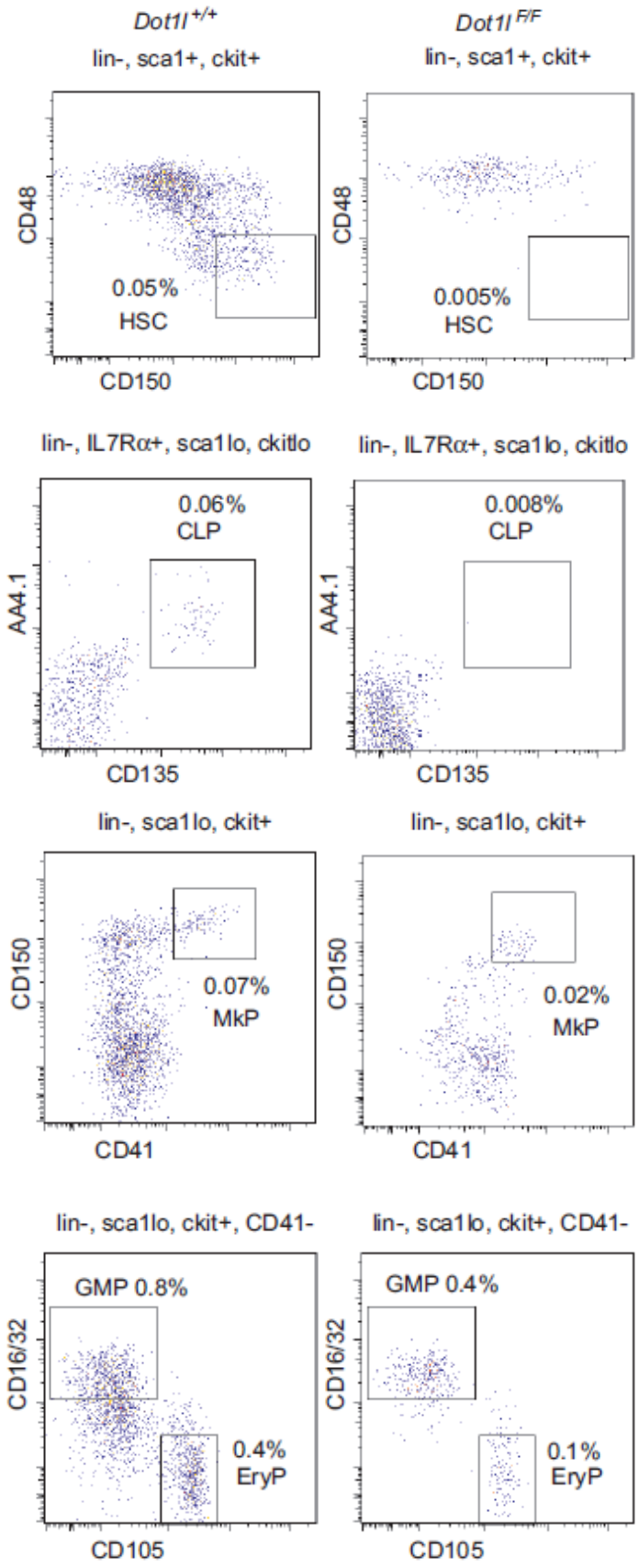

Figure 2.6. Deletion of *Dot1l* led to loss of HSCs and progenitors. (A) Staining profile of HSCs and progenitors 3 weeks after tamoxifen injection in *Dot1l*$^{+/+}$ and *Dot1l*$^{F/F}$ mice.

HSC: lineage-, sca1+, ckit+, CD48-, CD150+.

CLP: lineage-, IL7Rα+, sca1lo, ckitlo, AA4.1+, CD135+.

MkP: lineage-, sca1lo, ckit+, CD150+, CD41+.

GMP: lineage-, sca1lo, ckit+ CD41-, CD16/32+, CD105-.

EryP: lineage-, sca1lo, ckit+, CD41-, CD16/32-, CD105+.

Percentages are based on total live cell count.

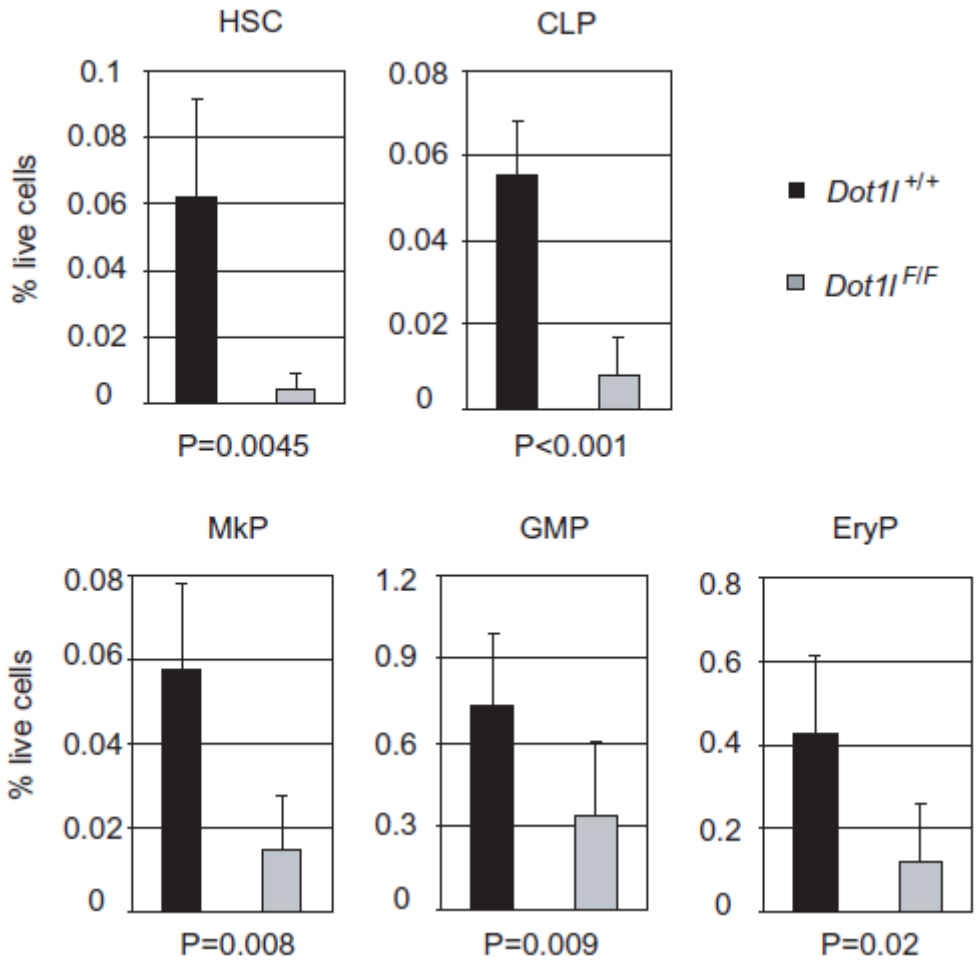

Figure 2.7. Bar graph of population frequencies as defined in Figure 2.6. *Dot1l* deletion led to a statistically significant decrease in HSCs and progenitors in all three lineages. Percentages are based on total live cell count. Data represent mean and standard deviation.

Dot1l deletion leads to depletion of functional HSCs

In order to rule out the persistence of functional HSCs with altered cell surface markers, we performed competitive bone marrow transplantation experiments. The origin of cells can be traced by utilizing two different CD45

alleles. Recipient and competitive donor cells have CD45.1 allele, while control and experimental donor cells have CD45.2 allele. Relative contribution of the donor cells in reconstituting the bone marrow can be examined by staining for CD45 expressing peripheral leukocytes. Dot1l+/+ or Dot1lF/F mice (CD45.2+) were injected with tamoxifen and bone marrow were harvested three days later. These cells were mixed with competitor cells (CD45.1+) at 1:1 or 3:1 ratio and injected via tail vein into lethally irradiated (900 rad) recipient mice (Figure 2.8).

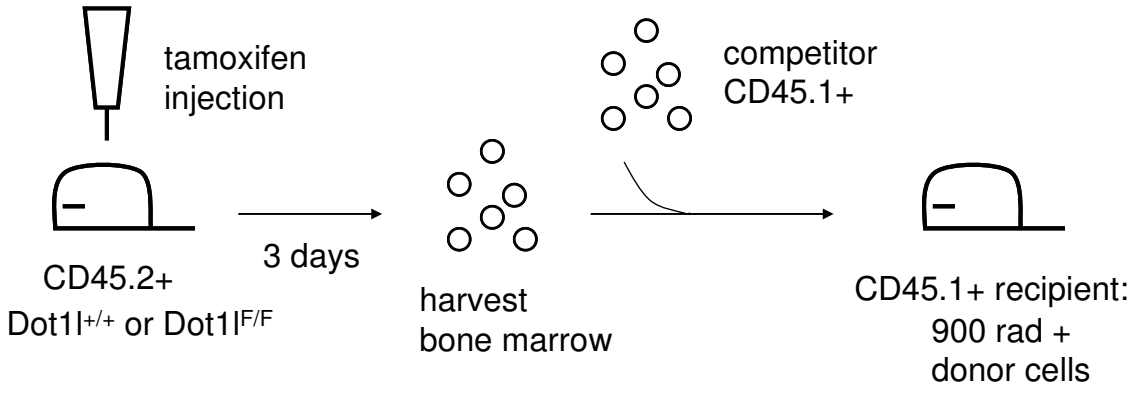

Figure 2.8. Schematic of competitive bone marrow transplantation experiment. CD45.2+ *Dot1l*$^{+/+}$ or *Dot1l*$^{F/F}$ mice were injected with tamoxifen and bone marrow cells were harvested and mixed with CD45.1+ competitors at 1:1 or 3:1 ratio. The mixture was transplanted into lethally irradiated CD45.1+ recipient.

Contribution of CD45.2+ cells were examined in myeloid, B lymphoid, and T lymphoid lineages (Figure 2.9). Peripheral blood was collected on indicated weeks after transplantation. There were markedly decreased contributions of *Dot1l*$^{F/F}$ CD45.2+ cells to the myeloid, B lymphoid, and T lymphoid lineages at all time points examined.

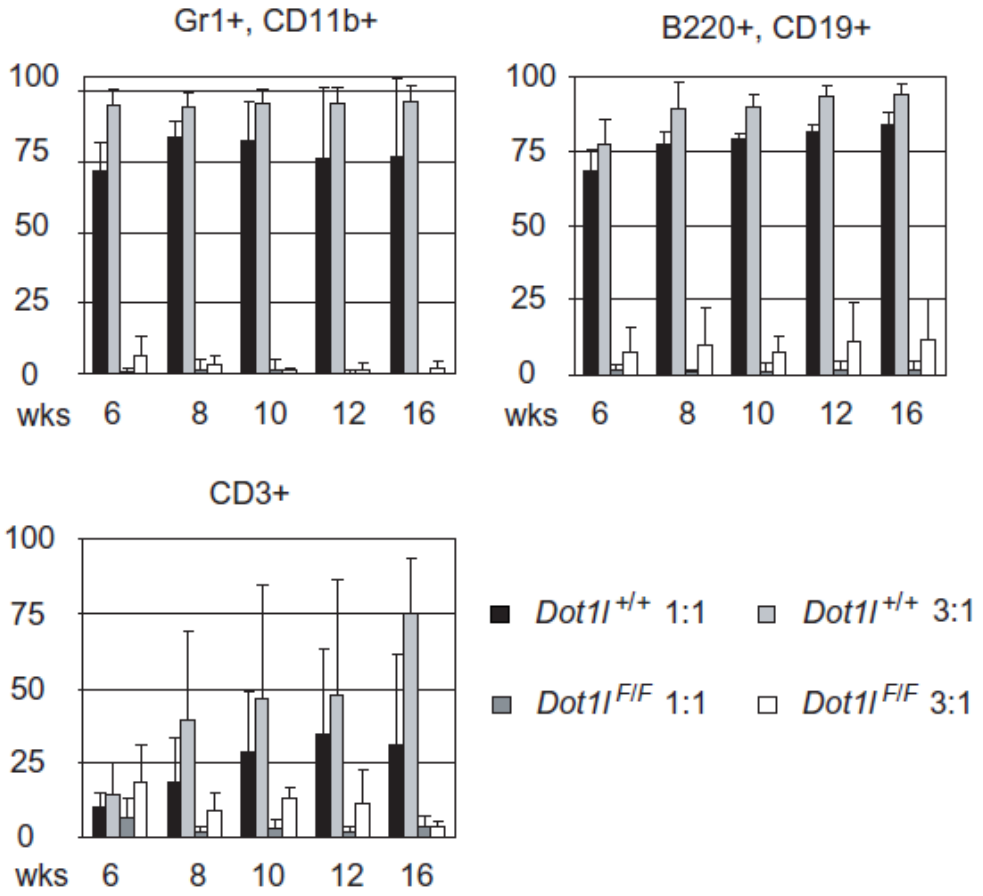

Figure 2.9. Bar graph of CD45.2+ cells in peripheral blood. Peripheral blood was stained for myeloid (Gr1+, CD11b+), B lymphoid (B220+, CD19+), and T lymphoid (CD3+) cells. Blood was collected from recipients on indicated weeks after transplantation. *Dot1l*$^{F/F}$ cells minimally constituted recipient peripheral blood. Data represent mean and standard deviation.

Bone marrow and thymus were harvested 16 weeks after transplantation and were similarly examined for contribution of CD45.2+ cells into the HSC, myeloid, B lymphoid, and developing T lymphoid compartments. Even at a 3:1 ratio, *Dot1l*$^{F/F}$ CD45.2+ cells minimally contributed to recipients' hematopoietic system (Figures 2.10 and 2.11). These results showed that Dot1l is required for functional HSC activity.

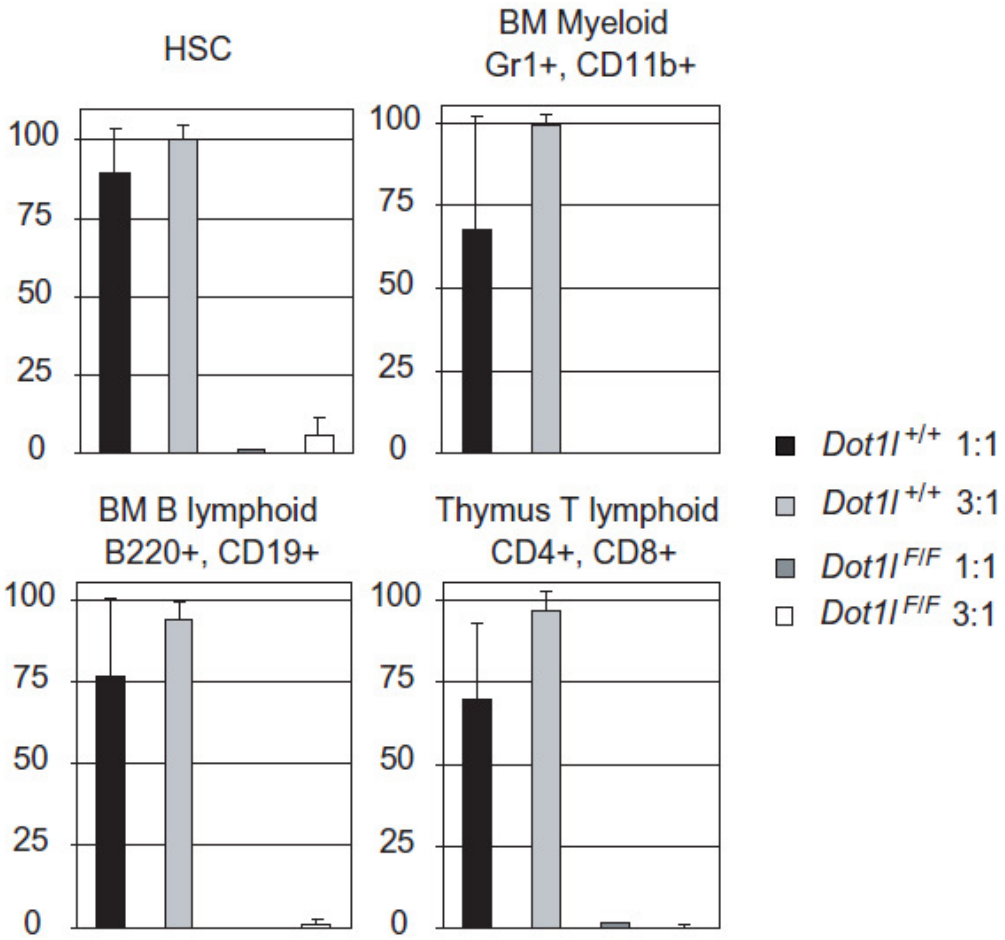

Figure 2.10. Bar graph of CD45.2+ cells in recipient bone marrow and thymus 16 weeks after transplantation. Cells were stained for HSCs (lineage-, sca1+, ckit+, CD48-, CD150+), myeloid (Gr1+, CD11b+), B lymphoid (B220+, CD19+) and developing T cells (CD4+, CD8+). Even at 3:1 ratio, *Dot1l*$^{F/F}$ cells failed to reconstitute recipient hematopoietic system. Data represent mean and standard deviation.

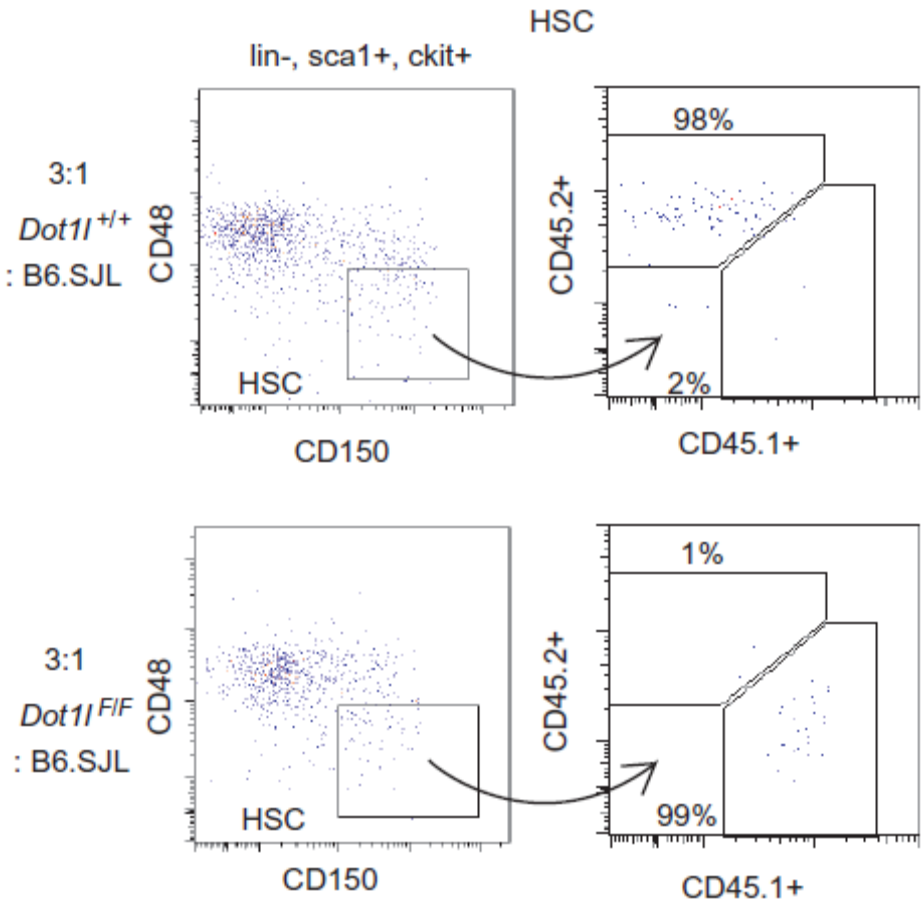

Figure 2.11. Staining profile of recipient HSCs (lineage-, sca1+, ckit+, CD48-, CD150+) 16 weeks after transplantation. Percentages are based on HSC gate. *Dot1l* lacking donor cells did not reconstitute recipient long-term HSCs.

Defect of HSCs after *Dot1l* deletion is cell-autonomous

After observing defects in *Dot1l* lacking HSCs, we examined if these defects were mediated in a cell-autonomous manner. Given that our mouse model led to excision of *Dot1l* from all cells through the ubiquitously expressed CreER, it is necessary to distinguish if the defects in HSCs are due to HSCs themselves or due to defects in stroma.

In order to study this, mixed bone marrow transplantation was performed without prior tamoxifen injection. CD45.2+ *Dot1l*$^{+/+}$ or *Dot1l*$^{F/F}$ bone marrow cells were transplanted with wild type CD45.1+ competitive cells at 1:1 ratio into lethally irradiated (900 rad) congenic CD45.1+ recipients. This created a condition in which Dot1l could be inactivated only in the donor-derived cohort of CD45.2+ cells in the presence of wild-type competitors and in a wild-type microenvironment. After measuring CD45.1/2 chimerism 8 weeks after transplantation, recipient mice were injected with tamoxifen (Figure 2.12). Peripheral blood was collected on indicated weeks after the tamoxifen injection to assess changes in CD45.1/2 chimerism. If the defects of Dot1l lacking HSCs were cell autonomous, contribution of Dot1l$^{F/F}$ CD45.2+ cells will decrease in peripheral blood, while if the HSC defects were due to stroma defects, Dot1l$^{F/F}$ CD45.2+ cells will continue to function in wild type stroma environment.

Injection of tamoxifen led to the rapid loss of CD45.2+ cells in all three lineages examined (Figure 2.13), indicating that defects in *Dot1l* lacking HSCs were cell-autonomous. The loss was particularly rapid and pronounced for the short-lived myeloid cells, which became profoundly depleted only two weeks after

tamoxifen injection. Examination of bone marrow HSCs, myeloid cells, B cells, and thymic T cells 16 weeks after the tamoxifen injection showed minimal contribution from Dot1l$^{F/F}$ CD45.2+ cells (Figure 2.14). These results showed that *Dot1l* deletion led to the loss of functional HSCs via cell-autonomous mechanisms.

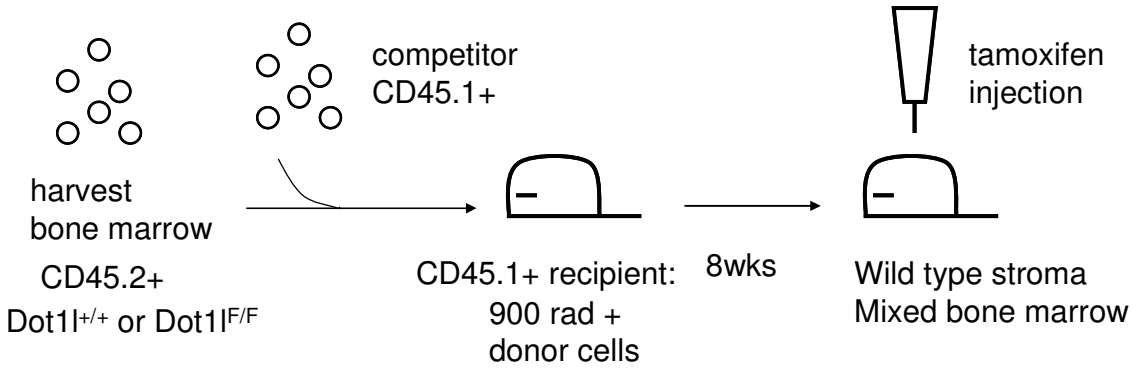

Figure 2.12. Schematic of bone marrow transplantation experiment for examining cell-autonomous HSC defect. CD45.2+ *Dot1l*$^{+/+}$ or *Dot1l*$^{F/F}$ cells and CD45.1+ competitors were mixed at 1:1 ratio and transplanted into lethally irradiated (900 rad) CD45.1+ recipients. Once bone marrow was reconstituted 8 weeks after transplantation, recipients were injected with tamoxifen.

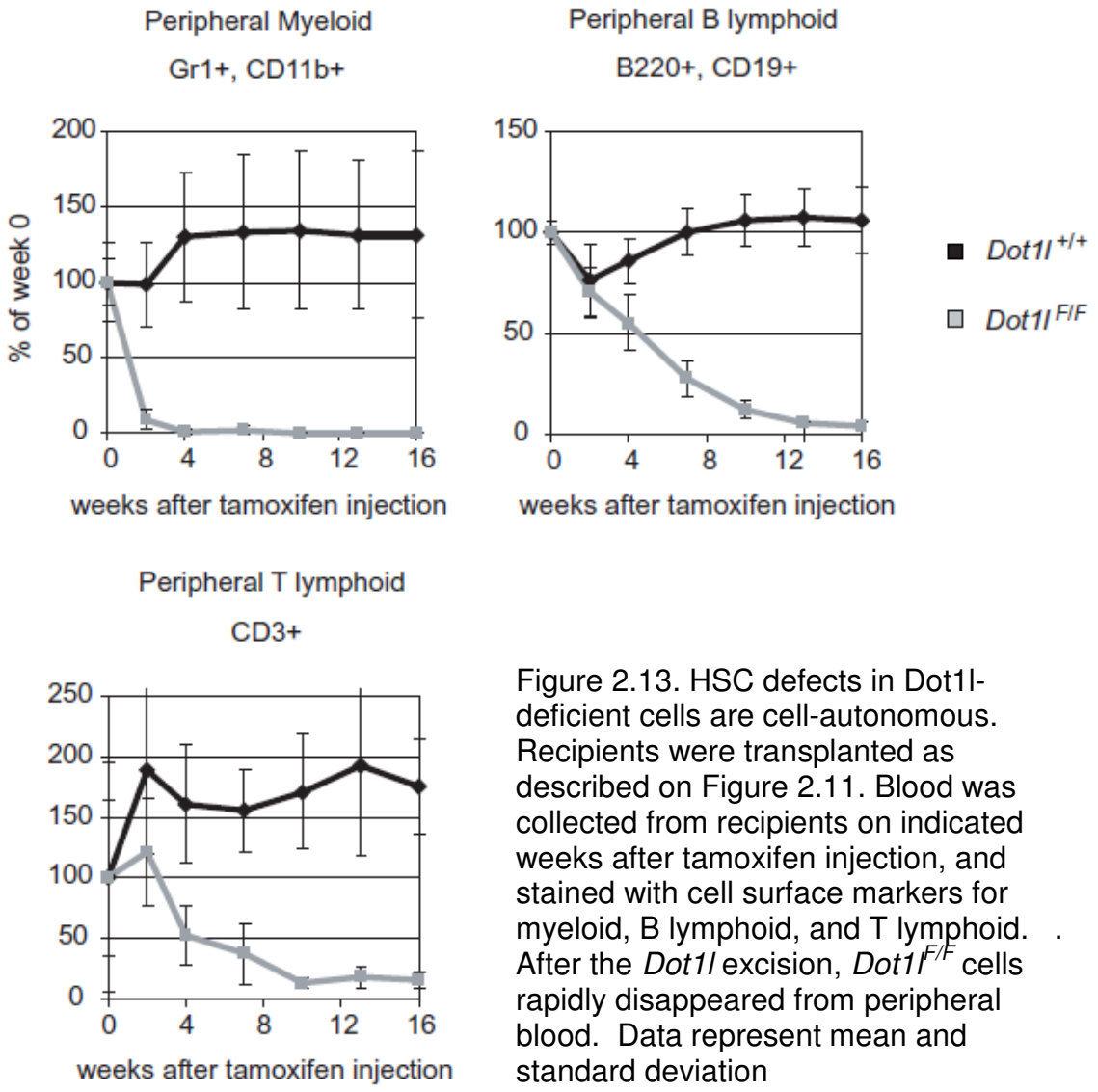

Figure 2.13. HSC defects in Dot1l-deficient cells are cell-autonomous. Recipients were transplanted as described on Figure 2.11. Blood was collected from recipients on indicated weeks after tamoxifen injection, and stained with cell surface markers for myeloid, B lymphoid, and T lymphoid. . After the *Dot1l* excision, *Dot1l*$^{F/F}$ cells rapidly disappeared from peripheral blood. Data represent mean and standard deviation

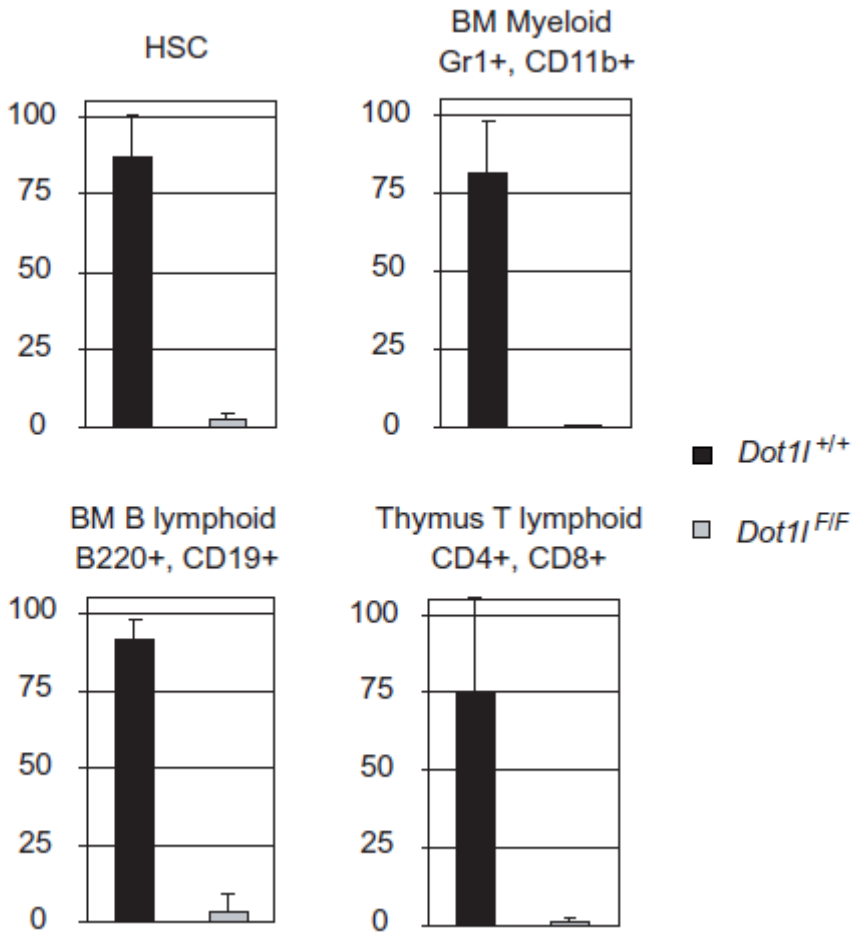

Figure 2.14. Bar graph of bone marrow and thymus reconstitution by CD45.2+ cells 16 weeks after tamoxifen injection. *Dot1l*$^{F/F}$ cells minimally remained in the recipients. Data represent mean and standard deviation.

CHAPTER III

The role of Dot1l in MLL fusion protein-mediated leukemogenesis

Because of the previous connection between Dot1l and *MLL* translocation leukemia, we examined further the role of Dot1l in MLL fusion protein-mediated leukemogenesis. Studies show a strong correlation between H3K4 methylation marks by MLL and H3K79 methylation marks by Dot1l at important MLL fusion protein downstream target loci (Krivtsov et al., 2008). This correlation has functional consequences since the loss of H3K79 methylation at target gene loci leads to decreased expression (Krivtsov et al., 2008; Monroe et al., 2010). Furthermore, loss of MLL fusion protein by conditional MLL-ENL-ER leads to decreased H3K79 methylation in the target gene loci (Milne et al., 2005). Our studies in normal HSCs also showed that Dot1l was required for stem cells, and we wanted to know if Dot1l is required for leukemia initiating cells (LICs) as well. Based on these studies, we examined in detail if Dot1l is required for *MLL* translocation leukemia and if this requirement for leukemia is universal or limited to MLL fusion oncogenes.

Materials and Methods

Dot1l excision

For *in vitro* experiments, 4-OHT (Sigma H7904) was used for *Dot1l* excision. 4-OHT was dissolved in 100% ethanol (EtOH) at 1mM stock solution, and equivalent volume of EtOH was used as control for 4-OHT treatment.

Cell culture

All cells were cultured in Iscove's Modified Dulbecco's Medium (Invitrogen 12440061) with 10ng/ml of IL3 (R & D Systems) and 1% penicillin/ streptomycin (P/S, Invitrogen 15140122). For cells with neomycin resistance gene, 1mg/ml G418 (Invitrogen 10131035) was added.

Plasmids, Retroviral Transductions and CFU Assay

Plasmids used for retrovirus generation were based on the Murine Stem Cell Virus (MSCV) vector (Clontech) derived from the murine embryonic stem cell virus (Grez et al., 1990; Hawley et al., 1994). The MSCVneo vector has a neomycin resistance gene, and the MigR1 vector has an internal ribosomal entry site followed by the GFP coding sequence for selection of transduced cells with either G418 or GFP, respectively. Retroviruses were generated by transfecting MigR1-MLL-AF9, MigR1-E2A-HLF, MigR1-Hoxa9, MigR1-Meis1, MSCVneo-HA-Dot1l or methyltransferase mutant Dot1l constructs (Kroon et al., 1998; Monroe et al., 2010; Muntean et al., 2008; Okada et al., 2005) into Plat-E cell line (Morita et al., 2000) with Fugene 6 (Roche). Fresh viral supernatants were used for all

experiments. Bone marrow cells were isolated from 6-8 week old mice 4 days after 150μg/g 5-fluoruracil (5-FU, Sigma) injection. 5-FU injection kills more differentiated bone marrow cells that go through cell division while low-cycling stem cells are minimally affected (Kopp et al., 2005). Hence, injection with 5-FU enriches for stem cells when harvesting bone marrow. Bone marrow cells were collected by flushing the femur and tibia with IMDM media (Invitrogen) with 1% P/S and 2% FBS (Stemcell Technologies) in a 27.5G needle. The harvested cells were placed overnight in 1% P/S, 10ng/ml IL3, IL6, and 100ng/ml SCF (R & D Systems), 15% FBS (Stemcell Technologies), and IMDM media (Invitrogen). Leaving the cells overnight in culture allows more differentiated cells to attach to flask and further enrich for stem cells in the supernatant. The cells were transduced twice with retrovirus by spinoculation at 3200 rpm for 90 minutes at room temperature. 2-3 days later, transduced cells were plated in Methocult media (Stem Cell Technologies, M3234) with 1% P/S, 10ng/ml IL3, IL6, GM-CSF, 100ng/ml SCF, 5nM 4-OHT or EtOH, and 1mg/ml G418 (Invitrogen 10131035). Colonies were scored 7-10 days after plating for three rounds. In the final round, colonies were stained with 0.1% p-iodonitrotetrazolium violet (INT, Sigma, 58030) for visualization.

Cell Growth, Cell Cycle, and Apoptosis Assays

Cell growth was assessed by the CellTiter-Glo assay (Promega G7572). The assay quantifies ATP levels in cell culture, which is a proxy for metabolically active live cells. Cells were treated with either 4-OHT or EtOH as control for

three days for the excision of *Dot1l*, and CellTiter-Glo assay was performed every day per manufacturer's instructions. Luminescence was measured by M5 microplate reader (Molecular Devices).

Similarly, 4 days after treatment with 4-OHT or ethanol, cells were incubated with 10ng/ml propidium iodide (Invitrogen P3566) and 100ng/ml RNase A (5 Prime 2500130) in standard buffer for 30 minutes at 37^{o}C for cell cycle analysis or stained with 1µg/ml DAPI (Sigma 9542) and Annexin V-APC (eBiosciences BMS306APC/100) in Annexin V Binding Buffer (Biolegend 422201) for 15 minutes at room temperature for apoptosis assay. Samples were run on LSRII (BD biosciences) and analyzed with Flowjo (Treestar).

RNA extraction, cDNA generation, and Quantitative PCR (qPCR)

RNA was extracted from cells after 4 days of 4-OHT or EtOH treatment using TRIzol Reagent (Invitrogen 15596026) and isopropanol precipitation. RNA was quantified with an Ultraspec 2100 (GE Healthcare) and 2-4 µg of RNA was converted to cDNA using SuperScript II (Invitrogen 18064022) according to the manufacturer's instructions. For qPCR reaction, SYBR (4367659) and Taqman mastermix (4304437) were used for duplex DNA and Fam fluorophore detection, respectively. An ABI7500 machine was used for reading qPCR plates.

Gene	Detector	Primers
5S rRNA	SYBR	F: TCTACGGCCATACCACCCTGA R: GCCTACAGCACCCGGTATTCC

HA-Dot1l	SYBR	F: GCCACCATGTACCCCTACGACGTG R: GATTTCCTCGCAGACCCACCGGAT
Hoxa9	Fam	Applied Biosystems (Mm00439364_m1)
Meis1	Fam	Applied Biosystems (Mm00487664_m1)

Table 3.1 qPCR primers.

Protein extraction and Western blot

Whole cell lysate samples were prepared by directly resuspending 500,000 cells in 100µl of Tris-Glycine SDS Sample Buffer (Novex LC2676) with 10% beta-mercaptoethanol (Sigma). Samples were then sonicated for 15 minutes (Bioruptor, Diagenode) and incubated at 95^{o}C for 5 minutes. Samples were run on 4-20% Tris-Glycine SDS page gels (Novex EC60285BOX).

Results

The MLL-AF9 oncogene requires Dot1l for transformation

Since the loss of Dot1l led to the loss of normal HSCs, we examined if LICs were also generally lost with *Dot1l* excision. Because Dot1l has been implicated in leukemia with *MLL* translocation, we wanted to know if the potential anti-leukemic effects of Dot1l loss are limited to *MLL* translocation alone or applicable to leukemia with other molecular signatures. Hence, we chose three different oncogenes and examined if Dot1l-deficient bone marrow cells could be

transformed. We selected MLL-AF9, an *MLL* translocation oncogene, Hoxa9/Meis1 proteins which are downstream targets of *MLL* translocation, and E2A-HLF, an oncogene unrelated to *MLL* translocation, for examination of transformation by colony forming unit (CFU) assay. CFU assay results are closely correlated with leukemogenesis *in vivo* (Lavau et al., 1997), and are a useful tool for studying leukemogenesis *in vitro*.

Bone marrow cells were harvested after 5-fluorouracil (5-FU) injection for HSC enrichment, transduced with oncogenes or MigR1 vector control, and plated on methylcellulose media in the presence of either 4-OHT for *Dot1l* excision or EtOH as control. Cells were replated every 7-10 days for three rounds and resulting colonies were counted and stained for visualization (Figure 3.1).

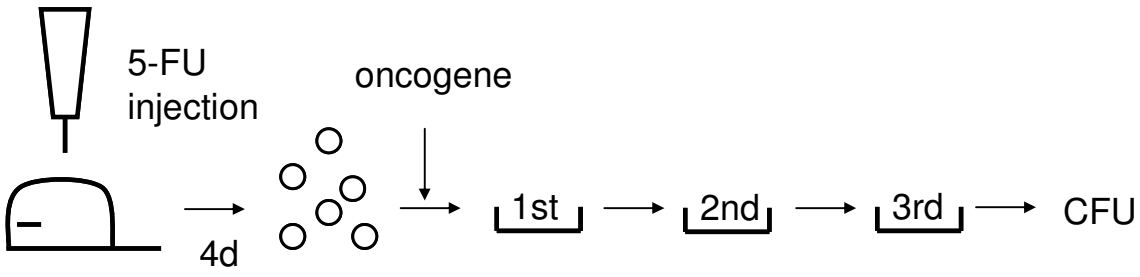

Figure 3.1. Schematic of colony forming unit (CFU) assay.

After the second round, cells were harvested and genomic DNA was extracted for checking excision efficiency. Genotyping showed high efficiency of *Dot1l* excision with 4-OHT treatment (Figure 3.2). There was some baseline excision occurring in Dot1l$^{F/F}$ cells treated with EtOH. However, these cells were

still able to form colonies (Figure 3.3) and H3K79 methylation was present in comparable levels to Dot1l$^{+/+}$ cells (Figure 3.7).

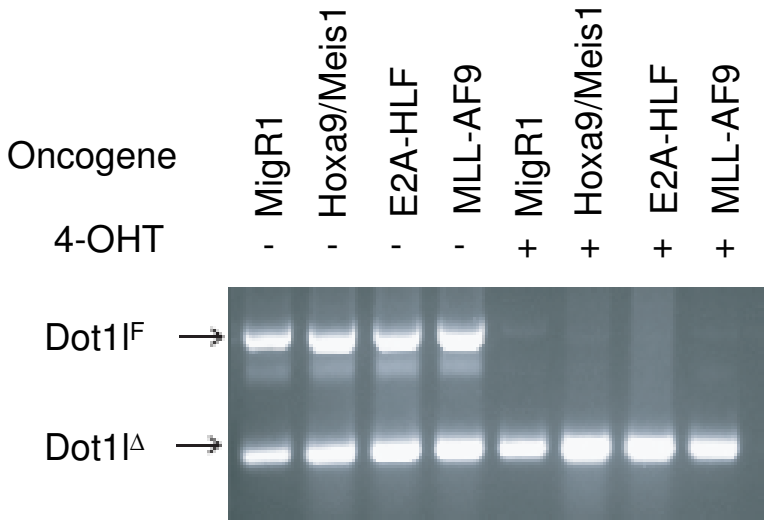

Figure 3.2. Genotyping of transduced cells after the second round. PCR reaction showed high excision efficiency with 4-OHT treatment in all cells. There was baseline excision (Dot1l$^{\Delta}$ allele in 4-OHT untreated cells), but this did not interfere with experiments.

While Hoxa9/Meis1 and E2A-HLF transformed cells were able to form colonies even upon *Dot1l* excision, MLL-AF9 transformed cells were unable to form colonies (Figures 3.3 and 3.4). MLL-AF9 transformed cells with 4-OHT treatment had colony counts on par with MigR1 control (3.4), and whole plate examination with INT dye showed very few staining colonies (3.3). Even after being grown in liquid culture for more than 8 weeks, MLL-AF9 transformed cells continued to require Dot1l for colony formation (Figures 3.5 and 3.6). These results suggested that Dot1l is selectively required for oncogenic transformation by MLL-AF9, but not Hoxa9/Meis1 or E2A-HLF.

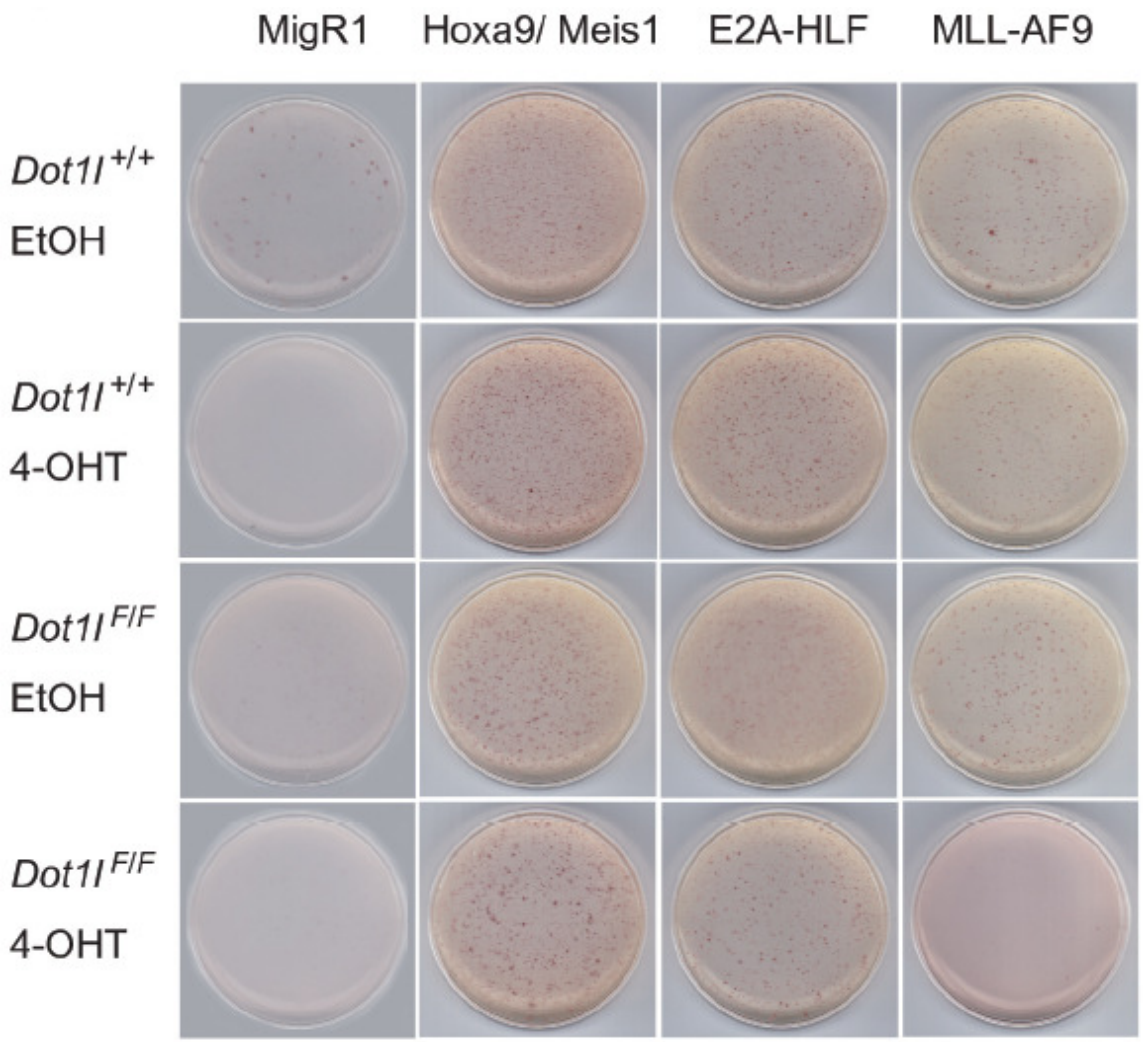

Figure 3.3. Colony formation on methocult plates. *Dot1l*$^{F/F}$ MLL-AF9 cells treated with 4-OHT failed to form colonies. INT stain of plates at final round.

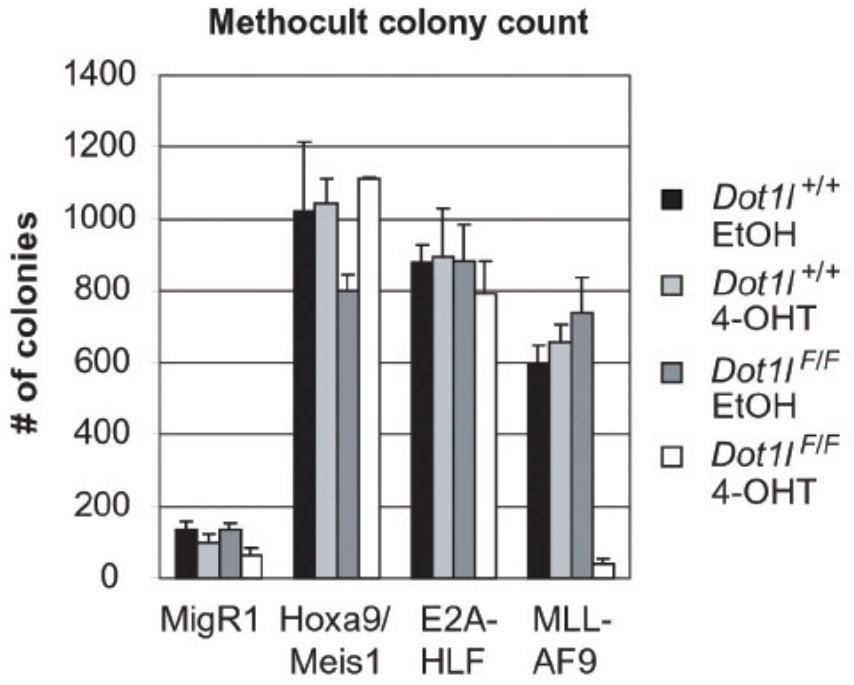

Figure 3.4. Bar graph of colony count at final round. Data represent mean and standard deviation. Dot1l is required for transformation by MLL-AF9 but not by Hoxa9/Meis1 and E2A-HLF

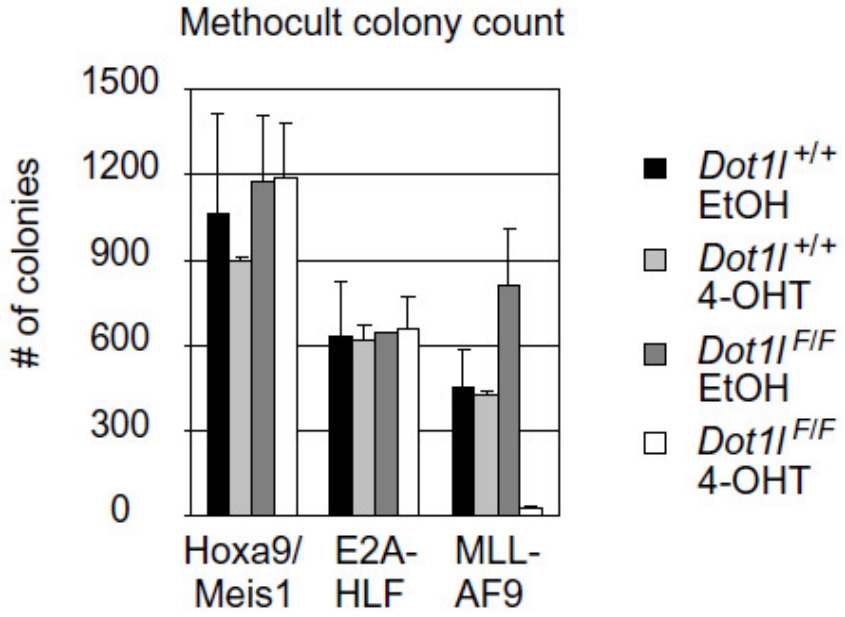

Figure 3.5. Bar graph of colony count with cells grown in liquid culture for >8 weeks. *Dot1l*$^{F/F}$ MLL-AF9 cells treated with 4-OHT failed to form colonies even after established transformation. Data represent mean and standard deviation.

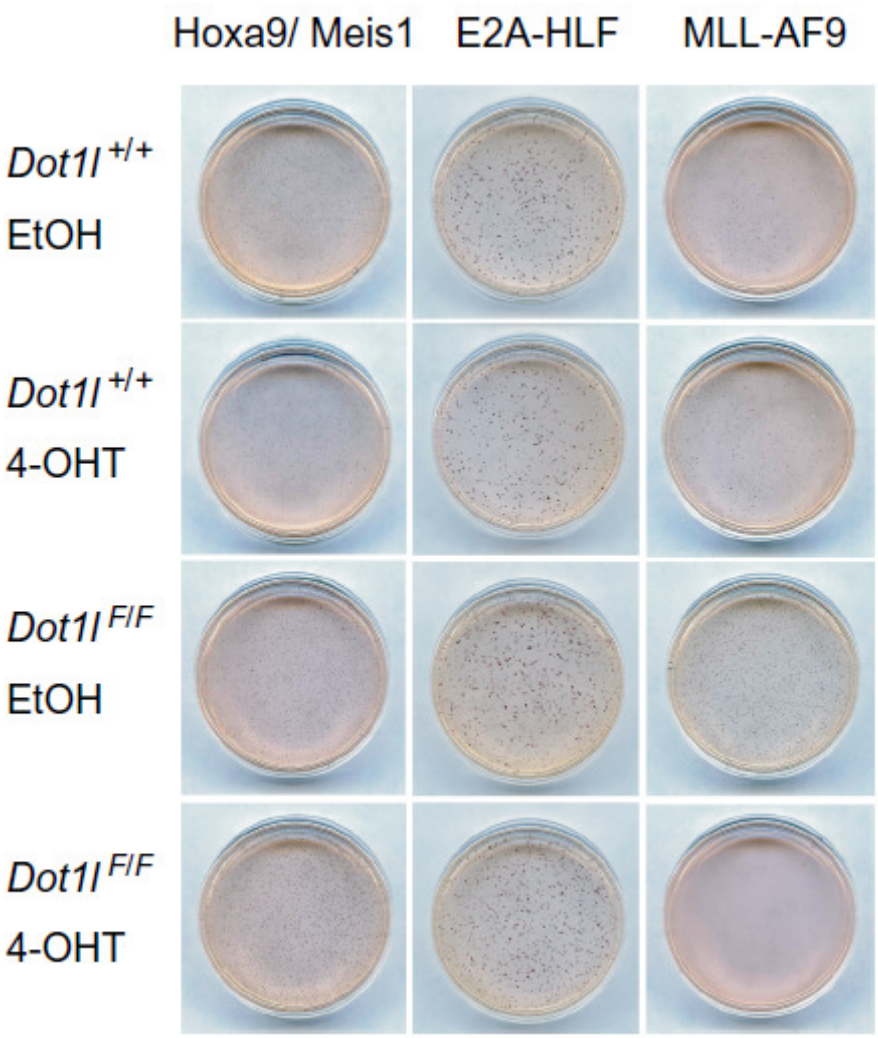

Figure 3.6. Colony formation on methocult plates. Dot1l is required for colony formation by MLL-AF9 cells even after established transformation. INT stain of plates.

Dot1l deletion leads to a cell cycle defect in MLL-AF9 transduced cells

We further examined the consequences of Dot1l loss in MLL-AF9 transformed cells in liquid culture. First, we confirmed that H3K79 methylation was abolished with Dot1l excision. Western blot after 4-OHT treatment of cells showed that H3K79me2 was comparably lost among all Dot1l$^{F/F}$ cell lines.

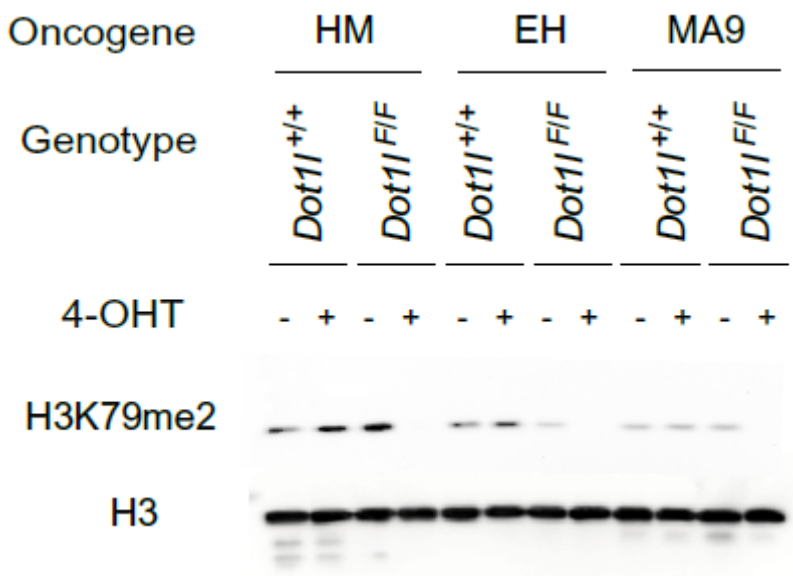

Figure 3.7. H3K79me2 western blot of Hoxa9/Meis1, E2A-HLF, and MLL-AF9 transformed cells. H3K79me2 western blot showed loss of methylation with 4-OHT treatment in all *Dot1l*$^{F/F}$ cell lines. Protein was harvested 4 days after EtOH or 4-OHT treatment. Histone 3 blot was used as loading control.

Next, we examined cell growth in liquid culture. Cells were treated with 4-OHT or EtOH for three days, and then moved to regular growth media. Cell toxicity was observed with prolonged culture in 4-OHT, and by day three *Dot1l* was reliably excised. In accordance with the CFU assay results, MLL-AF9 cells

stopped growing in liquid culture with 4-OHT treatment while Hoxa9/Meis1 and E2A-HLF cells continued to grow (Figure 3.8.). Cell growth was assessed with the CellTiter-Glo assay, which measures ATP levels and hence metabolically active live cells. The CellTiter-Glo assay was particularly useful compared to trypan blue staining and manual counting due to increased lightly staining cells, dead cells and debris. Also, technical and biological replicates were easy to obtain with the CellTiter-Glo assay, making the data more reliable.

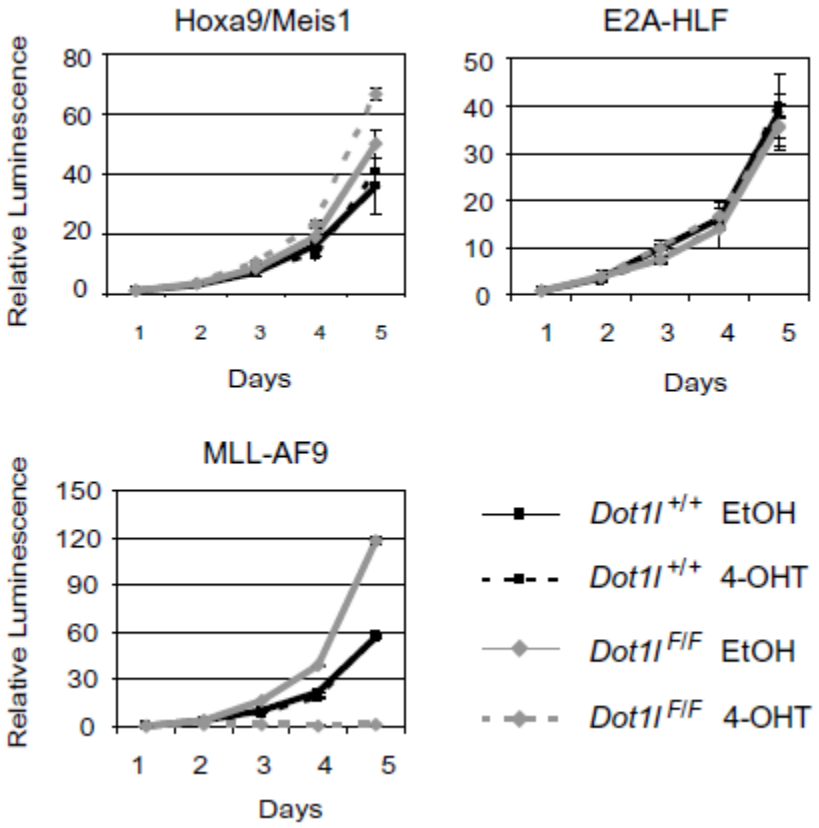

Figure 3.8. Loss of Dot1l leads to growth impairment for MLL-AF9 transformed cells but not for Hoxa9/Meis1 or E2A-HLF transformed cells. Cells were grown in culture for more than 8 weeks. Cell growth was measured by CellTiter-Glow assay with either ethanol (EtOH) as control or 4-OHT treatment for *Dot1l* excision. All values were normalized to day 1. Data represent mean and standard deviation.

Based on the liquid culture cell growth data, we picked several time points for examining the phenotype of Dot1l loss in more detail. First, the cell cycle was assessed using propidium iodide staining 1, 2, 3, and 4 days after 4-OHT treatment (Days 2, 3, 4, and 5 on growth curves) to identify the best time frame for further study. Propidium iodide is a DNA intercalating agent that can be used to quantify cell DNA content and hence its cell cycle stage (Crissman et al., 1976).

Cell cycle analysis using propidium iodide showed that there was a marked increase in G0-G1 phase in MLL-AF9 cells after *Dot1l* excision, while this effect was not present in Hoxa9/Meis1 or E2A-HLF cells (Figure 3.9 and 3.10). This suggested G1/S cell cycle arrest as the primary mechanism for decreased cell growth in MLL-AF9 cells. These data corroborate normal yolk sac cell data that show increases in G0-G1 as well (Feng et al., 2010) but are somewhat different from the embryonic stem cell data (Jones et al., 2008) that show increases in G2 phase. This difference in result is most likely due to different cell types.

The extent of G0-G1 block was greatest for MLL-AF9 transformed cells 4 days after treatment with 4-OHT. Further time points were not examined because cell splitting was necessary for some cell types, which might affect cell growth rate. From these data, day 4 was chosen for subsequent studies because the Dot1l loss phenotype was most pronounced.

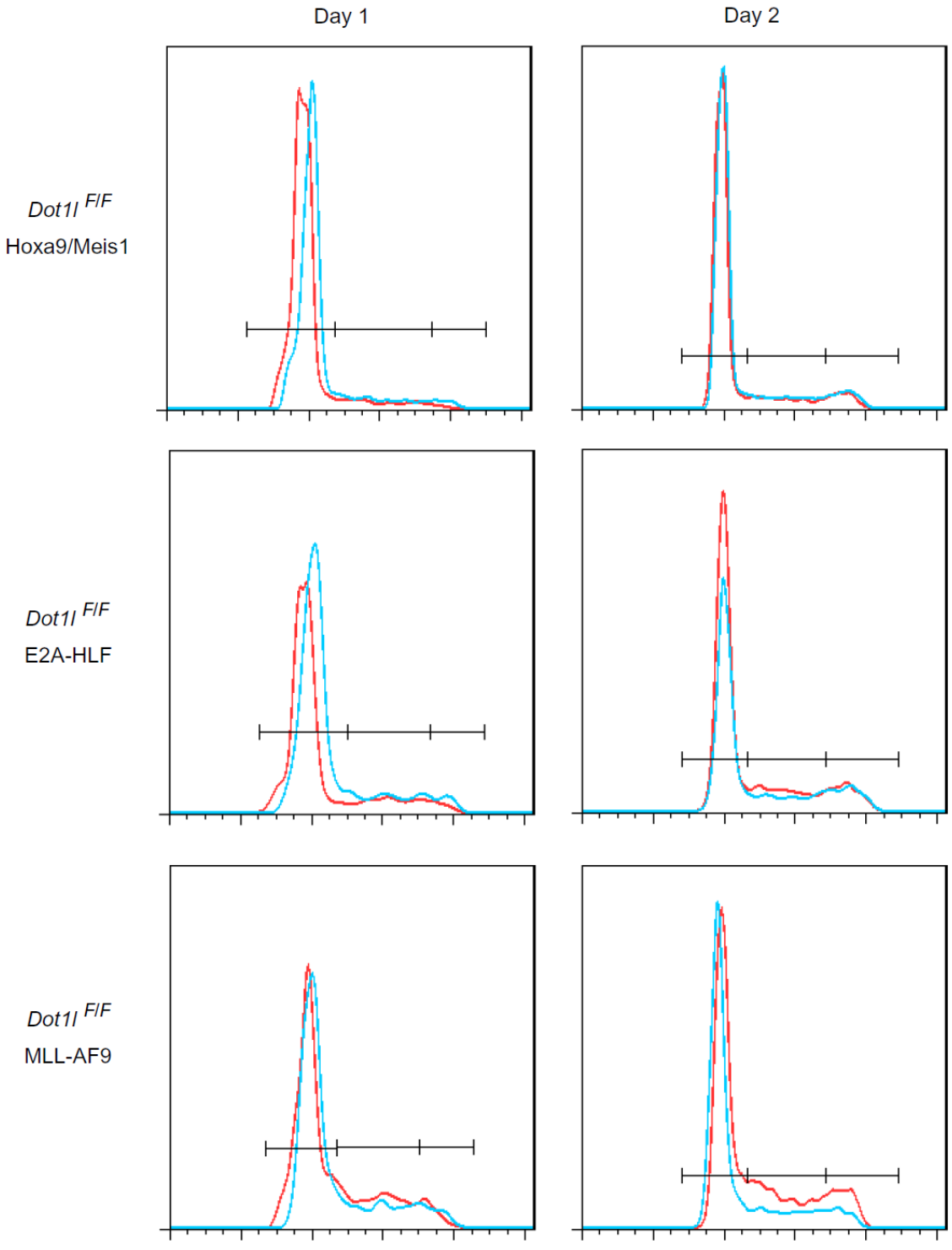
Day 1
Day 2
Dot1l F/F
Hoxa9/Meis1
Dot1l F/F
E2A-HLF
Dot1l F/F
MLL-AF9

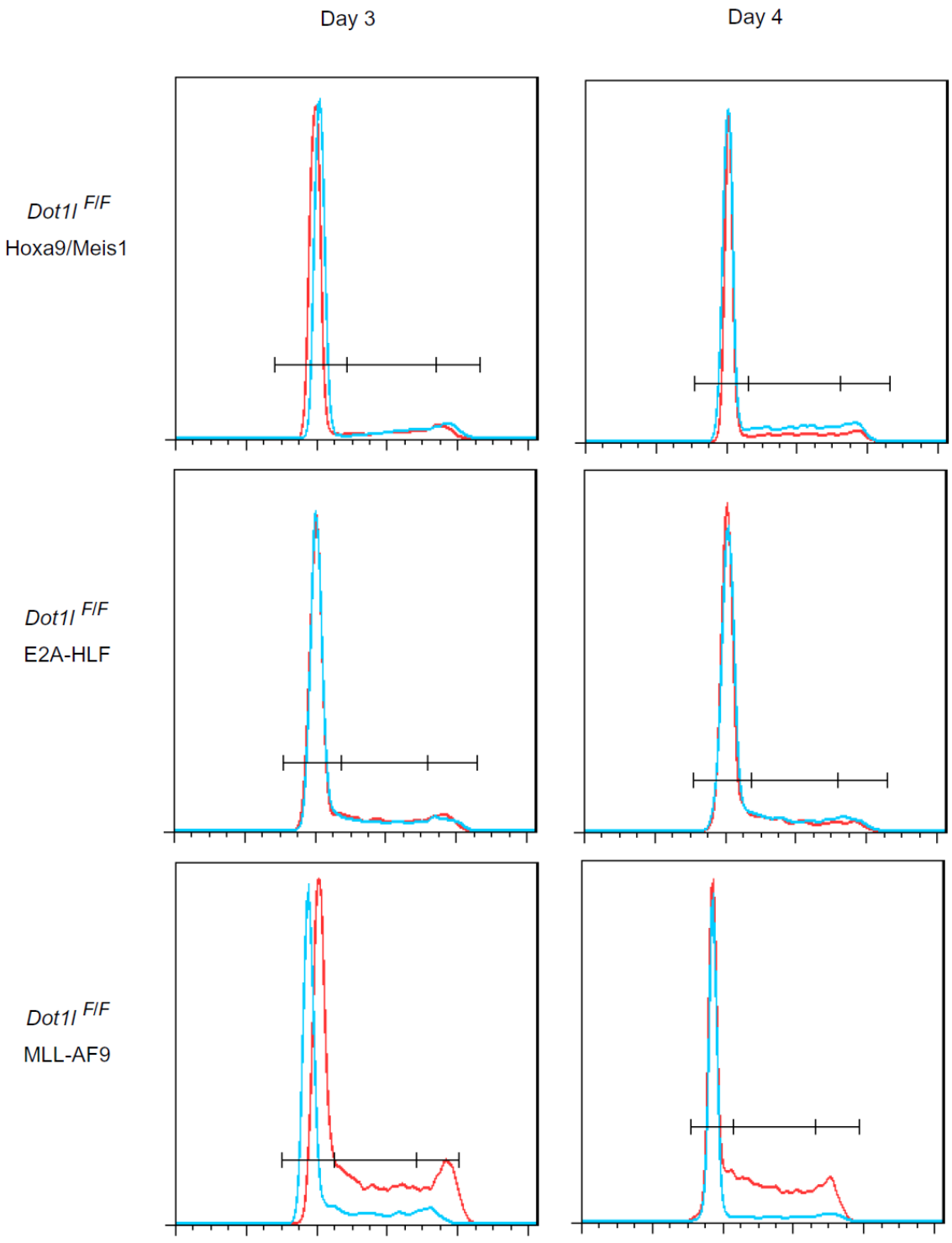

Figure 3.9. Time course of cell cycle analysis. EtOH 4-OHT Cells were treated with 4-OHT for *Dot1l* excision or EtOH and 3 days later moved to regular growth media. Propidium iodide staining was performed every day for the following 4 days to select the time point of maximal effect.

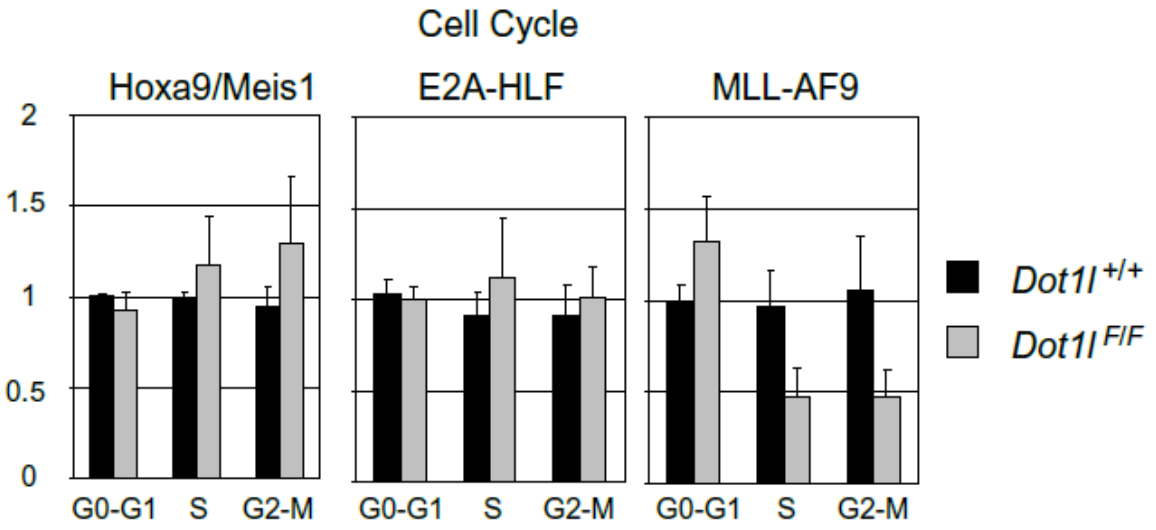

Figure 3.10. Quantification of cell cycle. Cells were stained with propidium iodide 4 days after EtOH or 4-OHT treatment. Values shown are ratio of 4-OHT treatment over EtOH treatment for respective cell lines. *Dot1l*$^{F/F}$ MLL-AF9 cell line showed increase in G0-G1 and decrease in S and G2-M phases with 4-OHT treatment. Data represent mean and standard deviation.

We then examined apoptosis of cells with *Dot1l* excision. From previous reports (Chang et al., 2010; Feng et al., 2010; Jones et al., 2008) we expected to see an increase in apoptosis. However, we noticed an increase in apoptosis from 4-OHT treatment alone for MLL-AF9 transformed cells and variably in E2A-HLF cells (Figure 3.11). Notably, this effect was most prominent in MLL-AF9 transformed cells in both Dot1$^{F/F}$ and Dot1l$^{+/+}$ cell lines compared to E2A-HLF and Hoxa9/Meis1 transformed cells. While the cause of the 4-OHT effect is not clear, it should be noted for future experimental designs that *MLL* translocation-containing leukemia may be more sensitive to 4-OHT treatment.

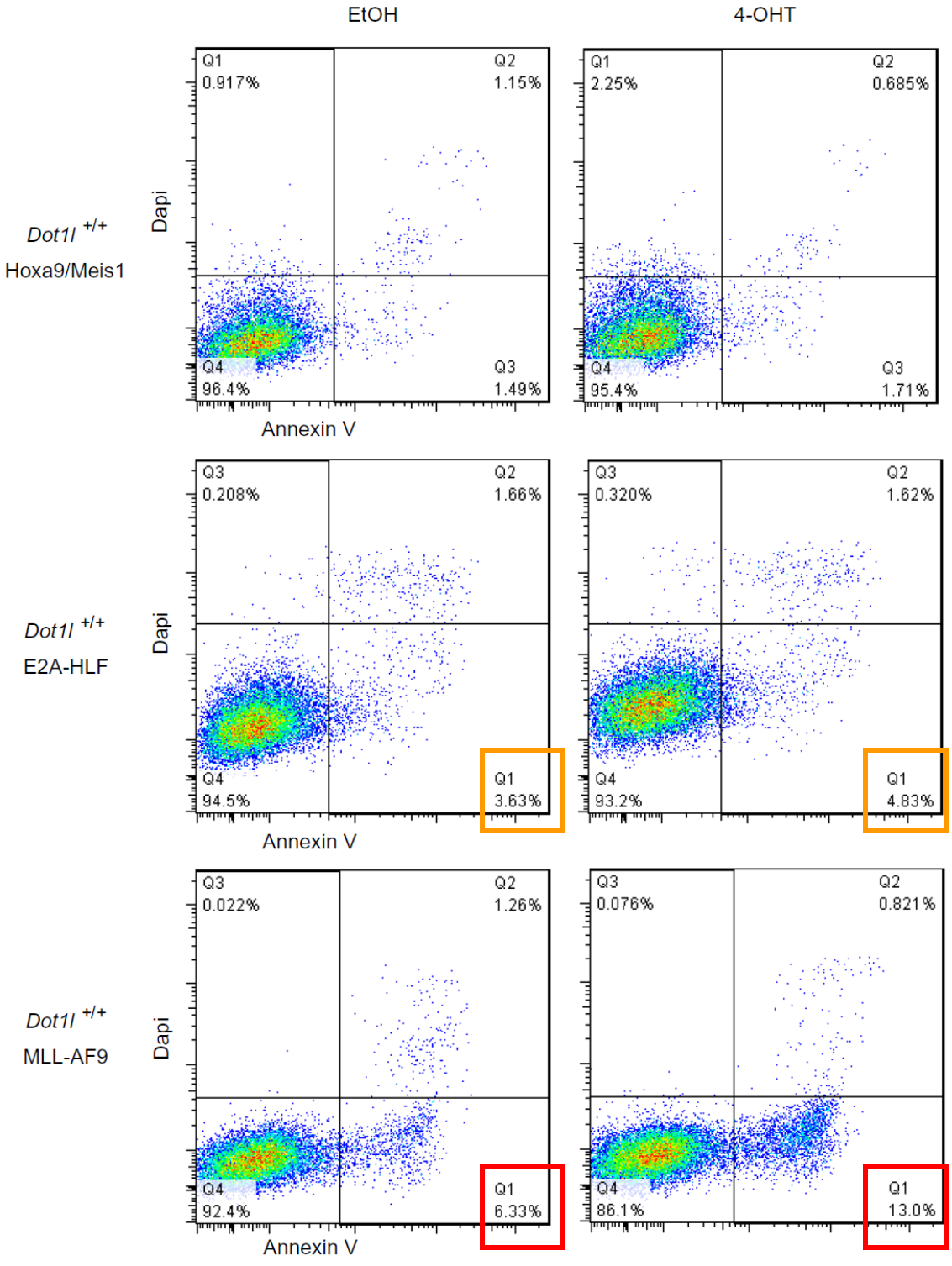
EtOH
4-OHT
Dot1l +/+
Hoxa9/Meis1
Dapi
Annexin V
Q1
0.917%
Q2
1.15%
Q4
96.4%
Q3
1.49%
Q1
2.25%
Q2
0.685%
Q4
95.4%
Q3
1.71%
Dot1l +/+
E2A-HLF
Q3
0.208%
Q2
1.66%
Q4
94.5%
Q1
3.63%
Q3
0.320%
Q2
1.62%
Q4
93.2%
Q1
4.83%
Dot1l +/+
MLL-AF9
Q3
0.022%
Q2
1.26%
Q4
92.4%
Q1
6.33%
Q3
0.076%
Q2
0.821%
Q4
86.1%
Q1
13.0%

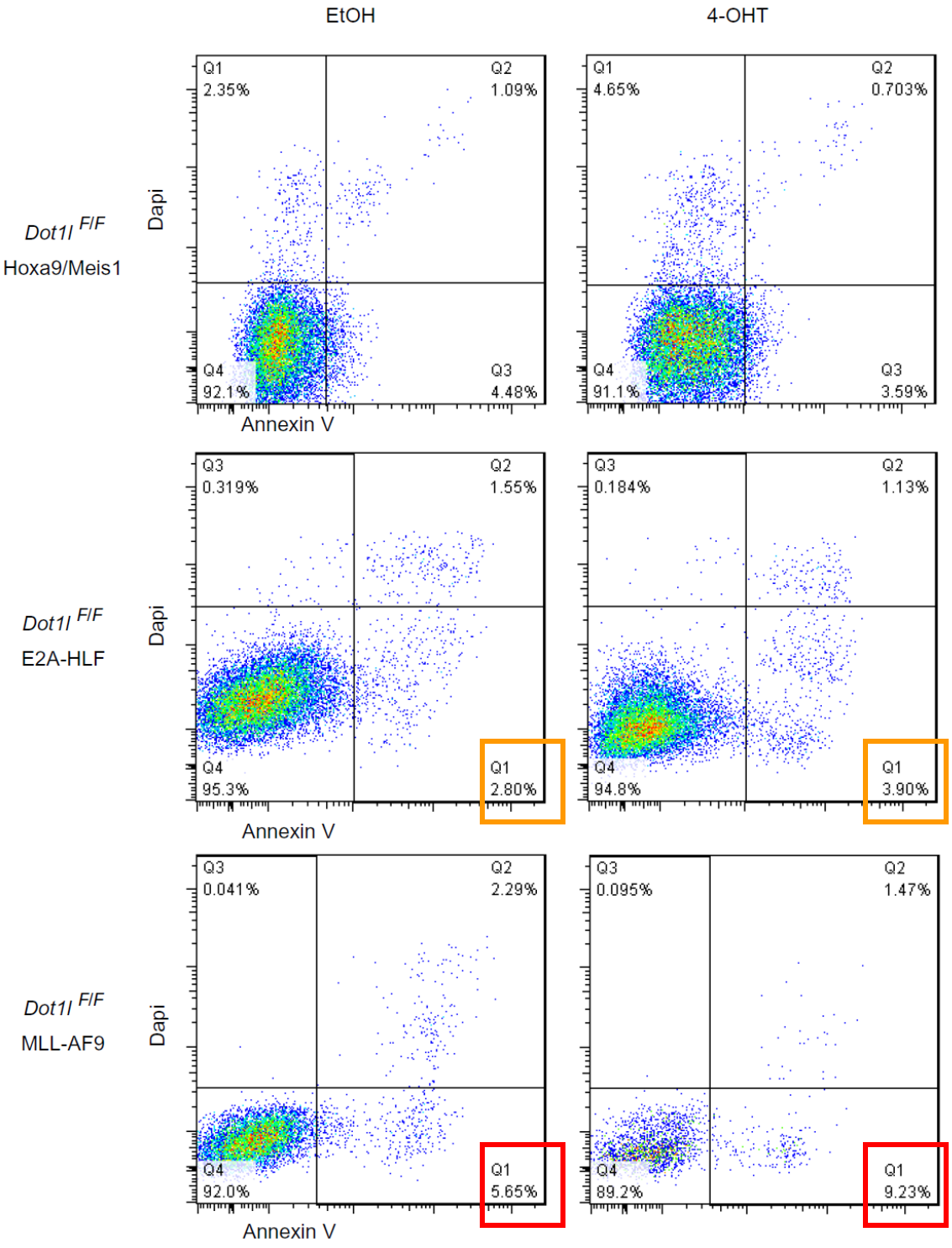

Figure 3.11. Annexin V staining of cell lines after *Dot1l* excision. There was almost doubling of Annexin V positive cells after 4-OHT treatment of MLL-AF9 transformed cells. For E2A-HLF cells the increase ranged from 25-40%. Hoxa9/Meis1 transformed cells were least affected.

The 4-OHT effect was taken into account by dividing the 4-OHT treatment over the EtOH treatment and comparing Dot1l$^{+/+}$ with Dot1l$^{F/F}$. The resulting ratios showed that there was no consistent change in apoptosis rate measured by annexin V staining (Figure 3.12).

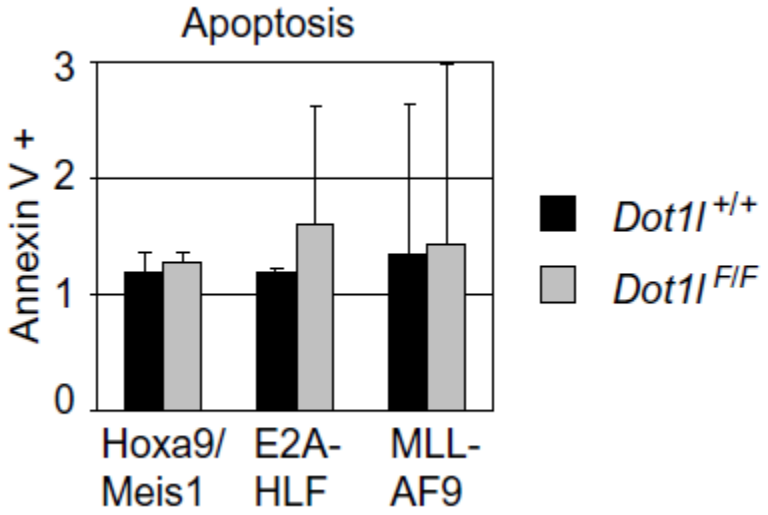

Figure 3.12. Annexin V staining for apoptosis assay. Cells were stained with annexin V 4 days after EtOH or 4-OHT treatment. Values shown are ratio of 4-OHT treatment over EtOH treatment for respective cell lines. There was no statistically significant change in apoptosis with *Dot1l* excision. Data represent mean and standard deviation.

We also examined if the expression of downstream targets of MLL-AF9 protein were affected by the loss of Dot1l. As reported from previous studies (Krivtsov et al., 2008; Monroe et al., 2010), qPCR showed loss of Dot1l in MLL-AF9 cells led to decreased expression of *Hoxa9* and *Meis1* (Figure 3.13), which are crucial for *MLL* translocation-mediated leukemia (Ayton and Cleary, 2003; Zeisig et al., 2004). Minimal changes in the gene expressions were noted in cells transformed by Hoxa9/Meis1 and E2A-HLF probably due to exogenous promoter driven

expression in Hoxa9/Meis1 cells and the already very low expression of Hoxa9 in E2A-HLF cells (E2A-HLF cells did not express detectable Meis1). In contrast, house-keeping genes such as *Beta actin* and *Gapdh* showed relatively stable expressions with *Dot1l* excision (Figure 3.13). These results showed that the loss of Dot1l in cells with MLL-AF9 led to cell cycle arrest and downregulation of key downstream targets, leading to failure of oncogenic transformation.

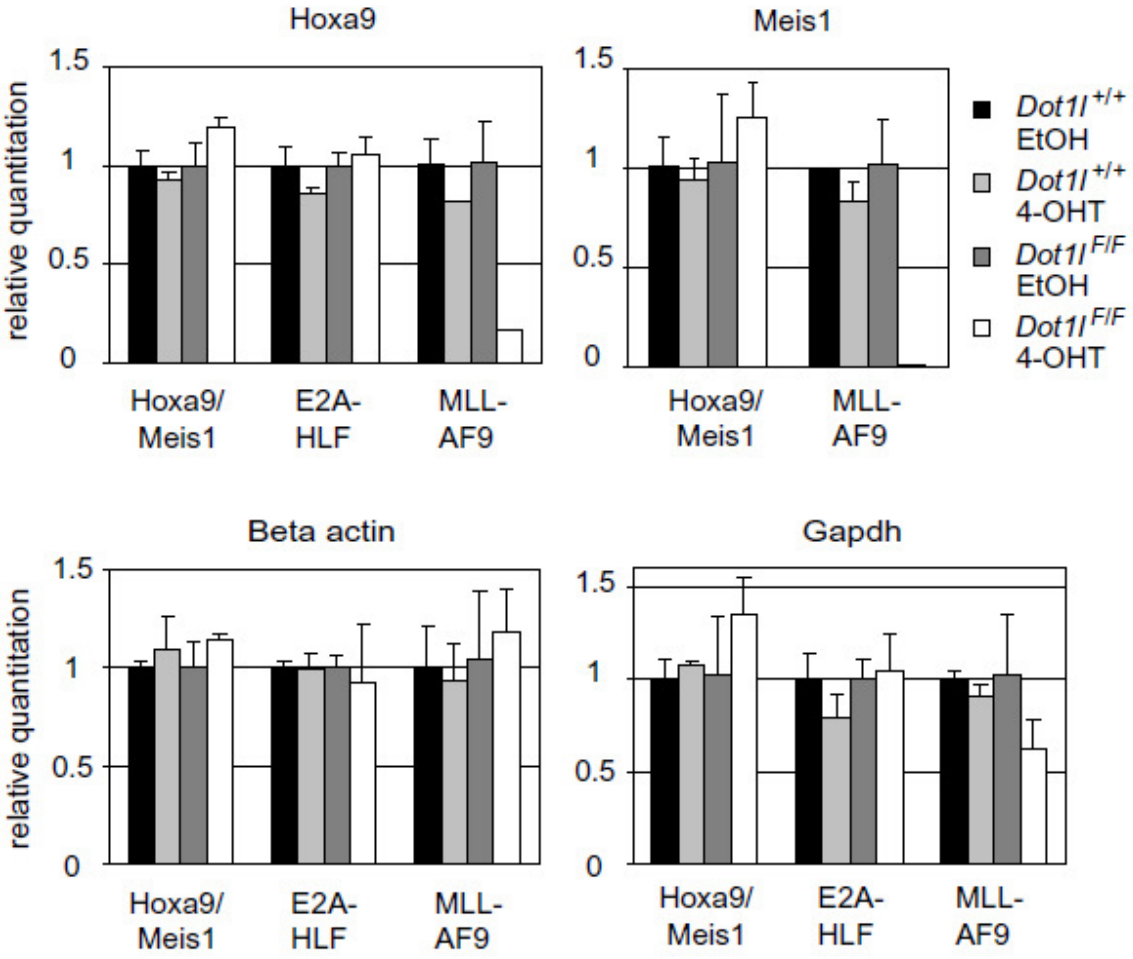

Figure 3.13. The loss of Dot1l leads to selective loss of critical downstream target gene expression in MLL-AF9 transformed cells. qPCR of *Hoxa9*, *Meis1*, and house keeping genes *Beta actin* and *Gapdh* expressions. Samples were collected 4 days after EtOH or 4-OHT treatment. Values were normalized to 5s rRNA internal control and EtOH treatment for respective cell lines. Data represent mean and standard deviation.

H3K79 methylation is required for transformation by MLL-AF9 oncogene

We then tried to identify the region of Dot1l that is necessary for transformation by MLL-AF9. The N-terminal 1-416 residues of Dot1l are sufficient for histone methyltransferase (HMT) activity (Min et al., 2003), while 827-1095 residues of Dot1l are important for interaction with *MLL* translocation partners and transcriptional elongation proteins (Mueller et al., 2009). In order to potentially distinguish the function of HMT versus protein interaction by Dot1l, we made HA-tagged constructs of Dot1l with point mutations or Dot1l fragments (Figure 3.14). The full-length wild type Dot1l construct was courtesy of Dr. Robert Slany (University of Erlangen). RCR is a full-length Dot1l construct with GSG to RCR mutation in the S-adenosylmethionine binding domain that lacks enzymatic activity (Min et al., 2003; Okada et al., 2005). Residues 1-416 of Dot1l HMT domain also were cloned for expression.

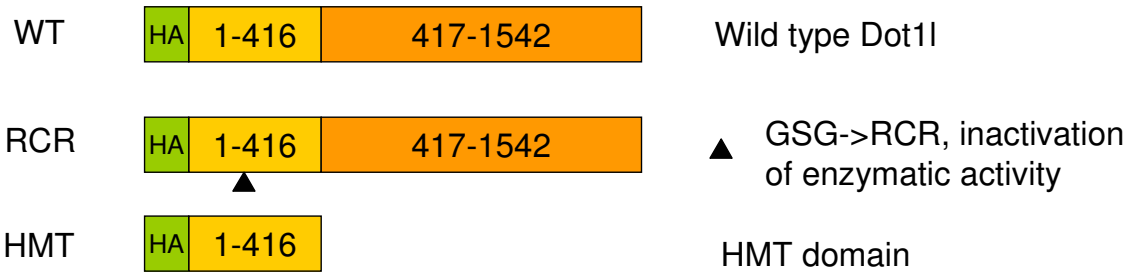

Figure 3.14. Schematic of Dot1l constructs. Wild type, HMT inactive (RCR) and HMT domain alone were used to determine if HMT activity of Dot1l is required for transformation or if protein interaction by Dot1l is sufficient for MLL-AF9 transformation.

We introduced these HA-tagged Dot1l constructs into Dot1l-deficient MLL-AF9 cells, and repeated the methocult CFU assay (Figure 3.1). Endogenous *Dot1l* excision was confirmed by PCR after the second round (Figure 3.15) and showed high efficiency of excision. The expression of exogenous Dot1l was confirmed by qPCR of HA tag sequences (primers in Table 3.1) compared to the neomycin vector control (Figure 3.16).

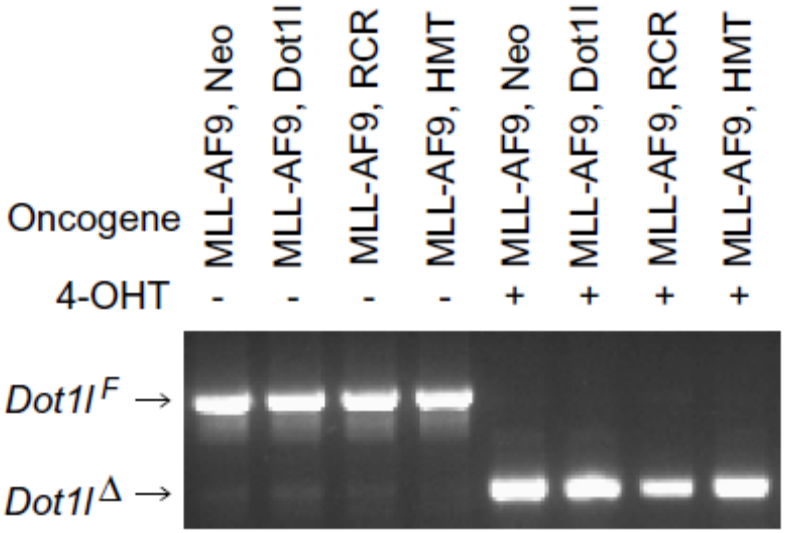

Figure 3.15. Genotyping of transduced cells after the second round. PCR reaction showed high excision efficiency of endogenous *Dot1l* with 4-OHT treatment in all cells.

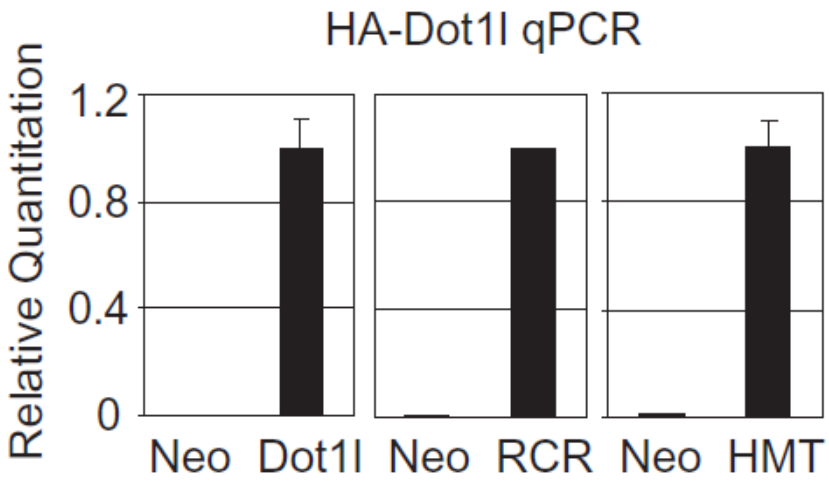

Figure 3.16. qPCR of exogenous Dot1l expression. All constructs show expression compared to Neo vector alone. Values were normalized to 5s rRNA internal control. Data represent mean and standard deviation.

Restoration of H3K79 methylation with construct expression was confirmed by western blot (Figure 3.17). Wild type HA-Dot1l was able to restore H3K79 methylation, but the HMT domain alone failed to do so. This result is in contrast to the many *in vitro* HMT assays where the HMT fragment was sufficient for H3K79 methylation of chromatin substrates (Feng et al., 2002; Min et al., 2003). Furthermore, Dot1l has a KKGR nuclear localization sequence identical to its yeast homologue (San-Segundo and Roeder, 2000) at residues 400-403, and hence the HMT construct (1-416) should enter the nucleus. Therefore, the inactivity of the HMT domain *in vivo* was somewhat unexpected. However, it is possible that for *in vivo* methylation, protein interactions are necessary for targeting Dot1l to proper loci and for catalytic activity.

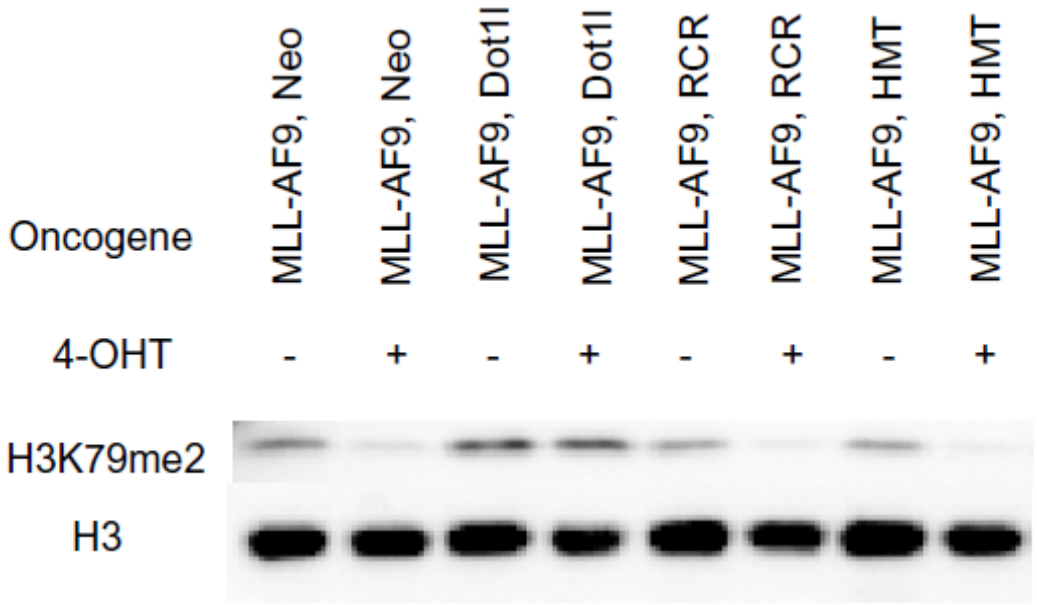

Figure 3.17. Western blot of H3K79me2 after second round. Western blot showed restoration of H3K79Me2 with the introduction of exogenous wild type Dot1l but not with RCR and HMT domain alone. Histone 3 blot was used as loading control.

Because of lack of methylation activity by the HMT construct *in vivo*, it was excluded from further studies. CFU assays showed that the RCR construct failed to rescue CFU loss after *Dot1l* deletion in MLL-AF9 cells, while the exogenous wild type Dot1l restored CFU formation (Figures 3.18 and 3.19). Because RCR is a full-length Dot1l construct, protein interaction should be intact even though it is catalytically inactive. These results suggested that H3K79 methylation is required for transformation by MLL-AF9, and protein interactions without HMT activity could not rescue CFU formation.

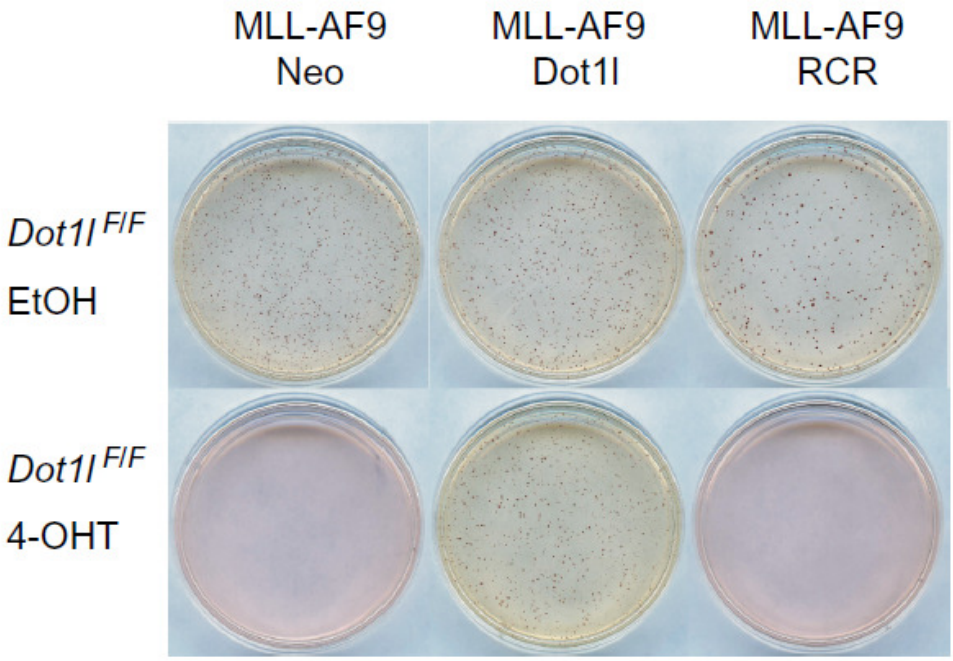

Figure 3.18. Colony formation on methocult plates. 4-OHT treated *Dot1l*$^{F/F}$ MLL-AF9 cells with wild type Dot1l were able to form colonies, but not those with RCR. INT stain of plates at final round.

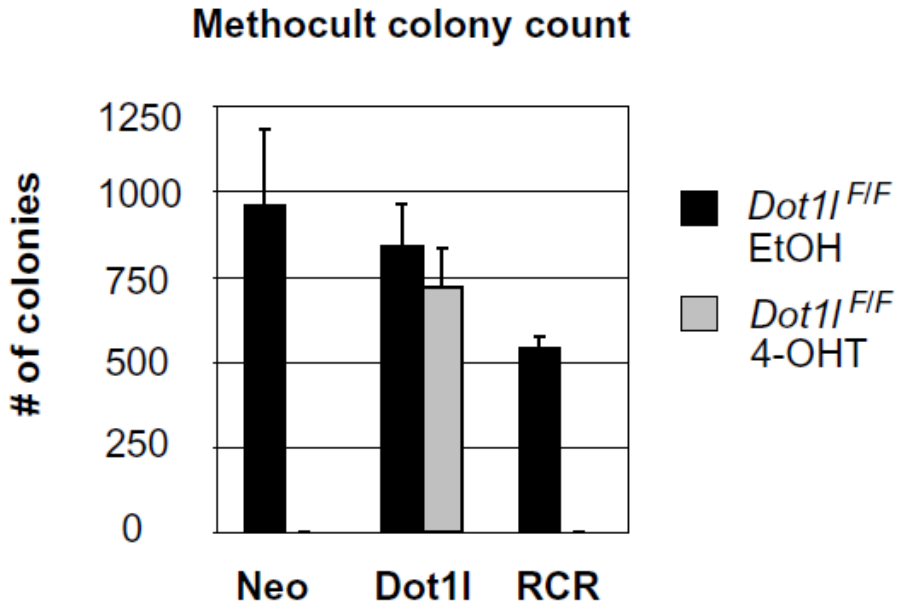

Figure 3.19. Bar graph of colony count at final round. Data represent mean and standard deviation.

Chapter IV

Analysis of Dot1l lacking Tissue Sections

Expression of Dot1l in embryos has been examined using a constitutive Dot1l knockout mouse line. Utilizing the beta-galactosidase gene, E9.5 embryos have been stained with X-gal and are shown to be constitutively expressed (Jones et al., 2008). However, there has been no examination of adult mammalian tissues for Dot1l expression.

Since CreER is ubiquitously expressed, we examined the major organs of mice after *Dot1l* excision with immunohistochemistry. We used H3K79me2 mark as the proxy for Dot1l expression because the antibody works very well. In addition, if complete loss of H3K79me2 was observed with Dot1l excision, it would corroborate that Dot1l is the only H3K79 methyltransferase. Necropsy was performed on moribund *Dot1l*$^{F/F}$ mice (Figure 2.2), and tissues from *Dot1l*$^{+/+}$ mice were collected once all *Dot1l*$^{F/F}$ mice were euthanized.

Materials and Methods

Tissue collection and fixation

Tissues were collected and immediately placed in 10% phosphate buffered formalin solution for fixation (Fisher SF100-4). Tissues were fixed for 22-26 hours and then placed in 70% ethanol solution for stopping over fixation. Fixed tissues were paraffin embedded, sectioned, and stained at the University of Michigan Cancer Center Tissue Core.

H3K79me2 immunohistochemial staining

Immunohistochemical staining was performed on the DAKO Autostainer (DAKO) using biotinylated goat anti-Rabbit IgG (Invitrogen, 1:250), streptavidin-HRP and diaminobenzidine as the chromogen. De-paraffinized sections of mouse formalin fixed tissue at five-micron thickness were labeled with anti-H3K79me2 antibody (Rabbit polyclonal antibody, 1:1500, ab3594, 30 minutes) after microwave citric acid epitope retrieval. Appropriate negative (no primary antibody) and positive controls (normal human liver) were stained in parallel with each set of tissues studied.

Results

H3K79me2 immunohistochemistry of conditional *Dot1l* knockout mice

Tissues were collected for H3K79me2 immunohistochemistry to confirm *Dot1l* deletion and to examine the tissue structure (Figure 4.1). In general, mice did not show gross abnormalities of organs except for the atrophy of seminiferous tubules. However, as evident Figure 4.1, foci of spermatogenesis

were observed though at decreased numbers. Most major organ tissues showed clear loss of H3K79me2 with loss of Dot1l. The exception was brain tissue, which showed remaining H3K79me2. Initially, we considered that the blood-brain barrier might hinder tamoxifen entry to the brain and hence decrease excision efficiency. However, presentations by Dr. Lieberman's lab (University of Michigan) using the same CreER mice showed clear excision of a floxed gene in brain tissue. Currently, we do not have a clear explanation for the discrepancy. It may be that for brain cells a higher tamoxifen concentration is required as we used less tamoxifen than the Lieberman lab for excision. More interestingly, neurons and glial cells may have special regulation preventing the loss of H3K79 methylation or there may be another H3K79 methyltransferase active only in the brain that can compensate the loss of Dot1l.

With the exception of brain, which showed remaining H3K79 methylation, most organs showed relatively normal histology despite the clear loss of H3K79me2 compared to bone marrow H & E sections (Figure 2.4). These results suggested that hematopoietic toxicity is the major consequence of *Dot1l* excision in our mouse model system.

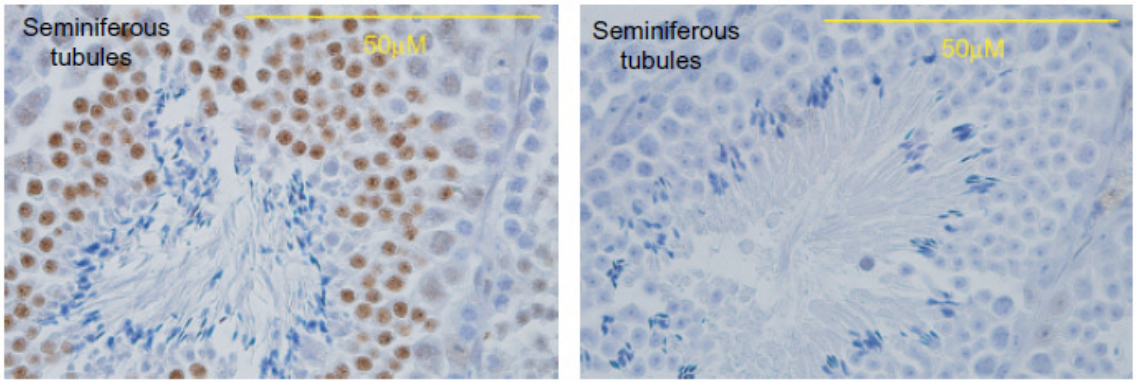

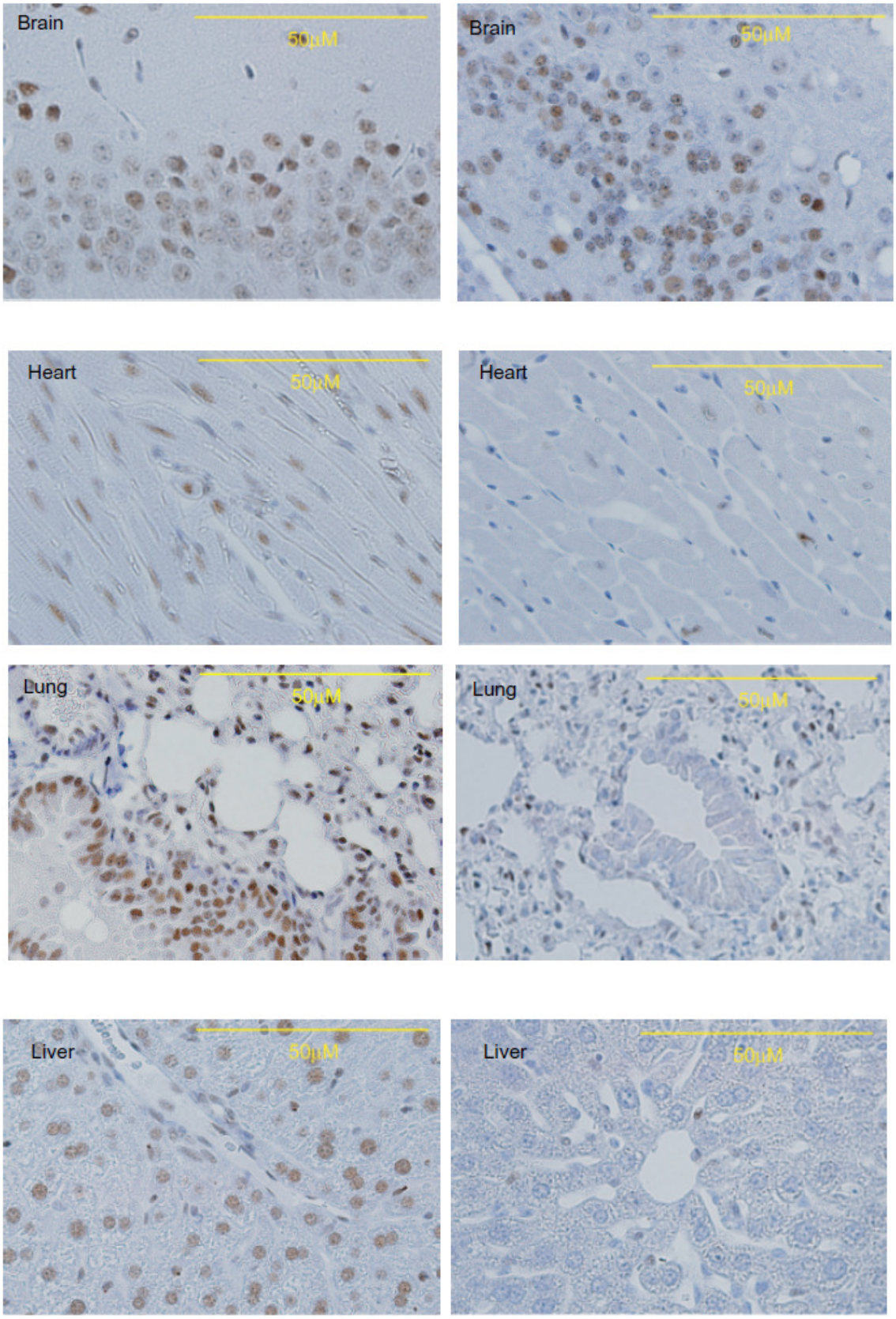
Brain
50μM
Brain
50μM
Heart
50μM
Heart
50μM
Lung
50μM
Lung
50μM
Liver
50μM
Liver
50μM

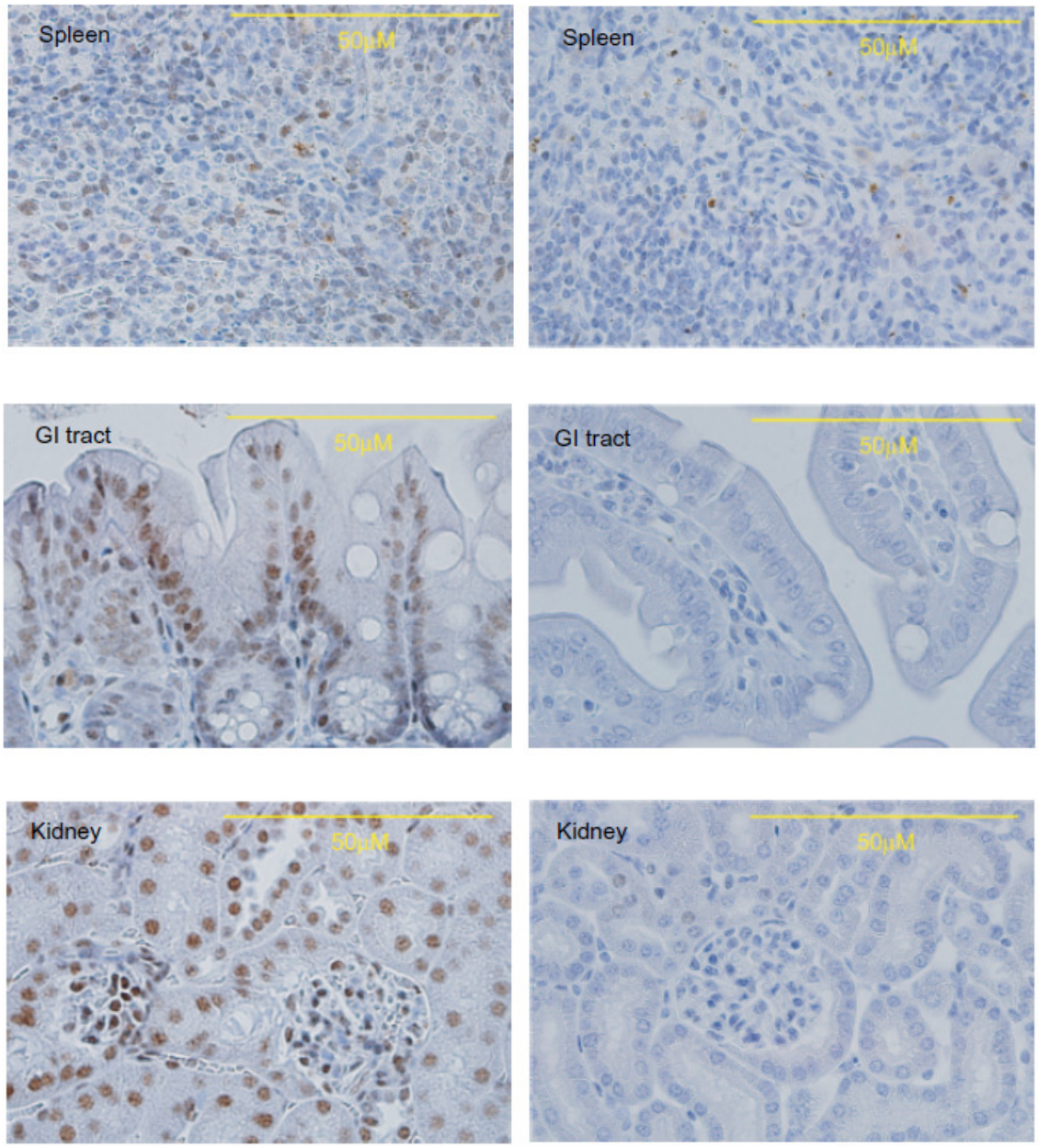

Figure 4.1. H3K79me2 immunohistochemical staining of representative *Dot1l*$^{+/+}$ and *Dot1l*$^{F/F}$ tissue sections. Tissues were collected when *Dot1l*$^{F/F}$ mice became moribund after long-term *Dot1l* excision (Figure 2.2). With the exception of brain tissue, most major organs showed complete loss of H3K79me2 with *Dot1l* excision.

Chapter V

Other Experiments and Preliminary Results: Expression Analysis of HSCs

Given our results regarding the role of Dot1l in normal hematopoiesis and leukemogenesis, we designed further experiments to address additional questions raised from these studies. A most interesting question remains that normal HSCs and MLL-AF9 LICs require proper Dot1l expression while Hoxa9/Meis1 and E2A-HLF LICs do not. Previous studies with embryonic stem cells and Dot1l knock down show that relatively small set of genes are changed with Dot1l loss (Barry et al., 2009). In order to identify potential effectors of Dot1l, we performed a microarray analysis on immunopurified HSCs after *Dot1l* excision.

Materials and Methods

HSC sorting and RNA extraction

6-10 week old mice were injected with tamoxifen 200µg/g weight by IP injection and euthanized 1 week later. HSC was immunophenotypically defined

as in Figure 2.5 and sorted using FACSAria (BD Biosciences). Cells were collected directly into pre-chilled TRIzol reagent. After chloroform extraction, the aqueous phase was mixed with an equal volume of 70% ethanol. The mixture was loaded onto an RNeasy MinElute column, DNase I treated, and the RNeasy micro kit protocol was followed (Qiagen 74004).

Amplification, cDNA conversion, biotin labeling and fragmentation

Total RNA from HSC was amplified using Ovation Pico WTA system (Nugen 3300), converted into double stranded cDNA using WT-Ovation Exon Module (Nugen 2000), biotin labeled and fragmented using Encore Biotin Module (Nugen 4200). Fragmented cDNA was hybridized on Mouse Gene ST 1.0 array (Affymetrix) by University of Michigan Microarray Core Facility.

Bioinformatics Analysis

Data from Microarray Core Facility included a list of genes with over 2 fold change and P-values. The list was further analyzed by first removing duplicate probes, and taking a cut off at P=0.05 for Cluster 3.0 (Stanford University) or P=0.2 for Gene Set Enrichment Analysis (GSEA, Broad Institute) programs. Cluster 3.0 program was used for heat map generation and was visualized with TreeView (Stanford University). Running the GSEAPreRanked program grouped genes in similar pathways together. The P-value cut off was less stringent for GSEA to allow inclusion of more genes for a particular pathway, which increased the possibility that a given pathway is a true positive.

EasySep Purification system

In order to quickly assess phenotypic difference between progenitors versus differentiated cells, EasySep Mouse Hematopoietic Progenitor Cell Enrichment kit (Stem Cell Technology 19756) was used according to manufacturer's instructions. The kit utilizes magnetic separation based on lineage markers and biotin-streptavidin interaction. Because it is a negative selection, the resulting purified cells could be used without possible confounding effects from the magnetic beads.

Results

Loss of H3K79 methylation upregulates differentiation promoting genes and polycomb target genes in HSCs

First we tried to pick the best time to collect HSCs after *Dot1l* excision. Given that by 3 weeks the vast majority of the HSCs were gone (Figure 2.6), we tried to examine the HSC population as early as possible. As a time course, bone marrow cells were collected and stained for HSCs 2, 4, and 7 days after tamoxifen injection. There were changes in sca1 and ckit staining profiles 2 and 4 days after tamoxifen injection, presumably from tamoxifen injury and recovery (Figure 5.1, refer to Figure 2.5 for normal staining profile of HSCs). This effect was largely gone by 7 days. Therefore, HSCs were sorted from $Dot1l^{F/F}$ and $Dot1l^{+/+}$ mice one week after tamoxifen injection.

For the experiment, each genotype had three individuals and all animals were between 6-10 weeks of age. Given that tamoxifen has hormonal effects, only males were used to exclude differences that might arise from gender. Hence, using female individuals or pooling male and females might give slightly different results. Between 1500-3000 HSCs were collected per individual mouse. The difference in HSC numbers were not due to genotype differences but correlated with flow rate during the cytometry run, with slower flow rates allowing higher collection rates and hence more cells. Cells were collected directly into pre-chilled TRIzol reagent and stored at -150^{o}C until RNA extraction, amplification, cDNA synthesis, biotin labeling and fragmentation as mentioned in the materials and methods.

HSC samples were hybridized onto Affymetrix Mouse Gene ST 1.0 arrays by the Affymetrix Core (University of Michigan). The results were first analyzed by Cluster 3.0 heat mapping software (Stanford University). 234 genes were significantly either upregulated or downregulated with loss of Dot1l with P-value cut off at 0.05 (Figure 5.2). Unfortunately, a lot of the highest hits on first pass did not seem very closely connected with each other (Table 5.1). Therefore, Gene Set Enrichment Analysis (GSEA, Broad Institute) was performed. With conventional P-value < 0.05, no enriched pathway was identified. Hence, a less stringent cut off of P=0.2 was used. The enriched pathways included EZH2 targets, , myeloid proliferation and renewal, and granulocyte/monocyte differentiation (Figures 5.3, 5.4, 5.5). The red box indicates genes that changed expression with P-value < 0.05. EZH2 is a H3K27 methyltransferase that is a

member of the polycomb group protein complex and has been implicated in many different cancers (Xiao, 2011). Upregulation of EZH2 targets made sense in that Dot1l and H3K79 methylation are generally associated with gene activation while EZH2 and polycomb proteins are associated with gene repression. Also, given the profound disappearance of HSCs, accelerated differentiation might be occurring with *Dot1l* excision. Based on the P-values of pathway components, myeloid proliferation and renewal pathway was the highest hit. These data were partially corroborated by a preliminary cell cycle analysis on lineage positive and lineage negative cell populations (Figure 5.6). Unfractionated bone marrow was used as lineage positive cells, while lineage negative cells were collected by EasySep Mouse Hematopoietic Progenitor Cell Enrichment kit (Stem Cell Technology). Cells were collected 1 week after tamoxifen injection. While the cell population was not very pure, data suggested that unfractionated Dot1l$^{F/F}$ cells have defects in cell cycle similar to MLL-AF9 transformed cells with *Dot1l* excision, while lineage negative cells show a comparable cell cycle profile between Dot1l$^{F/F}$ and Dot1l$^{+/+}$ with *Dot1l* excision. Better cell cycle analysis with methods such as BrdU incorporation with cell surface antibody is required to make further conclusions. Additional literature search is also necessary to determine the details on how myeloid proliferation and renewal pathway genes affect cell cycling. Based on these preliminary data, *Dot1l* excision might lead to induction of closed chromatin structure, accelerated differentiation and then cycling block of differentiated cells leading to failure of hematopoiesis.

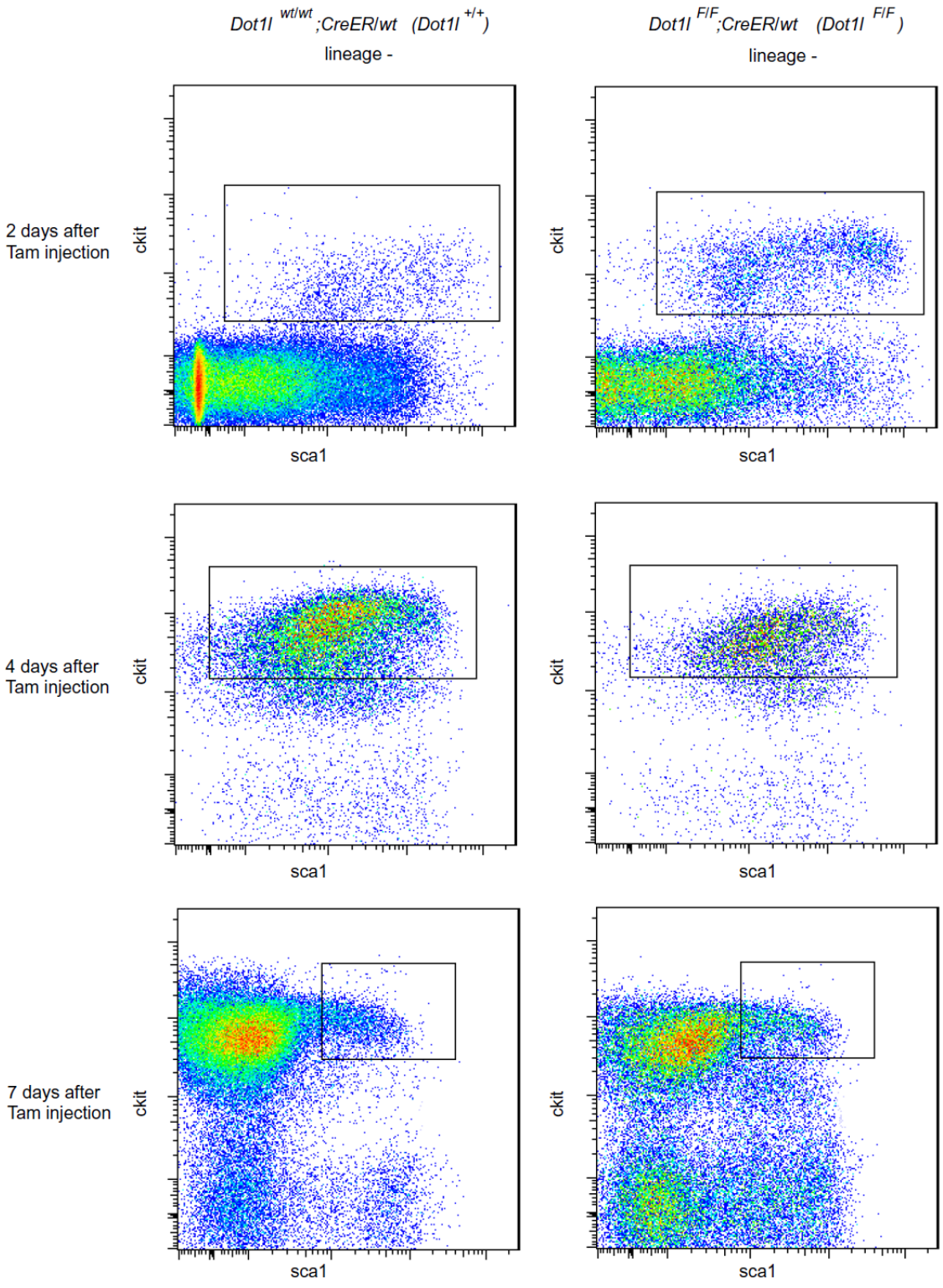

Figure 5.1. Time course of HSC staining profile after tamoxifen injection.

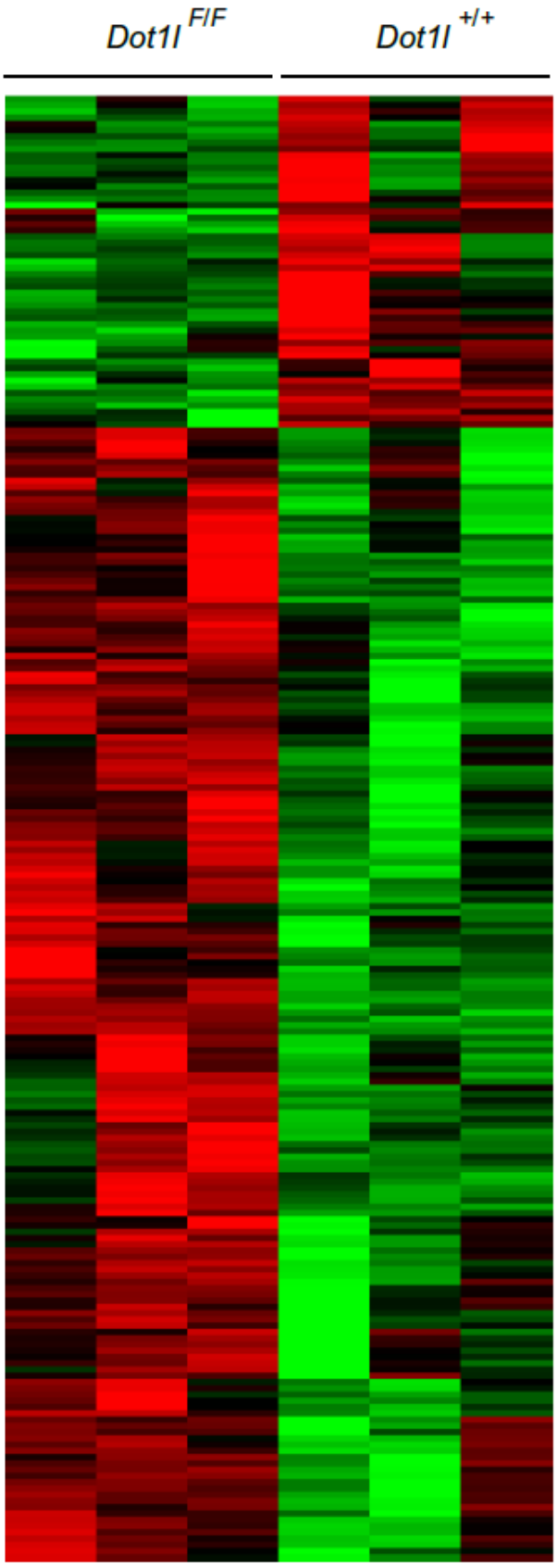

Figure 5.2. Heat map of altered gene expression with *Dot1l* excision in HSCs. P-value < 0.05 genes were selected. 234 genes were significantly changed.

Chd7	chromodomain helicase DNA binding protein 7
Insl6	insulin-like 6
Prkcq	protein kinase C, theta
Tacstd2	tumor-associated calcium signal transducer 2
Ube2h	ubiquitin-conjugating enzyme E2H
Slamf1	signaling lymphocytic activation molecule family member 1
Fmo5	flavin containing monooxygenase 5
Zfp273	zinc finger protein 273
Ccdc69	coiled-coil domain containing 69
Ankmy2	ankyrin repeat and MYND domain containing 2
Nupr1	nuclear protein 1
Polr3gl	polymerase (RNA) III (DNA directed) polypeptide G like
Rmi1	RMI1, RecQ mediated genome instability 1, homolog (S. cerevisiae)
Cnot8	CCR4-NOT transcription complex, subunit 8
Prim2	DNA primase, p58 subunit
Trip10	thyroid hormone receptor interactor 10
Arfgef2	ADP-ribosylation factor guanine nucleotide-exchange factor 2 (brefeldin A-inhibited)
Ppm1a	protein phosphatase 1A, magnesium dependent, alpha isoform
Trim13	tripartite motif-containing 13
Nkg7	natural killer cell group 7 sequence
Ebi3	Epstein-Barr virus induced gene 3

Table 5.1 Top 20 changed genes with *Dot1l* excision in HSCs.

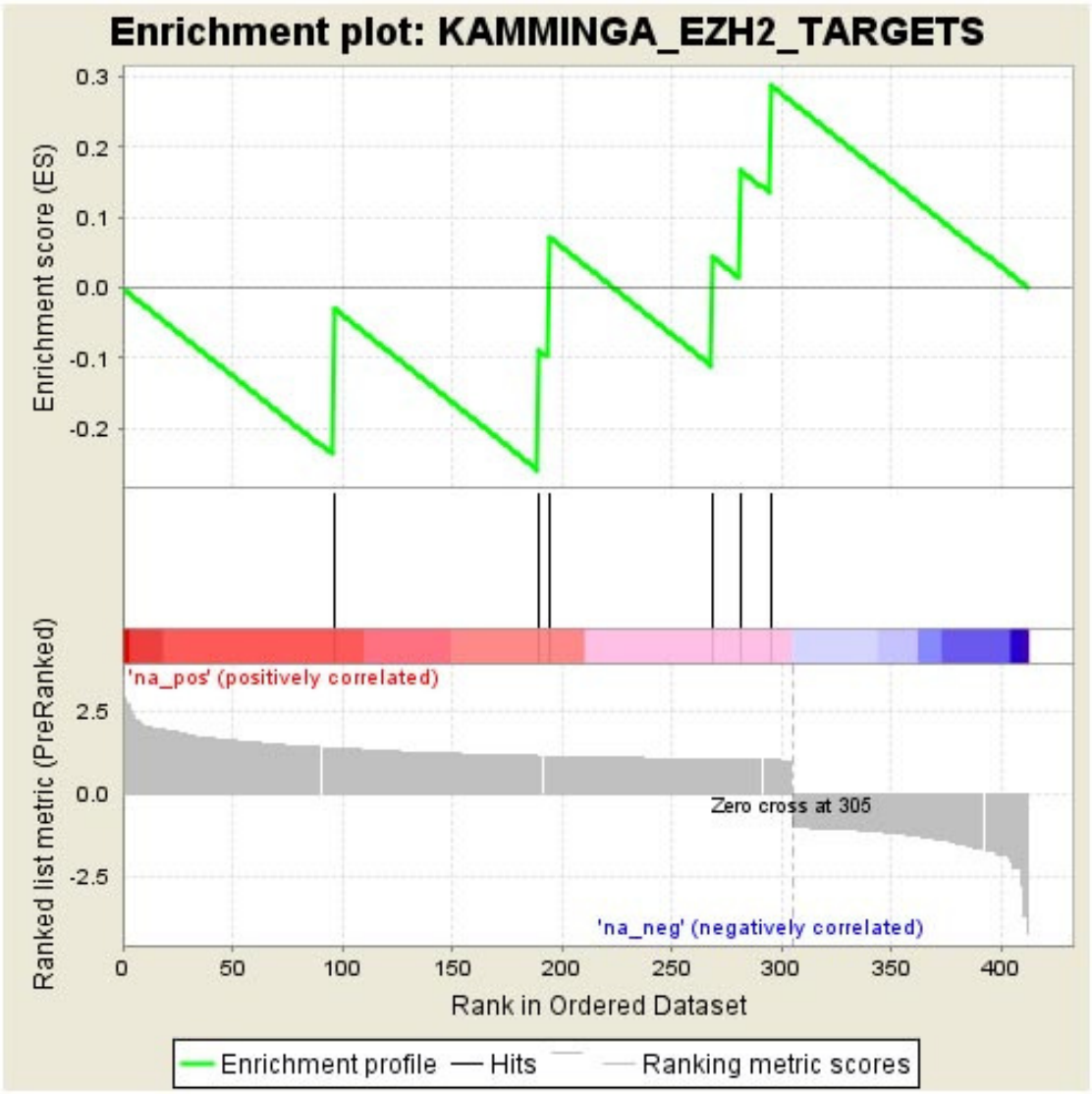

	PROBE	GENE SYMBOL	GENE_TITLE	RANK IN GENE LIST	RANK METRIC SCORE	RUNNING ES	CORE ENRICHMENT
1	Prc1			96	1.380	-0.0299	Yes
2	Ahcy			190	1.130	-0.0897	Yes
3	Mcm3			194	1.130	0.0715	Yes
4	Ccnb2			269	1.030	0.0435	Yes
5	Ect2			282	1.020	0.1662	Yes
6	Pole2			295	1.010	0.2875	Yes

Figure 5.3. GSEA pathway enrichment: EZH2 targets.

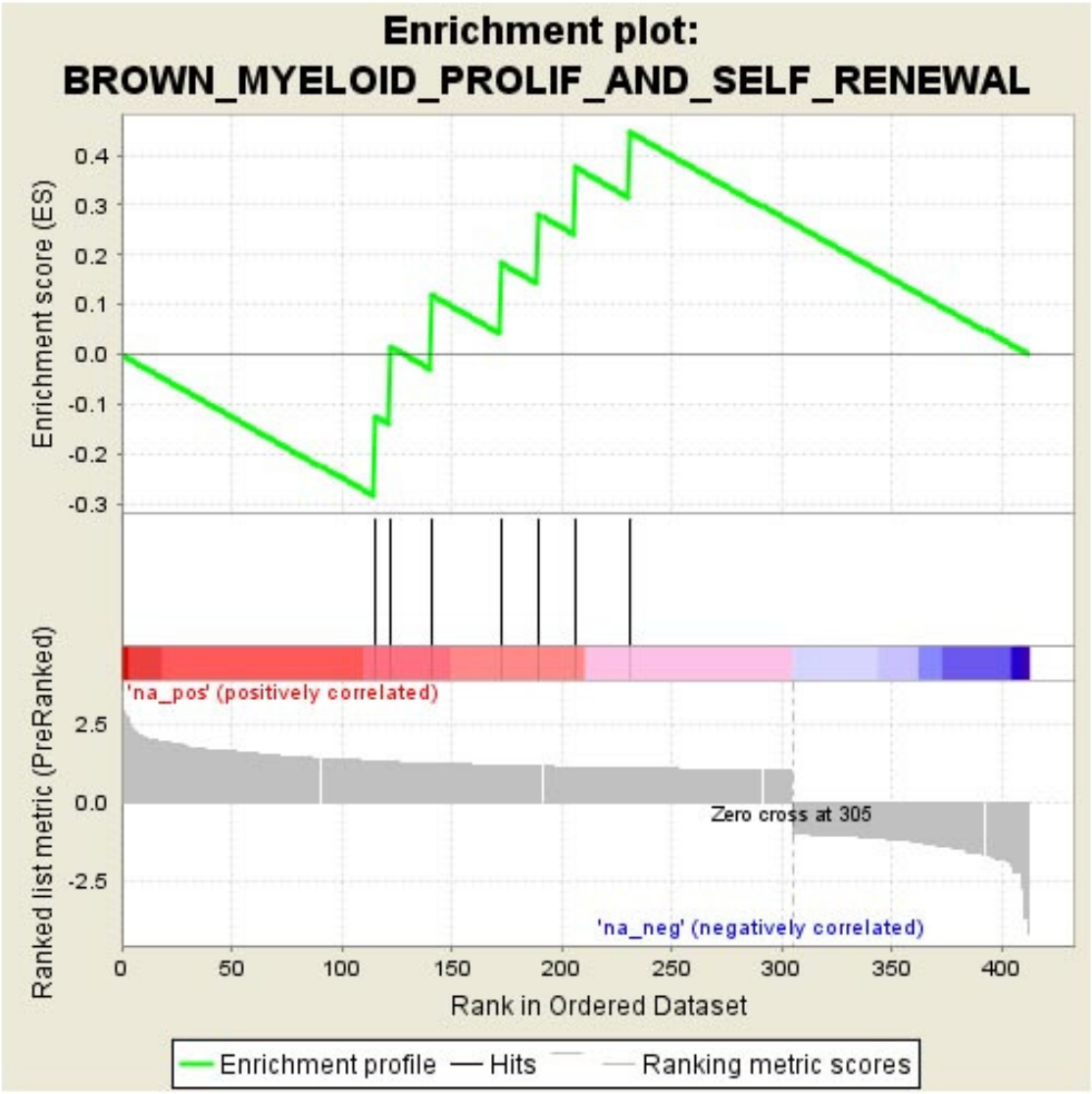

	PROBE	GENE SYMBOL	GENE_TITLE	RANK IN GENE LIST	RANK METRIC SCORE	RUNNING ES	CORE ENRICHMENT
1	H2-Ab1			115	1.320	-0.1248	Yes
2	Bzw2			122	1.290	0.0153	Yes
3	Fkbp4			141	1.230	0.1186	Yes
4	Slc7a5			173	1.170	0.1827	Yes
5	Ahcy			190	1.130	0.2790	Yes
6	Akr1c12			206	1.110	0.3753	Yes
7	Cd48			231	1.080	0.4458	Yes

Figure 5.4. GSEA pathway enrichment: Myeloid proliferation and self renewal.

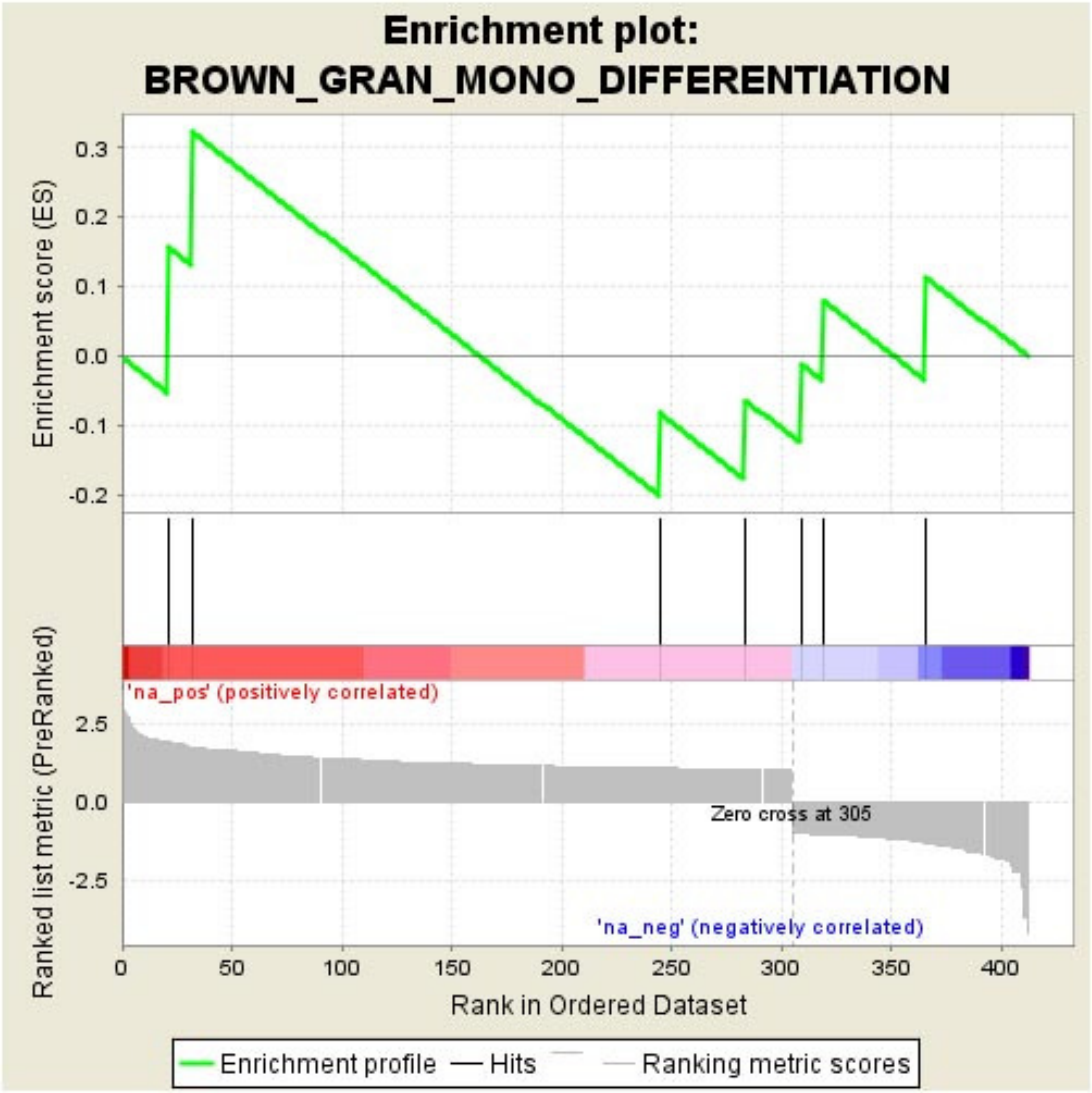

	PROBE	GENE SYMBOL	GENE_TITLE	RANK IN GENE LIST	RANK METRIC SCORE	RUNNING ES	CORE ENRICHMENT
1	Rpl13			21	1.900	0.1564	Yes
2	Cd68			32	1.740	0.3223	Yes
3	Scarb2			245	1.070	-0.0826	No
4	Gp5			284	1.020	-0.0645	No
5	Emcn			309	-1.020	-0.0119	No
6	Sepx1			319	-1.040	0.0798	No
7	Fpr1			366	-1.340	0.1133	No

Figure 5.5. GSEA pathway enrichment: Granulocyte and monocyte differentiation.

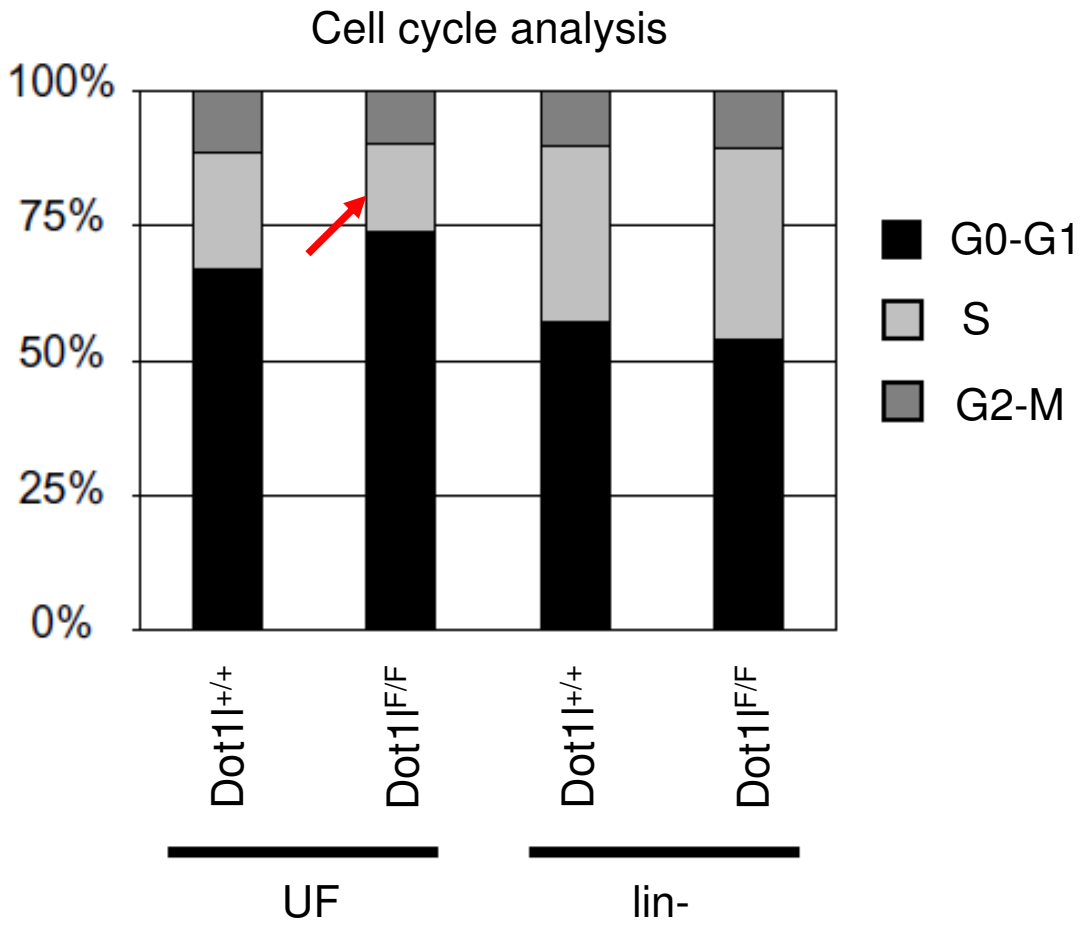

Figure 5.6. Propidium iodide cell cycle analysis of bone marrow cell population. UF: unfractionated bone marrow cells. Lin-: lineage-negative cells remaining after depletion of lineage-positive cells by EasySep kit.

Chapter VI

Other Experiments and Preliminary Results: Histone Cross-Talk

H2B ubiquitination has been shown to be required for H3K79 methylation and H3K4 methylation. In yeast and in human cell lines, loss of Rad6 (E2 ubiquitin ligase), Bre1 (E3 ubiquitin ligase for Rad6), or Paf1 complex components (required for Rad6-Bre1 activity) led to loss of H3K4 methylation and H3K79 methylation (Kim and Roeder, 2011; Ng et al., 2002b; Wood et al., 2003). On the contrary, loss of yeast Dot1 and H3K79 methylation does not lead to loss of H2B ubiquitination (Ng et al., 2002b). However, studies examining how the loss of H3K79 methylation affects H2B ubiquitination and H3K4 methylation in mammalian cells are lacking. With Dot1l$^{F/F}$ cells transformed by MLL-AF9, we examined if *Dot1l* excision leads to the loss of H3K4 methylation and H2B ubiquitination. Because of the close correlation between H3K79 methylation and H3K4 methylation in *MLL* translocation leukemia (Krivtsov et al., 2008; Milne et al., 2005) and the requirement of wild type Mll in MLL-AF9 transformation (Thiel et al., 2010), we examined the recruitment of wild type Mll to target gene loci as well. Since our HSC gene expression analysis indicated an increase of EZH2 targets with *Dot1l* excision, we also examined the changes of H3K27 methylation status.

Materials and Methods

Chromatin Immunoprecipitation (ChIP)

ChIP samples were prepared from Dot1l$^{F/F}$ cells transformed with MLL-AF9 and treated with either EtOH or 4-OHT. Four days after treatment, cells were harvested and cross-linked with 1% paraformaldehyde in growth media without cytokines for 15 minutes at room temperature. Cross-linked samples were lysed with lysis buffer (1% SDS, 10mM EDTA and 50mM Tris, pH 8.1) for 15 minutes on ice. 1ml of lysis buffer was used for 10 million cells. Lysed samples were divided into 250µl per microcentrifuge tube and sonicated for 15 minutes (Bioruptor, Diagenode) on ice and spun down at maximum speed for 15 minutes at 4^{o}C. Supernatant of samples were then pooled and diluted 1:10 with dilution buffer (0.01% SDS, 1.1% Triton X- 100, 1.2mM EDTA, 16.7mM Tris-HCl, pH 8.1, 167mM NaCl). 1% of samples were set aside as input. Diluted samples were divided and antibodies were added for incubation overnight on a rotor. Complete mini EDTA-free protease inhibitor cocktail tablet (Roche), 100µM PMSF in isopropanol, and 1:1000 aprotinin (Sigma A6279) was added to lysis buffer and elution buffer to prevent protein degradation. The next day, Dynabead Protein G (Invitrogen, 100-04D) was washed three times with 5% BSA in 1x PBS and 30µl was added per sample for immunoprecipitation. Dynabeads and samples were incubated for 1 hour at 4^{o}C on rotor. Dynabead-bound complex was separated with magnet and supernatant discarded. Samples were then washed with low salt buffer (0.1% SDS, 1% Triton X-100, 2mM EDTA, 20mM

Tris-HCl, pH 8.1, 150mM NaCl), high salt buffer (0.1% SDS, 1% Triton X-100, 2mM EDTA, 20mM Tris-HCl, pH 8.1, 500mM NaCl), LiCl buffer (0.25M LiCl, 1% IGEPAL CA630, 1% deoxycholic acid (sodium salt), 1mM EDTA, 10mM Tris, pH 8.1), and TE buffer (10mM Tris-HCl, pH 8.0, 1mM EDTA). The washed samples were eluted with 200µl of elution buffer (1%SDS, 0.1M $NaHCO_3$) at 42^{o}C for 30 minutes. Dynabeads were removed from the eluate by magnet and 8µl of 5M NaCl were added per sample. The samples were incubated overnight at 65 ^{o}C for reverse cross-linking. DNA was recovered from reverse cross-linked samples using QIAquick PCR purification kit (Qiagen 28106).

Antibodies for ChIP

Following antibodies were used for ChIP: H3 (Abcam, ab1791), H3K79me2 (Abcam, 3594), normal rabbit/mouse IgG (Santa Cruz sc 2027/sc-2025), H3K4me3 (Millipore 04-745), H3K27me3 (Millipore 17-622), H2BUb (Millipore 05-1312), Mll-C (courtesy of Dr. Yali Dou, University of Michigan).

Primers for ChIP

Primer	Taqman Probe	Forward	Reverse
Hoxa9-2	CCTGCGGTGGCAACCTCAGATCC	GCCATCAAGGCCTAATCGTG	AAGACCCGAAGCTCCTCCTG
Hoxa9-3	CCCACATCGAGGGCAGGAAACACT	CACCCGCGGCGTCTT	CGAACCAATGGATCTGGCA

Hoxa9-4	TGAATTTTCCCCCTTTTGGGCCAC	TAGACTCACAAGGACAATATCTCCTTTT	AGGTACTGAGTATTAAGCAGCTGTTTACA
Hoxa9-5	CCACCGCCCCTCCCATTAACAACA	CTGTTGCTTTGTGTTCCAGATTG	AAGTGAGAAGGCCACAGCCA
Hoxa9-6	CCTCTTGATGTTGACTGGCGATTTTCCC	TGACCCCTCAGCAAGACAAAC	TCCCGCTCCCCAGACTG
Hoxa9-7	AAGCGCCTGGCTGGCTTTCCA	AGGGTGATCTGGCCGATGT	AAAATGGGCTACCGACCCTAGT
Hoxa9-8	TGTTGGTCGCTCCTGACTTTCCACC	CACAGCGAGGCAAACGAAT	TTATTGTTTCGGAAGCCACACA
Hoxa9-9	ATTATGACTGCAAAACACCGGGCCATT	CGCGATCCCTTTGCATAAAA	CGTAAATCACTCCGCACGCT
Hoxa9-10	CTTCAGTCCTTGCAGCTTCCAGTCCAA	CAGCTCTGGCCGAACACC	TTCCACGAGGCACCAAACA
Hoxa9-11	TACCCTCCAGCCGGCCTTATGGC	GGTGCGCTCTCCTTCGC	GCATAGTCAGTCAGGGACAAAGTGT
Hoxa9-12	CCAACTGGCTACATGCTCGCTCCA	TCTCTCTCCCTCCGCAGATAAC	GGGCATCGCTTCTTCCG
Meis1-1	AATCTCCATTTCTTTCCACTCTGCAGACC	GCCTCTTTAGGGCAATCTATAGCTT	CACTTTGCCTTCCTCCAAACC
Meis1-2	CCGGCGCTGACTCGTGCAGAC	CTGCCGCTGGTGTGAACTAG	CGGAGCCTCCTAAGACAGCTT

Meis1-3	TTCCTTTCCTCCGGCCCTACGTCC	TCAAAGTGACAAAATGCAAGCA	CCCCCCGCTGTCAGAAG
Meis1-4	CATTCACCACGTTGACAACCTCGCC	GAAGAAGACAGAACGGACGATCA	GCCACTCCAGCTGTCAATCA
Meis1-5	CCCCCGCAGAGGTGGCTTCTTAAA	GCCTTGAAAGTAAACTGAGACAATGA	GGCCAAGACACAAATTATGCAA
Meis1-6	ACCGGTCCACCACCTGAACCACG	GCATGCAGCCAGGTCCAT	TAAAGCGTCATTGACCGAGGA

Table 6.1. ChIP-qPCR primers.

Data analysis for ChIP

ChIP samples were analyzed by qPCR with primers as indicated above. Fam-tamra probes were used with Taqman Mastermix (Applied Biosystems). Ct values of qPCR were normalized to input value as internal control and then divided with histone 3 (H3) ChIP value, which served as control for the amount of nucleosome present on the locus.

HA immunoprecipitation (IP)

293 cells were transfected with gene of interest with Fugene 6 (Roche). Cells were harvested 2 days later and lysed with BC300 lysis buffer (20mM Tris, pH 7.5, 10% glycerol, 300mM KCl, 1mM EDTA, 10mM beta-mercaptoethanol, 200μM PMSF, 0,1% NP-40) for 30 minutes on ice. Samples were sonicated with a Branson sonicator for 1 minute and spun at maximum speed to remove

debris, and then incubated with anti-HA Affinity Matrix from rat IgG (Roche 11815016001) overnight. The next day, complexes were washed three times with BC300 and proteins were eluted from the matrix by adding Tris-Glycine SDS Sample Buffer and heat denaturing for 5 minutes at 95^{o}C. 5% beta-mercaptoethanol (Sigma) was added to the eluates.

Results

Loss of H3K79 methylation leads to decrease of H3K4 methylation, MII-C, and H2B ubiquitination, and increase of H3K27 methylation at *Hoxa9* and *Meis1* loci

As in all previous experiments with the MLL-AF9 transformed cell line, cells were treated with 4-OHT for three days and then cultured for four more days in regular growth medium before cross-linking. Western blot of whole cell lysates with histone modification antibodies used for ChIP was performed to examine changes in global levels (Figure 6.1). As expected, H3K79me2 was dramatically lost with *Dot1l* excision. There might be a slight decrease in H3K4me3 in MLL-AF9 transformed cells, but H3K27me3 and H2B ubiquitination (H2Bub) remained mostly unchanged. Unchanged H3K27 and H3K4 methylation levels were also reported previously (Feng et al., 2010).

With the excision of *Dot1l*, H3K79 methylation was totally lost from *Hoxa9* and *Meis1* loci as expected (Figure 6.2). As in previous studies, a strong

correlation between H3K79 methylation and H3K4 methylation was observed (Krivtsov et al., 2008; Milne et al., 2005), and H3K4 methylation also dramatically decreased with some remaining methylation around transcriptional start site (Figure 6.3). We next examined if this loss of H3K4 methylation is due to loss of Mll recruitment or due to loss of enzymatic activity even with normal Mll recruitment. In order to differentiate between wild type Mll and MLL-AF9, antibody raised against the C-terminus of Mll (Mll-C) was used for ChIP. ChIP with Mll-C showed that recruitment of Mll to the loci was compromised as well (Figure 6.4). This result is notable because global levels of H3K4me3 were comparatively less changed (Figure 6.1) or reported unchanged (Feng et al., 2010). Western blot of Mll-C may be useful for examining if Dot1l regulates Mll expression directly. Given that there are multiple H3K4 methyltransferases in mammals (Shilatifard, 2008), Dot1l loss seemed to specifically affect H3K4 methylation on Mll target gene loci.

In contrast to H3K4 methylation, H3K27 methylation increased with *Dot1l* excision (Figure 6.5). This result corroborates GSEA HSC microarray data indicating upregulation of EZH2 targets with the loss of Dot1l. Similarly to H3K4me3 ChIP, these data are notable because there was no change in global H3K27 methylation according to western blot (Figure 6.1) and reported data (Feng et al., 2010).

We next examined H2Bub status with *Dot1l* excision. As mentioned above, H2Bub is required for normal H3K4 and H3K79 methylation in yeast and in mammals (Kim et al., 2009; Ng et al., 2002b; Wood et al., 2003). We wanted

to examine if reverse is also true with our Dot1l knockout model. H2Bub ChIP data showed that with loss of Dot1l, H2Bub also decreased (Figure 6.6). This result may be due to several reasons. With loss of Dot1l, expression of H2B ubiquitination machinery may be decreased and hence decrease H2Bub in general. However, this is not likely since global H2B ubiquitination levels did not change with *Dot1l* excision (Figure 6.1). Preliminary immunoprecipitation experiments also showed that Dot1l and Paf1 complex member Ctr9 (Rozenblatt-Rosen et al., 2005; Zhu et al., 2005) did not interact (Figure 6.7). It will be interesting to examine the expression and recruitment of Rad6, Bre1, and Paf1 complex components to the *Hoxa9* and *Meis1* loci as well. This result also raises interesting questions on histone cross-talk, because on specific loci H3K79 methylation seemed to affect other histone modification, but presumably not for all loci based on global western blot data.

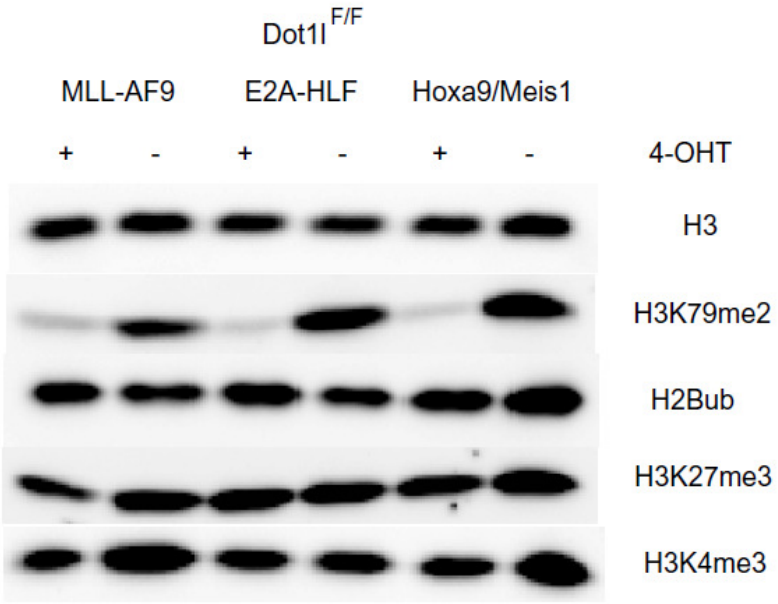

Figure 6.1. Western blot of whole cell lysate after *Dot1l* excision. In general, global levels of examined histone modifications other than H3K79 methylation remained stable.

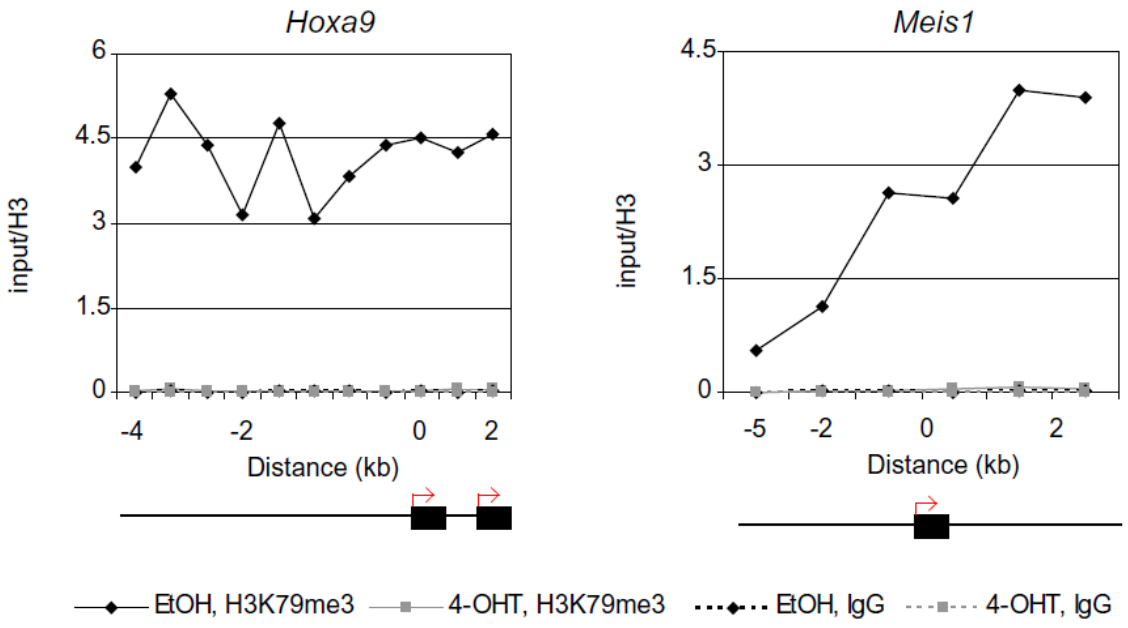

Figure 6.2. H3K79me2 ChIP of *Hoxa9* and *Meis1* loci after *Dot1l* excision. H3K79 methylation was completely lost.

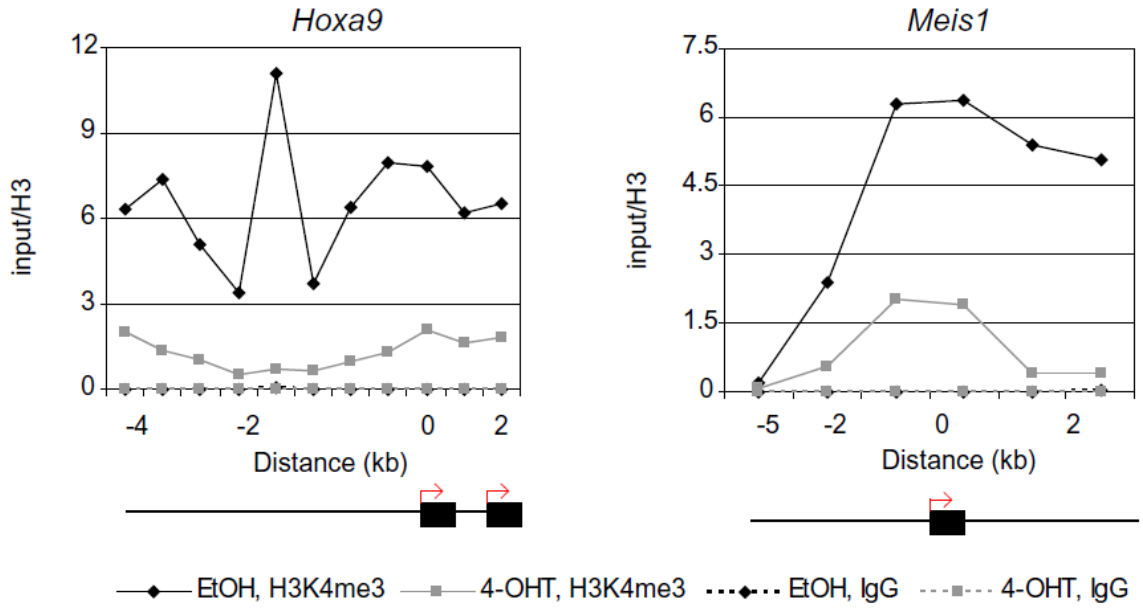

Figure 6.3. H3K4me3 ChIP of *Hoxa9* and *Meis1* loci after *Dot1l* excision. H3K4 methylation was dramatically reduced.

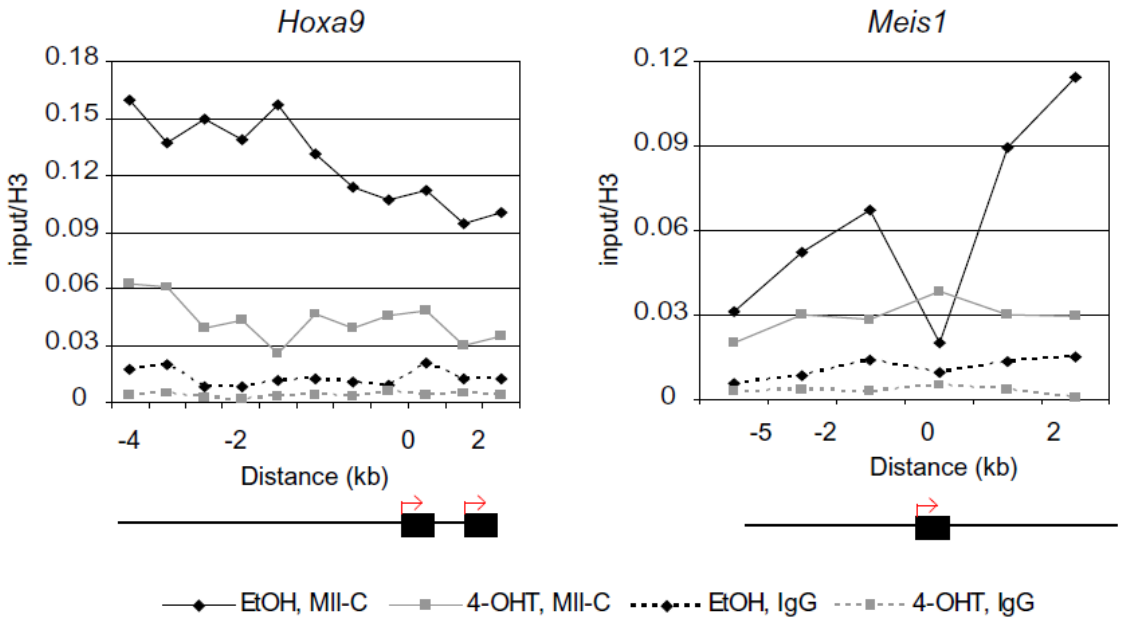

Figure 6.4. MII-C ChIP of *Hoxa9* and *Meis1* loci after *Dot1l* excision. Recruitment of wild type MII was compromised.

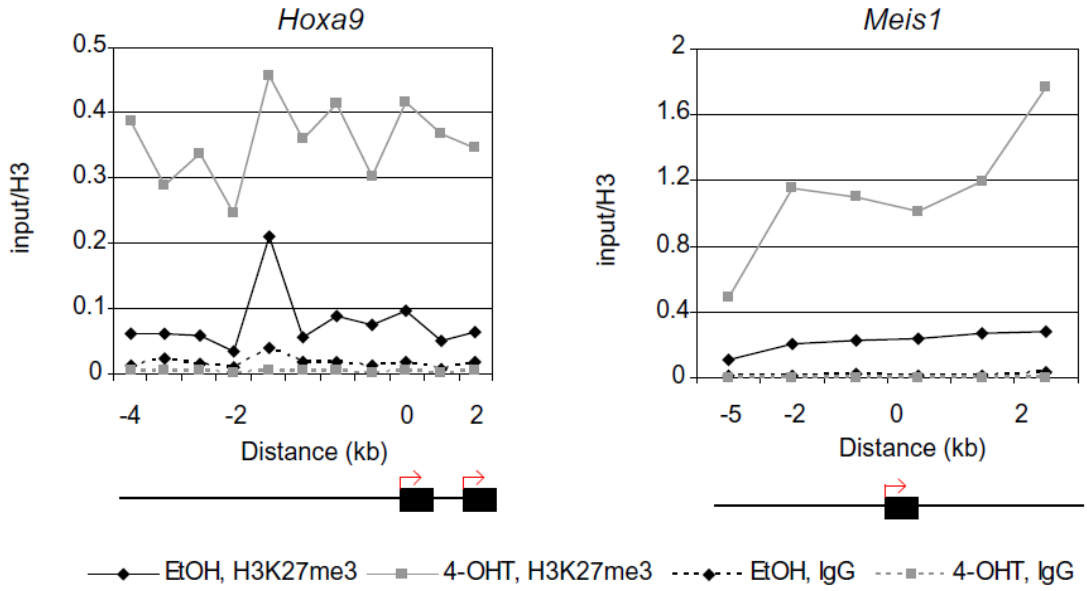

Figure 6.5. H3K27me3 ChIP of *Hoxa9* and *Meis1* loci after *Dot1l* excision. H3K27 methylation was greatly increased.

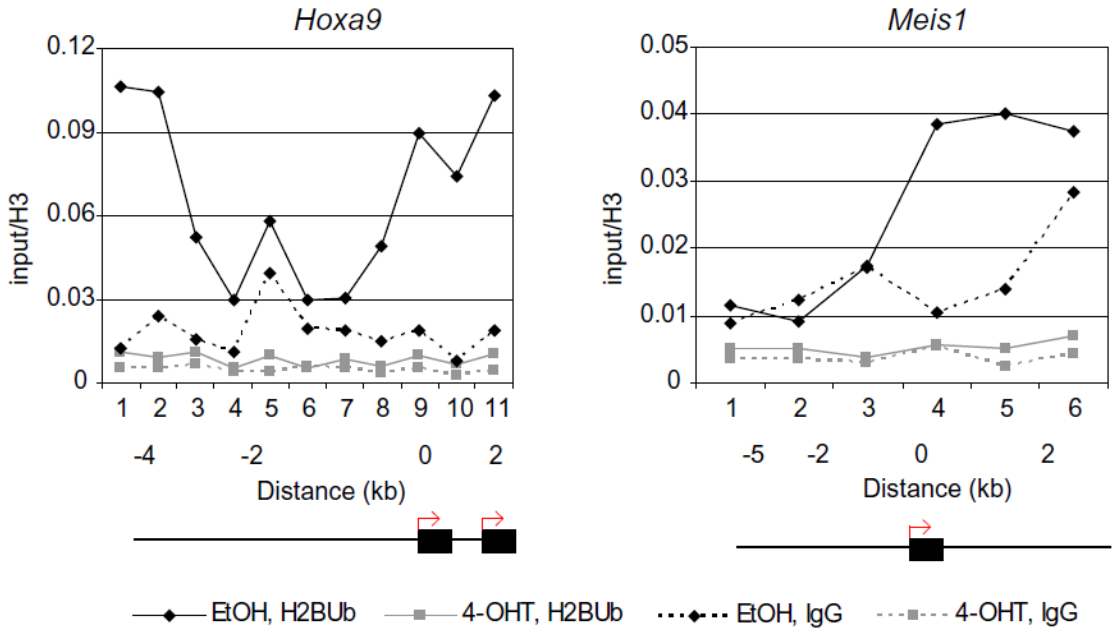

Figure 6.6. H2Bub ChIP of *Hoxa9* and *Meis1* loci after *Dot1l* excision. H2B ubiquitination was reduced.

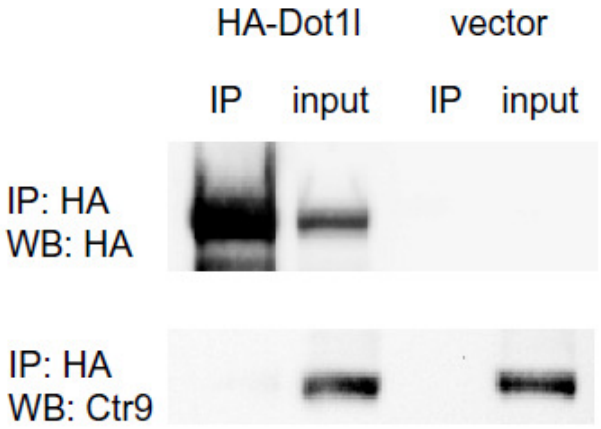

Figure 6.7. HA tagged Dot1l was overexpressed in 293 cells and immunoprecipitated (IP) with HA antibody. Western blot (WB) with HA show that HA-Dot1l was significantly enriched in IP sample but Paf complex component Ctr9 did not show interaction.

Chapter VII

Other Experiments and Preliminary Results: Dot1l-AF9/ENL interaction

In collaboration with Dr. Zaneta Nikolovska-Coleska's lab we examined the effects of Dot1l-AF9/ENL interaction in MLL-AF9 transformation. AF9 and ENL are both common MLL translocation partners, and the two proteins show high homology especially in the C-terminus which is involved in *MLL* translocation (Figure 7.1). Together, they constitute ~25% of acute lymphoid leukemia (ALL) and ~35% of acute myeloid leukemia (AML) with *MLL* translocations (Meyer et al., 2009). It was interesting as mentioned in Chapter III that MLL-AF9 transformed cells were specifically affected by Dot1l loss. Hence, Chenxi Shen from Dr. Nikolovska-Coleska's lab studied the interaction domain of Dot1l and AF9/ENL.

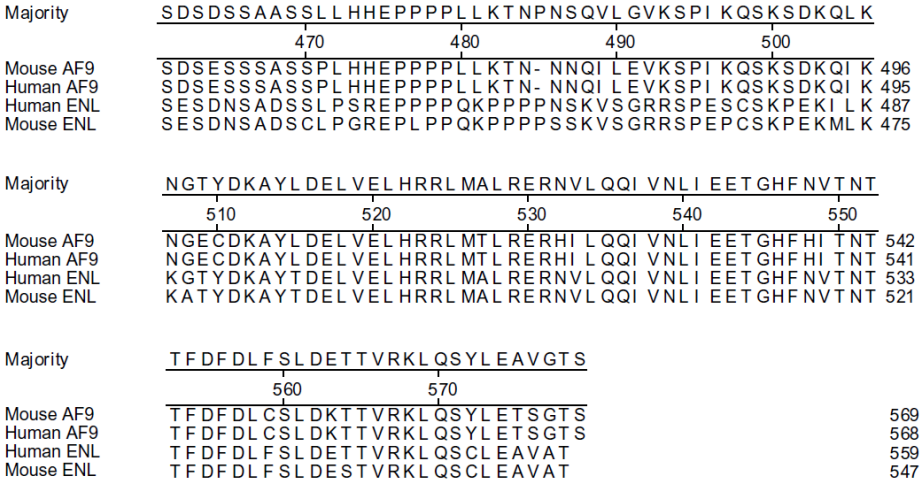

Figure 7.1. Alignment of C-terminus of human and mouse AF9 and ENL proteins.

She was able to narrow down the interaction region to 10 amino acids, showing that *in vitro* the 10 amino acid peptide can disrupt interaction between Dot1l and AF9/ENL. From these data, we examined the effect of these 10 amino acids on MLL-AF9 transformation. A full length HA-tagged Dot1l construct was made with the 10 amino acid deletion (10aaΛ). Rescue of transformation by this construct was compared to those of full length wild type Dot1l and enzymatically inactive Dot1l (RCR) constructs (Figures 3.18 and 3.19).

Materials and Methods

All methods for this section were as indicated in Chapter III. 150,000 MLL-AF9 transformed Dot1l$^{F/F}$ cells were transduced per Dot1l construct.

Results

10aaΛconstruct retains H3K79 methylation ability but loses transformation ability

MLL-AF9 transformed cells from Chapter III were used as starting point for experiments in Chapter VII. The MLL-AF9 transformed cell line was transduced twice with neomycin (Neo) vector control, wild type Dot1l, enzymatically inactive Dot1l (RCR), and AF9 interaction defective Dot1l (10aaΛ). 2-3 days after the

last transduction, cells were plated on methocult media with EtOH or 4-OHT. Once the plates became confluent 5-7 days later, cells were replated onto methocult media. Colony formation were count from the 2nd plating (Figure 7.2)

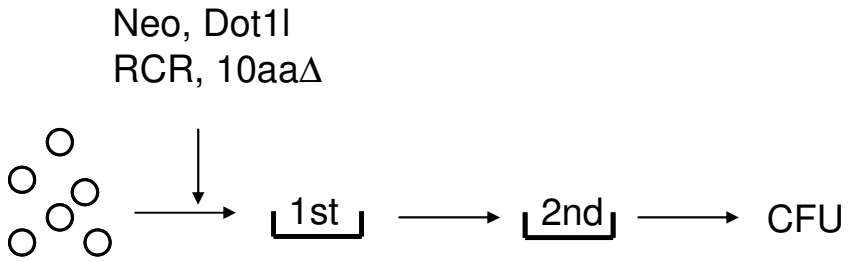

Figure 7.2. Schematic of transduction of MLL-AF9 transformed cells.

Cells left over from the 1st plating were used for genomic DNA, RNA, and protein extraction. PCR reaction of genomic DNA showed clear excision of endogenous *Dot1l* loci (Figure 7.3).

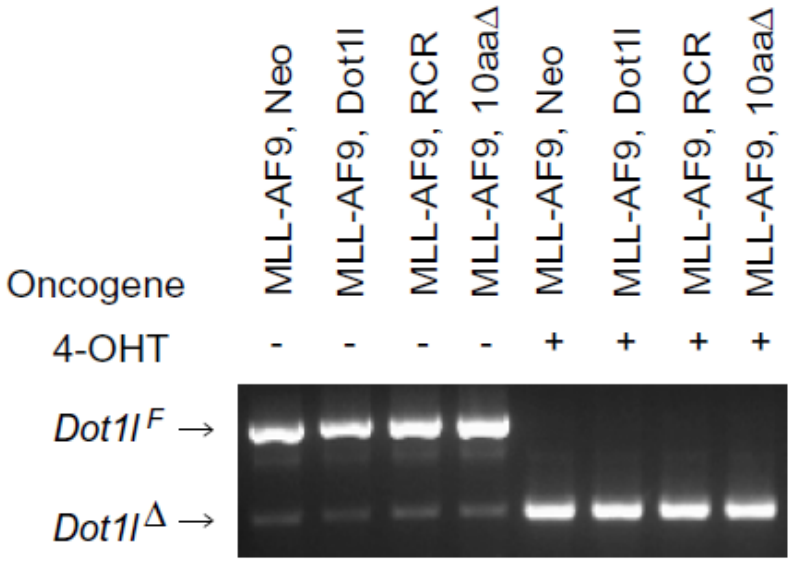

Figure 7.3. Genotyping of transduced bone marrow cells after first round. PCR reaction showed high excision efficiency with 4-OHT treatment in all cells.

qPCR of HA tag showed that all exogenous Dot1l constructs were expressed compared to neomycin vector control (Figure 7.4).

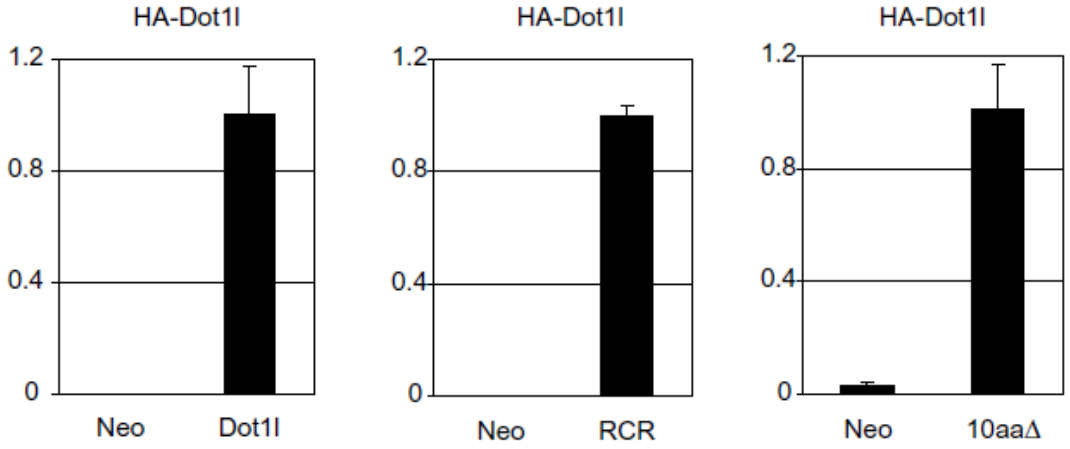

Figure 7.4. qPCR of HA tag and N-terminus of Dot1l. All Dot1l constructs showed high expression compared to vector alone.

The functionality of the 10aaΛ construct was examined by western blot. Western blot of H3K79me2 showed that H3K79 methylation was restored with expression of exogenous wild type Dot1l and 10aaΛ constructs, but not with RCR construct (Figure 7.5). Restoration of H3K79 methylation by the 10aaΛ construct is in contrast to the HMT domain construct (Figure 7.5 and Figure 3.17). This result suggested that for *in vivo* H3K79 methylation the C-terminal region of Dot1l is also required, unlike for *in vitro* methylation assays (Feng et al., 2002; Min et al., 2003). Given the restoration of H3K79 methylation, the transformation ability of the 10aaΛ construct was of particular interest. Unlike the wild type Dot1l construct, expression of the AF9/ENL interaction domain lacking 10aaΛ construct failed to rescue colony formation after endogenous *Dot1l* excision (Figures 7.6 & 7.7).

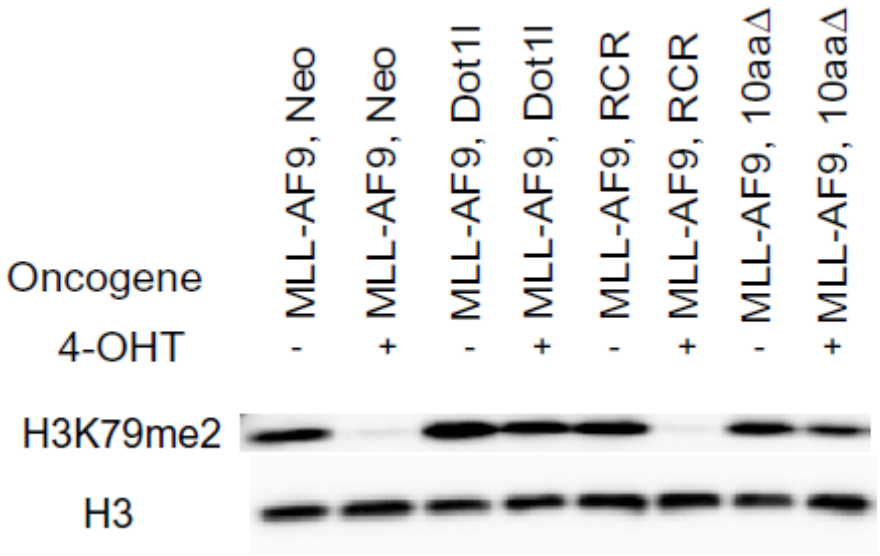

Figure 7.5. Western blot of H3K79Me2 after first round. Western blot showed restoration of H3K79Me2 with the introduction of exogenous wild type Dot1l and 10aaΔ but not with RCR. Histone 3 blot was used as loading control.

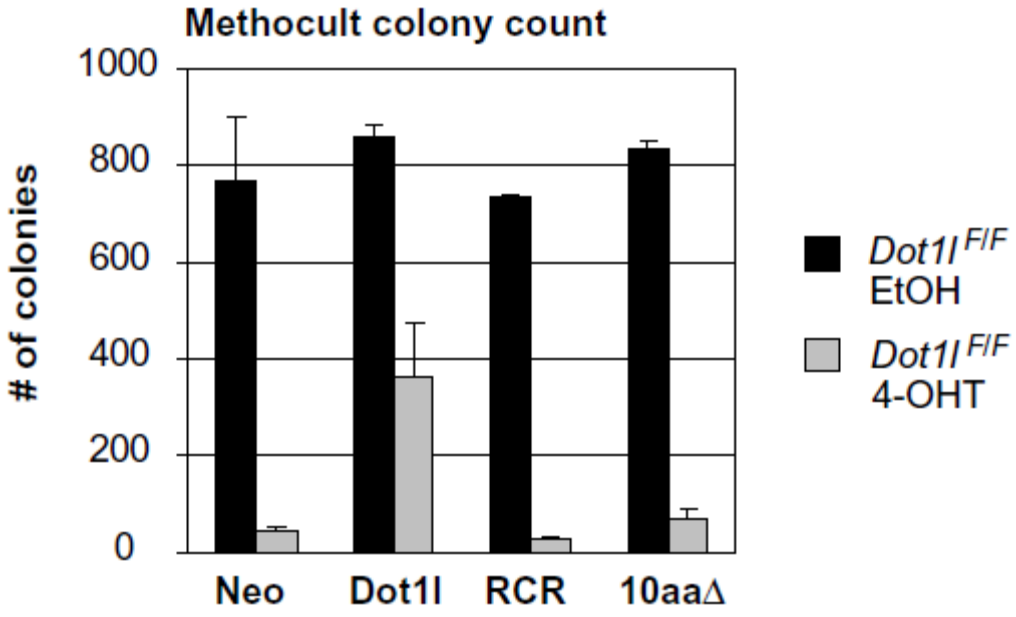

Figure 7.6. Quantification of colony formation by MLL-AF9 transformed cells with endogenous *Dot1l* excision and exogenous Dot1l constructs (wild type-Dot1l, methyltransferase inactive-RCR and AF9/ENL interaction domain lacking-10aaΔ).

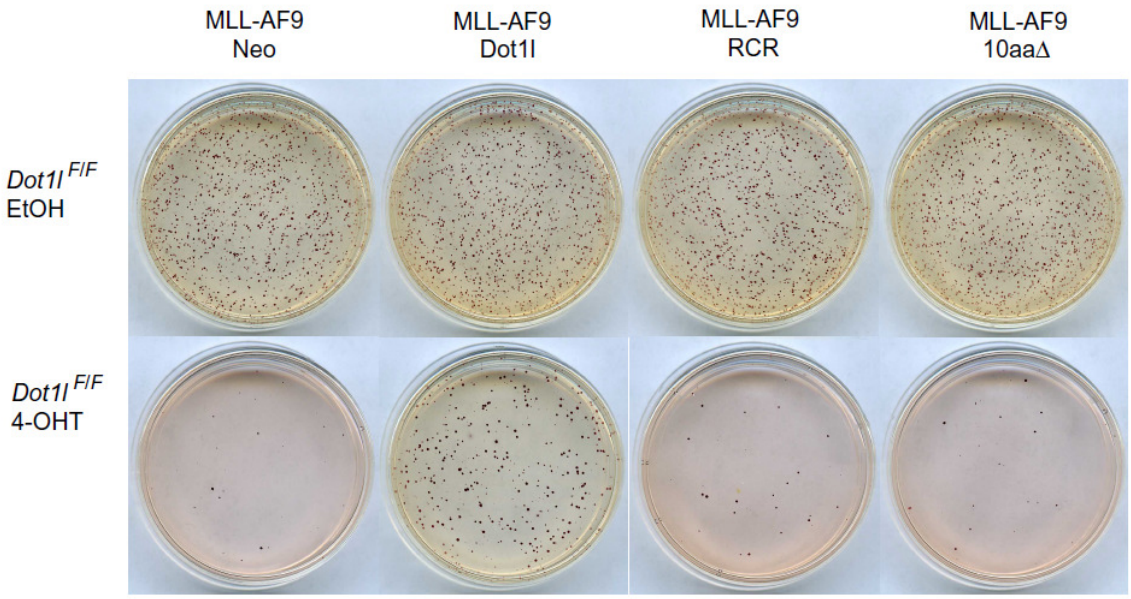

Figure 7.7. Whole plate image of colony formation by MLL-AF9 transformed cells after endogenous *Dot1l* excision and exogenous Dot1l expression. INT staining at 2nd round.

In fact, despite the restoration of H3K79 methylation, colony formation by the 10aaΛ construct mimicked that of neomycin vector control and RCR constructs. This result is significant because it suggested that interrupting this key interaction with a peptide or small molecule could also disrupt colony formation by MLL-AF9 transformed cells, which in the clinic could lead to remission. Due to high homology between AF9 and ENL (Figure 7.1) and identical interaction residues on Dot1l, similar results are expected with MLL-ENL. Further studies will be necessary to determine if other *MLL* translocation proteins will be affected by targeting these interaction residues on Dot1l. It will also be interesting to perform a detailed analysis of interaction domains between Dot1l and other known interacting proteins.

Chapter VIII

Discussion

This thesis focuses on the biological role of Dot1l in mammalian hematopoietic system. With our conditional Dot1l knockout mouse model, we showed that Dot1l is required for maintaining postnatal hematopoiesis as well as leukemogenesis by *MLL* translocation. *Dot1l* deletion led to the failure of hematopoietic homeostasis and to the loss of functional HSCs in a cell-autonomous manner. Moreover, Dot1l was selectively required for the transformation by *MLL* translocation proteins but not by Hoxa9/Meis1 and E2A-HLF oncogenes. Interestingly, both the histone methyltransferase activity of Dot1l and the protein interaction by Dot1l were important in transformation by the MLL-AF9 oncogene. In addition, Dot1l loss led to upregulation of polycomb target genes and differentiation-related genes in HSCs, and the loss of H3K79 methylation affected histone modification status on selected gene loci in MLL-AF9 transformed cells instead of leading to global changes.

Dot1l and normal hematopoiesis

Our studies clearly show the requirement of Dot1l in normal postnatal hematopoiesis. Extended Dot1l loss (~8 weeks) led to bone marrow atrophy and

pancytopenia that was more extensive compared to other organs (Figures 2.2, 2.3 and 4.1). Transplantation experiments showed that Dot1l lacking HSCs could not reconstitute bone marrow, and this effect was cell autonomous. The excision of *Dot1l* in normal hematopoietic microenvironment with competitors showed that even relatively short period of Dot1l loss (~2 weeks) led to profound disappearance of Dot1l-deficient cells particularly for short-lived myeloid cells (Figure 2.13).

From our data, question arises on how *Dot1l* excision affects HSCs, progenitors and circulating blood cells. By third week, HSCs and progenitors of all blood lineages showed significant decrease in frequency (Figure 2.6). However, animals survived and CBC did not drop significantly until ~8 weeks after *Dot1l* excision (Figure 2.3). This suggested that effects of Dot1l loss are likely not due to indiscriminant toxicity to cells. If loss of Dot1l and H3K79 methylation led to generalized chromosomal defects, then all nucleated cells would be affected catastrophically. On the other hand, it is possible that there were a few cells that escaped excision and that these cells were responsible for the reduced toxicity observed in these mice. The repopulation of peripheral blood by cells that escaped excision was observed by PCR reaction at 4-5 weeks after initial tamoxifen injection, and for this reason tamoxifen was injected every 4 weeks to ensure *Dot1l* excision. Peripheral blood was used for excision check before and after each tamoxifen injection (3-5 days before and after the injection date), and with the every 4 week injection schedule there was no detectable unexcised allele from PCR. However, the presence of PCR-undetectable cells

that escaped excision cannot be completely ruled out. If this were the case, then it will suggest that in fact Dot1l loss is catastrophically toxic and that there is a huge selection against Dot1l loss. One way to possibly test this hypothesis is to perform transplantation experiment without the competitor cells. In the absence of competitor cells, the few cells that escaped excision may be able to repopulate the recipient bone marrow. Another way to examine this hypothesis is to analyze chromosomal structure of cells after *Dot1l* excision with time course metaphase spread. If there are chromosomal defects shortly after excision in most of the cells with a few exceptions (presumable those that escaped excision), then it will suggest that in fact Dot1l loss is extremely toxic to cells. It is also notable that enzymatic demethylation of H3K79 residue has not been reported. Hence, H3K79 methylation may persist longer than other histone modifications that can be enzymatically removed especially for slow-cycling cells. This may contribute to delayed toxicity. For example, demethylase LSD1 has been shown to remove H3K4 methylation mark (Shi et al., 2004). Eight week survival by Dot1l lacking mice is in contrast to Mll lacking mice that died by three weeks after excision (Jude et al., 2007).

Gene expression data from HSC microarray suggested a possible mechanism of Dot1l action in hematopoiesis. GSEA data indicated upregulation of EZH2 targets (Figure 5.3), with many of them associated with cell cycle, such as Prc1 (Jiang et al., 1998), Mcm3 (Madine et al., 1995), and Ccnb2 (Gong and Ferrell, 2010). GSEA data also indicated upregulation of myeloid proliferation and self-renewal genes (Figure 5.4). Combined with possible increase in HSC

cell cycle, this data might imply acceleration of differentiation into myeloid lineage, with depletion of HSCs and lymphocyte, megakaryocyte, and erythrocyte lineage progenitors. Loss of renewable HSCs will eventually lead to depletion of myeloid lineage progenitors as well. Frequency of cell population roughly correlates with this hypothesis, with HSC loss being most severe, then CLP (furthest from myeloid pathway), then MkP similar to EryP (separated from myeloid pathway later than CLP), and GMP being least depleted (Figure 2.7). In addition, GSEA data suggested that granulocyte and monocyte differentiation downstream of the initial myeloid commitment may be affected by Dot1l loss (Figure 5.5). While it is unclear if and how these genes affect cell cycle, preliminary cell cycle analysis implied that there may be cell cycle block in more differentiated cells (Figure 5.6). From these data, it can be hypothesized that Dot1l loss leads to increased cycling and accelerated myeloid differentiation of HSCs and then cell cycle block near the end of differentiation pathway, eventually leading to hematopoietic failure.

Several experiments can be proposed to test this hypothesis. Firstly, HSCs and progenitor population frequency can be examined after shorter period of *Dot1l* excision. Although use of tamoxifen for *Dot1l* excision led to staining profile changes in bone marrow and precluded analysis prior to one week (Figure 5.1), we can perform time course experiment for population analysis between one and three weeks. If the hypothesis of accelerated differentiation into myeloid pathway is true, then there might be a time period where frequencies of HSCs and other lineage progenitors are decreasing but there is no change or increase

in GMPs. Similarly, cell cycle analysis of individual cell population can be performed in a time course. There are two approaches to cell cycle analysis. One is first staining for cell surface markers, sorting and collecting cell populations, fixing the cells, and using DNA intercalating agents such as propidium iodide or DAPI for examining DNA content. Use of DAPI is preferable to propidium iodide because it interferes less with emissions of other fluorophores. This approach is limited in analyzing low frequency population because of the inherent loss of cells while fixing and staining small number of cells, and at least 5000-10000 events are necessary during the second flow cytometer run to get good DNA content profile (example Figure 3.9). On the other hand, this approach separates efficiency of cell surface marker staining and DNA content analysis. Once the cells are sorted and collected by the surface marker profile, the population of cells is set and any incompatibility of surface marker antibodies and fixation treatment or intercalating reagent is not very important. Also, this approach does not require any prior treatment of animals or cells unlike the second approach. The second approach is using BrdU and anti-BrdU antibody. Animals are injected with BrdU 12 hours prior to analysis, bone marrow cells or peripheral blood cells are harvested and stained for cell surface markers, and cells are fixed, permeabilized and stained for BrdU-antibody. BrdU staining requires cell surface antibodies to remain bound and fluorophores to be intact through fixation and permeabilization processes. BrdU itself may also be toxic to the cells, although the effects are likely to be minimal with only 12 hour exposure. If good surface staining can be obtained, BrdU staining can be useful

in examining all cell population. With detailed cell cycle analysis with time course, effects of *Dot1l* excision on HSCs, progenitors and differentiated cells can be compared. If our hypothesis of accelerated HSC myeloid differentiation and cell cycle block downstream is true, then there may be initial increase in HSC cycling and then decrease in GMP cycling. Additionally, gene expression profiles of populations other than HSCs can be examined and compared to understand the effects of *Dot1l* excision in more differentiated cells.

Another interesting question is determining the relative importance of HMT activity of Dot1l and protein interaction by Dot1l in normal hematopoiesis. This question is derived in part from Chapter VII of the thesis, where deletion of Dot1l-AF9 interaction residues of Dot1l was as detrimental to MLL-AF9 transformation as removing enzymatic activity of Dot1l. If normal hematopoiesis can be rescued by 10aaΔ construct that retains HMT activity but cannot interact with AF9, then there will be a very high therapeutic index targeting Dot1l-AF9 interaction region. Several experiments can be designed to test this idea. Transplantation experiments can be done in two ways. Bone marrow cells can be harvested from Dot1l$^{F/F}$ mice and transduced with either vector control or 10aaΔ construct. The cells can then be treated with 4-OHT *in vitro* for *Dot1l* excision and transplanted into lethally irradiated recipient mice with varying ratios of competitive cells. If experimental cells can reconstitute recipient bone marrow in the presence of competitors, then it is a very strong evidence that Dot1l-AF9 interaction is non-essential in HSC activity. Or, the transduced cells can be transplanted first into recipients and allowed to reconstitute recipient bone marrow. Then the recipients

will be injected with tamoxifen for *Dot1l* excision *in vivo*. The second method assures that experimental cells are not competed out at the initial engraftment stage before 10aaΛ construct expression is stable and also examine if any observed phenotype is cell autonomous. More sophisticated method of examining the activity of 10aaΛ construct in hematopoiesis is to generate transgenic mice from the conditional Dot1l knockout line. One approach is starting with our homozygous Dot1$^{F/F}$ mice and expressing 10aaΛ construct. A vector with ubiquitously expressed promoter such as ROSA26 with transcriptional termination sequences flanked with loxp sequences can be used (Soriano, 1999). 10aaΛ construct can be cloned into this vector 3' to the flanked transcriptional termination sequences. The embryos will be microinjected with this vector for random integration into genome. This approach has the disadvantage of exogenous promoter driven expression and random integration while having the advantage of expressing Dot1l protein with just the minimal 10 amino acid deletion required for Dot1l-AF9 interaction. Alternatively, exon 20 that contains the Dot1l-AF9 interaction residues can be deleted out similarly to exon 2 deletion conditional knockout mice generated in this thesis (Figure 2.1). However, exon 20 is 484 base pairs long, so more than the 10 amino acids required for the interaction will be lost. However, this approach has the advantage of being endogenous promoter driven expression and no random integration. In both cases, Cre induction will lead to expression of Dot1l that cannot interact with AF9. If hematopoietic homeostasis can be maintained in these animals after endogenous *Dot1l* excision, then it will strongly suggest that

targeting Dot1l-AF9 interaction will yield high therapeutic index and also suggest that Dot1l-AF9 interaction is dispensable for hematopoietic homeostasis, indicating that Dot1l acts through other proteins to affect hematopoiesis. This mice model may also be more physiologically similar to patients who may be taking a drug targeting Dot1l-AF9 interaction. In addition to hematopoiesis, Dot1l-AF9 interaction has been shown to be important in both brain development (Büttner et al., 2010) and regulation of sodium channels in kidneys (Zhang et al., 2006). As more biological roles of Dot1l-AF9 interactions are reported, generation of these mice may prove to be useful. Similar studies can also be performed with a good inhibitor targeting Dot1l-AF9 interaction region.

The role of Dot1l in HSCs versus LICs

One of the most interesting findings of this thesis is the selective nature of Dot1l function depending on cell type. Remarkably, normal HSCs and MLL-AF9 LICs required proper Dot1l expression while Hoxa9/Meis1 and E2A-HLF LICs did not. It is notable that cells with MLL-AF9 oncogene showed phenotype similar to normal HSCs instead of acting similarly to cells with other leukemic oncogenes. There are some evidences indicating that *MLL* translocation ALL and AML may be a separate category apart from other ALL and AML. As the name *Mixed Lineage Leukemia* suggests, *MLL* translocation can lead to either ALL or AML. Gene expression profiling study shows that ALL and AML with *MLL* translocation clusters together instead of clustering with other ALL and AML cases (Zangrando et al., 2009). Hence, despite the phenotypic similarity to ALL and AML with other

oncogenes, *MLL* translocation leukemia seems to have separate gene regulation, which may be similar to HSCs.

Dependence on major *MLL* translocation target genes may be a possible explanation for the phenotypic distinction between cell types with *Dot1l* excision. Both normal HSCs and *MLL* translocation leukemia are dependent on Hoxa9 and Meis1. Previous studies on Hoxa9 and Meis1 knockout mice show that both proteins, especially Meis1, are critical for normal HSCs (Hisa et al., 2004; Lawrence et al., 1997). Similarly, it is well documented that Hoxa9 and Meis1 are important in the maintenance of *MLL* translocation leukemia (Ayton and Cleary, 2003; Zeisig et al., 2004). Dot1l binds directly to the *Hoxa9* and *Meis1* loci and H3K79 methylation levels are closely correlated with gene expression (Monroe et al., 2010), indicating that Dot1l is a direct regulator of these genes. In contrast, Hoxa9/Meis1 transformed cells have high expression of both proteins through exogenous promoters, and E2A-HLF cells do not upregulate *Hoxa9* and *Meis1* expression. The varying dependence on Hoxa9 and Meis1 in different cell types might explain the different response to *Dot1l* deletion. It will be interesting to compare gene expression changes with Dot1l loss among normal HSCs and cells transformed with MLL-AF9, Hoxa9/Meis1, and E2A-HLF.

Dot1l as a therapeutic target

The requirement of Dot1l by *MLL* translocation protein makes Dot1l an attractive target for therapy, particularly since Dot1l-deficient mice did not show overt toxicity for the first 7-8 weeks of *Dot1l* excision. From our data,

hematopoietic toxicity may complicate the long-term use of DOT1L inhibitors. However, many myelotoxic drugs are successfully used clinically. A pulse of DOT1L inhibition may not be unmanageably toxic, especially with supporting therapies such as transfusion. In addition, it is possible that a partial reduction in Dot1l activity may show greater toxicity for leukemia cells compared to normal HSCs based on the concept of oncogene addiction (Sharma and Settleman, 2010). Furthermore, the use of DOT1L inhibition may be broadened by targeting other leukemias with upregulated *HOXA9* and *MEIS1* expression such as those with CDX2/CDX4 and NPM1 mutations (Renneville et al., 2008). DOT1L may downregulate *HOXA9* and *MEIS1* expression in these other leukemias and have similar anti-leukemia effect.

It is notable that in addition to targeting HMT activity of Dot1l, targeting Dot1l interaction with an important co-activator for a particular cell type can be equally biologically effective. Inactivating HMT domain or deleting protein interaction domain of Dot1l had similar effects in suppressing colony formation on methocult (Figures 7.6 and 7.7), suggesting that either function can be targeted for therapeutic effects. Given that the Dot1l construct lacking AF9/ENL interaction residues retained H3K79 methylation (Figure 7.5), targeting the region might have lower toxicity compared to targeting the HMT domain for treating MLL-AF9 and MLL-ENL leukemias. In addition to *MLL* translocation partners, Dot1l has been shown to interact with Wnt pathway components (Mohan et al., 2010). Different interaction partners of Dot1l probably bind slightly different residues of Dot1l. By identifying specific residues of Dot1l responsible for

interacting with essential co-activator and targeting them, it may be possible to achieve high therapeutic index and broaden the use of Dot1l targeting drugs.

Gene regulation by Dot1l, H3K79 methylation, and co-activators

ChIP results in MLL-AF9 transformed cells revealed interesting histone cross-talk in mammalian cells. Previous studies show that H2B ubiquitination is required for H3K4 and H3K79 methylation (Kim et al., 2009; Ng et al., 2003; Wood et al., 2003), and H3K79 methylation closely correlates with H3K4 methylation in *MLL* translocation leukemia cells (Krivtsov et al., 2008; Lin et al., 2009). Our preliminary ChIP data on *Hoxa9* and *Meis1* loci clearly showed that both H3K4 methylation and H2B ubiquitination decreased with H3K79 methylation loss. These modification changes were likely loci specific because total modification levels did not change with *Dot1l* excision (Figure 6.1). It will be interesting to perform ChIP-seq of histone modifications before and after *Dot1l* excision and study which modifications vary together at which loci and correlate the data with gene expression analysis.

As mentioned above, H3K79 methylation by Dot1l and Dot1l-AF9 interaction were required for transformation by the MLL-AF9 oncogene. MLL-AF9 transformed cells with HA-tagged Dot1l, RCR, and 10aaΔ constructs provide a unique system to study gene regulation by Dot1l and H3K79 methylation. Recruitment of the Dot1l and H3K79 methylation status in cells with HA-tagged Dot1l, RCR, and 10aaΔ constructs through ChIP-seq in conjunction with gene expression profile can be performed. Comparing cells with wild type

Dot1l and those with RCR will shed light on genes that are specifically regulated by H3K79 methylation. In addition, comparing cells with wild type Dot1l and those with 10aaΔ will show more subtle regulation of loci that require Dot1l-AF9/ENL interaction.

Dot1l and other organ systems

The biological role of Dot1l is likely to be beyond hematopoiesis and leukemia. A study shows that DOT1L is involved in regulation of tumor suppressor gene expression in human colon carcinoma cell lines (Jacinto et al., 2009). Dot1l has also been shown to be important in gut development (Mahmoudi et al., 2010) and kidney function (Zhang et al., 2006). Also, a recent study shows that Dot1l loss in cardiac muscle leads to defects in heart development, arrhythmia, and death (Nguyen et al., 2011). Our observations also showed atrophy of seminiferous tubules and decreased but not abolished sperm production. It will be interesting to study if these sperm are actually functional. Furthermore, Dot1l and AF9 have been shown to be important for proper brain development (Büttner et al., 2010). In the case of our conditional Dot1l knockout mice, tissue immunohistochemistry after *Dot1l* excision showed that the brain tissue retained H3K79 methylation (Figure 4.1). Because Dot1l is the only H3K79 methyltransferase and current studies not support secondary methyltransferases for the H3K79 residue, it was initially suspected that the blood-brain barrier might have prevented uptake of tamoxifen into the brain. However, presentation by Dr. Andrew Lieberman's lab (University of Michigan)

showed that complete excision of a target gene was observed in the brain with identical ROSA-CreER system. Hence, further examination will be necessary to explain this discrepancy.

Concluding remarks

In summary, our studies showed that Dot1l is an important histone modifier with interesting biological functions. We established the requirement of Dot1l in normal postnatal hematopoiesis and the essential role of Dot1l in *MLL* translocation mediated leukemogenesis. Tissue immunohistochemistry, gene expression analysis, ChIP-qPCR, and mutant Dot1l construct rescue experiments further shed light on the subtle gene regulation by Dot1l and opened up questions for future studies. We hope that these findings broaden the understanding of the regulation of HSCs and the pathogenesis of *MLL* translocation leukemia, and contribute to targeted therapies in the future.

References

Ayton, P.M., and Cleary, M.L. (2003). Transformation of myeloid progenitors by MLL oncoproteins is dependent on Hoxa7 and Hoxa9. Genes Dev *17*, 2298-2307.
Barry, E., Krueger, W., Jakuba, C., Veilleux, E., Ambrosi, D., Nelson, C., and Rasmussen, T. (2009). ES cell cycle progression and differentiation require the action of the histone methyltransferase Dot1L. Stem Cells *27*, 1538-1547.
Barry, E.R., Corry, G.N., and Rasmussen, T.P. (2010). Targeting DOT1L action and interactions in leukemia: the role of DOT1L in transformation and development. Expert Opin Ther Targets *14*, 405-418.
Benedikt, A., Baltruschat, S., Scholz, B., Bursen, A., Arrey, T.N., Meyer, B., Varagnolo, L., Müller, A.M., Karas, M., Dingermann, T.*, et al.* (2011). The leukemogenic AF4-MLL fusion protein causes P-TEFb kinase activation and altered epigenetic signatures. Leukemia *25*, 135-144.
Bitoun, E., Oliver, P., and Davies, K. (2007). The mixed-lineage leukemia fusion partner AF4 stimulates RNA polymerase II transcriptional elongation and mediates coordinated chromatin remodeling. Hum Mol Genet *16*, 92-106.
Bursen, A., Schwabe, K., Rüster, B., Henschler, R., Ruthardt, M., Dingermann, T., and Marschalek, R. (2010). The AF4.MLL fusion protein is capable of inducing ALL in mice without requirement of MLL.AF4. Blood *115*, 3570-3579.
Büttner, N., Johnsen, S.A., Kügler, S., and Vogel, T. (2010). Af9/Mllt3 interferes with Tbr1 expression through epigenetic modification of histone H3K79 during development of the cerebral cortex. Proc Natl Acad Sci U S A *107*, 7042-7047.
Chandrasekharan, M.B., Huang, F., and Sun, Z.W. (2010). Histone H2B ubiquitination and beyond: Regulation of nucleosome stability, chromatin dynamics and the trans-histone H3 methylation. Epigenetics *5*.
Chang, M.J., Wu, H., Achille, N.J., Reisenauer, M.R., Chou, C.W., Zeleznik-Le, N.J., Hemenway, C.S., and Zhang, W. (2010). Histone H3 lysine 79 methyltransferase Dot1 is required for immortalization by MLL oncogenes. Cancer Res *70*, 10234-10242.
Crissman, H.A., Oka, M.S., and Steinkamp, J.A. (1976). Rapid staining methods for analysis of deoxyribonucleic acid and protein in mammalian cells. J Histochem Cytochem *24*, 64-71.
Dou, Y., and Hess, J.L. (2008). Mechanisms of transcriptional regulation by MLL and its disruption in acute leukemia. Int J Hematol *87*, 10-18.
Dou, Y., Milne, T.A., Ruthenburg, A.J., Lee, S., Lee, J.W., Verdine, G.L., Allis, C.D., and Roeder, R.G. (2006). Regulation of MLL1 H3K4 methyltransferase activity by its core components. Nat Struct Mol Biol *13*, 713-719.
Dou, Y., Milne, T.A., Tackett, A.J., Smith, E.R., Fukuda, A., Wysocka, J., Allis, C.D., Chait, B.T., Hess, J.L., and Roeder, R.G. (2005). Physical association and

coordinate function of the H3 K4 methyltransferase MLL1 and the H4 K16 acetyltransferase MOF. Cell *121*, 873-885.
Feng, Q., Wang, H., Ng, H., Erdjument-Bromage, H., Tempst, P., Struhl, K., and Zhang, Y. (2002). Methylation of H3-lysine 79 is mediated by a new family of HMTases without a SET domain. Curr Biol *12*, 1052-1058.
Feng, Y., Yang, Y., Ortega, M.M., Copeland, J.N., Zhang, M., Jacob, J.B., Fields, T.A., Vivian, J.L., and Fields, P.E. (2010). Early mammalian erythropoiesis requires the Dot1L methyltransferase. Blood *116*, 4483-4491.
Gong, D., and Ferrell, J.E. (2010). The roles of cyclin A2, B1, and B2 in early and late mitotic events. Mol Biol Cell *21*, 3149-3161.
Grez, M., Akgün, E., Hilberg, F., and Ostertag, W. (1990). Embryonic stem cell virus, a recombinant murine retrovirus with expression in embryonic stem cells. Proc Natl Acad Sci U S A *87*, 9202-9206.
Hanson, R.D., Hess, J.L., Yu, B.D., Ernst, P., van Lohuizen, M., Berns, A., van der Lugt, N.M., Shashikant, C.S., Ruddle, F.H., Seto, M.*, et al.* (1999). Mammalian Trithorax and polycomb-group homologues are antagonistic regulators of homeotic development. Proc Natl Acad Sci U S A *96*, 14372-14377.
Hawley, R.G., Lieu, F.H., Fong, A.Z., and Hawley, T.S. (1994). Versatile retroviral vectors for potential use in gene therapy. Gene Ther *1*, 136-138.
Hermiston, M.L., Xu, Z., and Weiss, A. (2003). CD45: a critical regulator of signaling thresholds in immune cells. Annu Rev Immunol *21*, 107-137.
Hisa, T., Spence, S.E., Rachel, R.A., Fujita, M., Nakamura, T., Ward, J.M., Devor-Henneman, D.E., Saiki, Y., Kutsuna, H., Tessarollo, L.*, et al.* (2004). Hematopoietic, angiogenic and eye defects in Meis1 mutant animals. EMBO J *23*, 450-459.
Huret, J.L., Dessen, P., and Bernheim, A. (2001). An atlas of chromosomes in hematological malignancies. Example: 11q23 and MLL partners. Leukemia *15*, 987–989.
Jacinto, F.V., Ballestar, E., and Esteller, M. (2009). Impaired recruitment of the histone methyltransferase DOT1L contributes to the incomplete reactivation of tumor suppressor genes upon DNA demethylation. Oncogene *28*, 4212-4224.
Jiang, W., Jimenez, G., Wells, N.J., Hope, T.J., Wahl, G.M., Hunter, T., and Fukunaga, R. (1998). PRC1: a human mitotic spindle-associated CDK substrate protein required for cytokinesis. Mol Cell *2*, 877-885.
Jones, B., Su, H., Bhat, A., Lei, H., Bajko, J., Hevi, S., Baltus, G., Kadam, S., Zhai, H., Valdez, R.*, et al.* (2008). The histone H3K79 methyltransferase Dot1L is essential for mammalian development and heterochromatin structure. PLoS Genet *4*, e1000190.
Jude, C., Climer, L., Xu, D., Artinger, E., Fisher, J., and Ernst, P. (2007). Unique and independent roles for MLL in adult hematopoietic stem cells and progenitors. Cell Stem Cell *1*, 324-337.
Karlić, R., Chung, H., Lasserre, J., Vlahovicek, K., and Vingron, M. (2010). Histone modification levels are predictive for gene expression. Proc Natl Acad Sci U S A *107*, 2926-2931.

Kiel, M., Yilmaz, O., Iwashita, T., Terhorst, C., and Morrison, S. (2005). SLAM family receptors distinguish hematopoietic stem and progenitor cells and reveal endothelial niches for stem cells. Cell *121*, 1109-1121.
Kim, J., Guermah, M., McGinty, R.K., Lee, J.S., Tang, Z., Milne, T.A., Shilatifard, A., Muir, T.W., and Roeder, R.G. (2009). RAD6-Mediated transcription-coupled H2B ubiquitylation directly stimulates H3K4 methylation in human cells. Cell *137*, 459-471.
Kim, J., and Roeder, R.G. (2011). Nucleosomal H2B ubiquitylation with purified factors. Methods.
Komura, K., Itakura, K., Boyse, E.A., and M., J. (1975). *Ly-5*: a new lymphocyte antigen system. Immunogenetics *1*, 452-456.
Kopp, H.G., Avecilla, S.T., Hooper, A.T., and Rafii, S. (2005). The bone marrow vascular niche: home of HSC differentiation and mobilization. Physiology (Bethesda) *20*, 349-356.
Krivtsov, A., Feng, Z., Lemieux, M., Faber, J., Vempati, S., Sinha, A., Xia, X., Jesneck, J., Bracken, A., Silverman, L.*, et al.* (2008). H3K79 methylation profiles define murine and human MLL-AF4 leukemias. Cancer Cell *14*, 355-368.
Krivtsov, A.V., and Armstrong, S.A. (2007). MLL translocations, histone modifications and leukaemia stem-cell development. Nat Rev Cancer *11*, 823-833.
Kroon, E., Krosl, J., Thorsteinsdottir, U., Baban, S., Buchberg, A.M., and Sauvageau, G. (1998). Hoxa9 transforms primary bone marrow cells through specific collaboration with Meis1a but not Pbx1b. EMBO J *17*, 3714-3725.
Lavau, C., Szilvassy, S.J., Slany, R., and Cleary, M.L. (1997). Immortalization and leukemic transformation of a myelomonocytic precursor by retrovirally transduced HRX-ENL. EMBO J *16*, 4226-4237.
Lawrence, H.J., Helgason, C.D., Sauvageau, G., Fong, S., Izon, D.J., Humphries, R.K., and Largman, C. (1997). Mice bearing a targeted interruption of the homeobox gene HOXA9 have defects in myeloid, erythroid, and lymphoid hematopoiesis. Blood *89*, 1922-1930.
Lee, J., Shukla, A., Schneider, J., Swanson, S., Washburn, M., Florens, L., Bhaumik, S., and Shilatifard, A. (2007). Histone crosstalk between H2B monoubiquitination and H3 methylation mediated by COMPASS. Cell *131*, 1084-1096.
Lin, Y., Kakadia, P., Chen, Y., Li, Y., Deshpande, A., Buske, C., Zhang, K., Zhang, Y., Xu, G., and Bohlander, S. (2009). Global reduction of the epigenetic H3K79 methylation mark and increased chromosomal instability in CALM-AF10-positive leukemias. Blood *114*, 651-658.
Madine, M.A., Khoo, C.Y., Mills, A.D., and Laskey, R.A. (1995). MCM3 complex required for cell cycle regulation of DNA replication in vertebrate cells. Nature *375*, 421-424.
Mahmoudi, T., Boj, S.F., Hatzis, P., Li, V.S., Taouatas, N., Vries, R.G., Teunissen, H., Begthel, H., Korving, J., Mohammed, S.*, et al.* (2010). The leukemia-associated Mllt10/Af10-Dot1l are Tcf4/β-catenin coactivators essential for intestinal homeostasis. PLoS Biol *8*, e1000539.

Maillard, I., Chen, Y., Friedman, A., Yang, Y., Tubbs, A., Shestova, O., Pear, W., and Hua, X. (2009). Menin regulates the function of hematopoietic stem cells and lymphoid progenitors. Blood *113*, 1661-1669.
Martin, M.E., Milne, T.A., Bloyer, S., Galoian, K., Shen, W., Gibbs, D., Brock, H.W., Slany, R., and Hess, J.L. (2003). Dimerization of MLL fusion proteins immortalizes hematopoietic cells. Cancer Cell *4*, 197-207.
Meyer, C., Kowarz, E., Hofmann, J., Renneville, A., Zuna, J., Trka, J., Ben Abdelali, R., Macintyre, E., De Braekeleer, E., De Braekeleer, M.*, et al.* (2009). New insights to the MLL recombinome of acute leukemias. Leukemia *23*, 1490-1499.
Milne, T.A., Briggs, S.D., Brock, H.W., Martin, M.E., Gibbs, D., Allis, C.D., and Hess, J.L. (2001). MLL targets SET domain methyltransferase activity to Hox gene promoters. Mol Cell *10*, 1107-1117.
Milne, T.A., Martin, M.E., Brock, H.W., Slany, R.K., and Hess, J.L. (2005). Leukemogenic MLL fusion proteins bind across a broad region of the Hox a9 locus, promoting transcription and multiple histone modifications. Cancer Res *65*, 11367-11374.
Min, J., Feng, Q., Li, Z., Zhang, Y., and Xu, R. (2003). Structure of the catalytic domain of human DOT1L, a non-SET domain nucleosomal histone methyltransferase. Cell *112*, 711-723.
Mohan, M., Herz, H.M., Takahashi, Y.H., Lin, C., Lai, K.C., Zhang, Y., Washburn, M.P., Florens, L., and Shilatifard, A. (2010). Linking H3K79 trimethylation to Wnt signaling through a novel Dot1-containing complex (DotCom). Genes Dev *24*, 574-589.
Monroe, S., Jo, S., Sanders, D., Basrur, V., Elenitoba-Johnson, K., Slany, R., and Hess, J. (2010). MLL-AF9 and MLL-ENL alter the dynamic association of transcriptional regulators with genes critical for leukemia. Exp Hematol.
Morita, S., Kojima, T., and Kitamura, T. (2000). Plat-E: an efficient and stable system for transient packaging of retroviruses. Gene Ther *7*, 1063-1066.
Mueller, D., Bach, C., Zeisig, D., Garcia-Cuellar, M., Monroe, S., Sreekumar, A., Zhou, R., Nesvizhskii, A., Chinnaiyan, A., Hess, J.*, et al.* (2007). A role for the MLL fusion partner ENL in transcriptional elongation and chromatin modification. Blood *110*, 4445-4454.
Mueller, D., García-Cuéllar, M., Bach, C., Buhl, S., Maethner, E., and Slany, R. (2009). Misguided transcriptional elongation causes mixed lineage leukemia. PLoS Biol *7*, e1000249.
Muntean, A.G., Giannola, D., Udager, A.M., and Hess, J.L. (2008). The PHD fingers of MLL block MLL fusion protein-mediated transformation. Blood *112*, 4690-4693.
Nakamura, T., Mori, T., Tada, S., Krajewski, W., Rozovskaia, T., Wassell, R., Dubois, G., Mazo, A., Croce, C.M., and Canaani, E. (2002). ALL-1 is a histone methyltransferase that assembles a supercomplex of proteins involved in transcriptional regulation. Mol Cell *10*, 1119-1128.
Ng, H., Feng, Q., Wang, H., Erdjument-Bromage, H., Tempst, P., Zhang, Y., and Struhl, K. (2002a). Lysine methylation within the globular domain of histone H3

by Dot1 is important for telomeric silencing and Sir protein association. Genes Dev *16*, 1518-1527.
Ng, H., Xu, R., Zhang, Y., and Struhl, K. (2002b). Ubiquitination of histone H2B by Rad6 is required for efficient Dot1-mediated methylation of histone H3 lysine 79. J Biol Chem *277*, 34655-34657.
Ng, H.H., Dole, S., and Struhl, K. (2003). The Rtf1 component of the Paf1 transcriptional elongation complex is required for ubiquitination of histone H2B. J Biol Chem *278*, 33625-33628.
Nguyen, A.T., Xiao, B., Neppl, R.L., Kallin, E.M., Li, J., Chen, T., Wang, D.Z., Xiao, X., and Zhang, Y. (2011). DOT1L regulates dystrophin expression and is critical for cardiac function. Genes Dev *25*, 263-274.
Okada, Y., Feng, Q., Lin, Y., Jiang, Q., Li, Y., Coffield, V., Su, L., Xu, G., and Zhang, Y. (2005). hDOT1L links histone methylation to leukemogenesis. Cell *121*, 167-178.
Okada, Y., Jiang, Q., Lemieux, M., Jeannotte, L., Su, L., and Zhang, Y. (2006). Leukaemic transformation by CALM-AF10 involves upregulation of Hoxa5 by hDOT1L. Nat Cell Biol *8*, 1017-1024.
Pronk, C., Rossi, D., Månsson, R., Attema, J., Norddahl, G., Chan, C., Sigvardsson, M., Weissman, I., and Bryder, D. (2007). Elucidation of the phenotypic, functional, and molecular topography of a myeloerythroid progenitor cell hierarchy. Cell Stem Cell *1*, 428-442.
Renneville, A., Roumier, C., Biggio, V., Nibourel, O., Boissel, N., Fenaux, P., and Preudhomme, C. (2008). Cooperating gene mutations in acute myeloid leukemia: a review of the literature. Leukemia *22*, 915-931.
Rozenblatt-Rosen, O., Hughes, C.M., Nannepaga, S.J., Shanmugam, K.S., Copeland, T.D., Guszczynski, T., Resau, J.H., and Meyerson, M. (2005). The parafibromin tumor suppressor protein is part of a human Paf1 complex. Mol Cell Biol *25*, 612-620.
Rubnitz, J.E., Link, M.P., Shuster, J.J., Carroll, A.J., Hakami, N., Frankel, L.S., Pullen, D.J., and Cleary, M.L. (1994). Frequency and prognostic significance of HRX rearrangements in infant acute lymphoblastic leukemia: a Pediatric Oncology Group study. Blood *84*, 570-573.
San-Segundo, P.A., and Roeder, G.S. (2000). Role for the silencing protein Dot1 in meiotic checkpoint control. Mol Biol Cell *11*, 3601-3615.
Sharma, S.V., and Settleman, J. (2010). Exploiting the balance between life and death: targeted cancer therapy and "oncogenic shock". Biochem Pharmacol *80*, 666-673.
Shen, F.W., Saga, Y., Litman, G., Freeman, G., Tung, J.S., Cantor, H., and Boyse, E.A. (1985). Cloning of Ly-5 cDNA. Proc Natl Acad Sci U S A *82*, 7360-7363.
Shi, Y., Lan, F., Matson, C., Mulligan, P., Whetstine, J.R., Cole, P.A., and Casero, R.A. (2004). Histone demethylation mediated by the nuclear amine oxidase homolog LSD1. Cell *119*, 941-953.
Shilatifard, A. (2008). Molecular implementation and physiological roles for histone H3 lysine 4 (H3K4) methylation. Curr Opin Cell Biol *20*, 341-348.

Silverman, L.B. (2007). Acute Lymphoblastic Leukemia in Infancy. Pediatr Blood Cancer *49*, 1070–1073.
Singer, M., Kahana, A., Wolf, A., Meisinger, L., Peterson, S., Goggin, C., Mahowald, M., and Gottschling, D. (1998). Identification of high-copy disruptors of telomeric silencing in Saccharomyces cerevisiae. Genetics *150*, 613-632.
Slany, R.K. (2009). The molecular biology of mixed lineage leukemia. Haematologica *94*, 984-993.
So, C.W., Lin, M., Ayton, P.M., Chen, E.H., and Cleary, M.L. (2003). Dimerization contributes to oncogenic activation of MLL chimeras in acute leukemias. Cancer Cell *4*, 99-110.
Soriano, P. (1999). Generalized lacZ expression with the ROSA26 Cre reporter strain. Nat Genet *21*, 70-71.
Steger, D., Lefterova, M., Ying, L., Stonestrom, A., Schupp, M., Zhuo, D., Vakoc, A., Kim, J., Chen, J., Lazar, M.*, et al.* (2008). DOT1L/KMT4 recruitment and H3K79 methylation are ubiquitously coupled with gene transcription in mammalian cells. Mol Cell Biol *28*, 2825-2839.
Taki, T., Ida, K., Bessho, F., Hanada, R., Kikuchi, A., Yamamoto, K., Sako, M., Tsuchida, M., Seto, M., Ueda, R.*, et al.* (1996). Frequency and clinical significance of the MLL gene rearrangements in infant acute leukemia. Leukemia *10*, 1303-1307.
Terranova, R., Agherbi, H., Boned, A., Meresse, S., and Djabali, M. (2006). Histone and DNA methylation defects at Hox genes in mice expressing a SET domain-truncated form of Mll. Proc Natl Acad Sci U S A *103*, 6629-6634.
Thiel, A.T., Blessington, P., Zou, T., Feather, D., Wu, X., Yan, J., Zhang, H., Liu, Z., Ernst, P., Koretzky, G.A.*, et al.* (2010). MLL-AF9-induced leukemogenesis requires coexpression of the wild-type Mll allele. Cancer Cell *17*, 148-159.
Vakoc, C., Sachdeva, M., Wang, H., and Blobel, G. (2006). Profile of histone lysine methylation across transcribed mammalian chromatin. Mol Cell Biol *26*, 9185-9195.
van Leeuwen, F., Gafken, P., and Gottschling, D. (2002). Dot1p modulates silencing in yeast by methylation of the nucleosome core. Cell *109*, 745-756.
Wood, A., Schneider, J., Dover, J., Johnston, M., and Shilatifard, A. (2003). The Paf1 complex is essential for histone monoubiquitination by the Rad6-Bre1 complex, which signals for histone methylation by COMPASS and Dot1p. J Biol Chem *278*, 34739-34742.
Xiao, Y. (2011). Enhancer of zeste homolog 2: A potential target for tumor therapy. Int J Biochem Cell Biol *43*, 474-477.
Yokoyama, A., and Cleary, M.L. (2008). Menin critically links MLL proteins with LEDGF on cancer-associated target genes. Cancer Cell *14*, 36-46.
Yokoyama, A., Somervaille, T.C., Smith, K.S., Rozenblatt-Rosen, O., Meyerson, M., and Cleary, M.L. (2005). The menin tumor suppressor protein is an essential oncogenic cofactor for MLL-associated leukemogenesis. Cell *123*, 207-218.
Yokoyama, A., Wang, Z., Wysocka, J., Sanyal, M., Aufiero, D.J., Kitabayashi, I., Herr, W., and Cleary, M.L. (2004). Leukemia proto-oncoprotein MLL forms a SET1-like histone methyltransferase complex with menin to regulate Hox gene expression. Mol Cell Biol *24*, 5639-5649.

Yu, B.D., Hess, J.L., Horning, S.E., Brown, G.A., and Korsmeyer, S.J. (1995). Altered Hox expression and segmental identity in Mll-mutant mice. Nature *378*, 505-508.
Zangrando, A., Dell'orto, M.C., Te Kronnie, G., and Basso, G. (2009). MLL rearrangements in pediatric acute lymphoblastic and myeloblastic leukemias: MLL specific and lineage specific signatures. BMC Med Genomics *2*, 36.
Zeisig, B., Milne, T., García-Cuéllar, M., Schreiner, S., Martin, M., Fuchs, U., Borkhardt, A., Chanda, S., Walker, J., Soden, R.*, et al.* (2004). Hoxa9 and Meis1 are key targets for MLL-ENL-mediated cellular immortalization. Mol Cell Biol *24*, 617-628.
Zhang, W., Xia, X., Reisenauer, M.R., Hemenway, C.S., and Kone, B.C. (2006). Dot1a-AF9 complex mediates histone H3 Lys-79 hypermethylation and repression of ENaCalpha in an aldosterone-sensitive manner. J Biol Chem *281*, 18059-18068.
Zhu, B., Mandal, S.S., Pham, A.D., Zheng, Y., Erdjument-Bromage, H., Batra, S.K., Tempst, P., and Reinberg, D. (2005). The human PAF complex coordinates transcription with events downstream of RNA synthesis. Genes Dev *19*, 1668-1673.